Investigating Postnatal Ontogeny in the Craniofacial Complex of Human Juveniles

A Dissertation Presented for the

Doctor of Philosophy

Degree

The University of Tennessee, Knoxville

Amber Davis Wheat

May 2015

To Austin,

for being the true rockstar of this journey.

You are *still* my world!

ACKNOWLEDGMENTS

This dissertation was accomplished with the help of many people, and I am more than grateful for everyone's support, assistance, and kindness. I would first like to thank Dr. Ben Auerbach for serving as my committee chair and mentor for the last five years. Words cannot express the appreciation I have for your intellectual guidance, advice, and patience during my time as your graduate student at the University of Tennessee. A big thank you to the members of my committee: Dr. Richard Jantz, Dr. Andrew Kramer, and Dr. James Fordyce. Dr. Richard Jantz not only provided assistance with some of the data formatting for this project, but also applied his knowledge of human craniofacial variation to the review of my work. Your insightful advice has greatly enhanced this project. I would also like to thank Dr. Andrew Kramer. Not only have you become an inspiration for my teaching practices, but you offered valuable advice in the creation of this project. I am also indebted to Dr. James Fordyce. I greatly appreciate that you were so willing to join my committee and offer your expertise. Together, the influence of my committee members has made this dissertation become exceedingly more than I ever expected. I sincerely thank each of you for your part in this project.

I would also like to thank the researchers and colleagues that were not on my committee that played an integral part in making this project possible. I am indebted to Dr. David Hatcher at the Digital Diagnostic Imaging Center. After months of trying to locate data to be used in this project, you generously provided me with access to CT scans. This project would not have been successful without your help. I would also like to thank Dr. David Wiley who provided me with a great deal of assistance in learning the imaging software used in this project. Dr. Valerie DeLeon, thank you for all the conversations that made this dissertation become better. Your advice throughout this project is greatly appreciated. In addition, I sincerely thank Dr. Timothy

Cole. Just when I was about to give up on using EDMA as an analytical tool in this dissertation, you graciously stepped in and wrote special software to aid in my research. Thank you for your countless advice related to my EDMA-issues. Thank you also to the Forensic Anthropology Center for funding a portion of this project through the Leitner Award and the Bass Endowment.

My time at the University of Tennessee was made enjoyable by the friendships of many people. Thank you to Bridget Algee-Hewitt for your unwavering support in all of my research endeavors. You have offered countless advice and have taught me so much about the world of geometric morphometrics. Thank you to Nicole Reeves, Courtney Eleazer, Becky Kelso, Brannon Hulsey, and Frankie Pack. You all inspire me to be a better thinker, educator, and person. Thank you for all of the coffee breaks, laughter, and the shared experience of being 'OVAL' office mates. You kept me going all the way to the end.

I am eternally grateful to all my friends and family for your support and encouragement. To my friends: Ashleigh Thomas, Camille Fritz, Kara Malone, Heather Story, and Amber Smith. Thank you for your unwavering support and your continuous prayers. I am truly blessed to have each of you in my life. Mali Collins, thank you for being a part of 'Team Wheat'. Your part in this journey does not go unrecognized. Thank you for loving on my babies like they were your own. Thank you to my parents for your continuous support in all of my endeavors. Mom, you have always encouraged me to reach for the stars when it came to my education. Thank you for your support throughout this entire journey. Dad, thank you for your continued interest in my research. I will always cherish our conversations about science. I also want to thank my grandparents and in-laws. Your unconditional love, support, and prayers means more to me than you will ever know. Thank you for supporting me in my decision to keep attending school. Abram and Dove, of all the accomplishments in my graduate career, you two are the ones of

which I am most proud.

And finally, thank you to my husband, Austin Wheat. You have earned your sticky note that will be placed on my diploma. Thank you for your unconditional support in this journey. When I wanted to give up and walk away, you kept me going. Thank you for becoming a full-time bread-winner, Daddy, house cleaner, dish washer, and chef during these last few months. None of this would have been possible without you.

"I can do all things through Christ who strengthens me." Philippians 4:13

ABSTRACT

Researchers have analyzed the developmental processes contributing to craniofacial variation from genetic, evolutionary, biomechanical and forensic perspectives, yet no study has clearly demonstrated the exact anatomical processes that occur in the craniofacial complex during postnatal growth to establish ultimate adult morphologies. Furthermore, previous research has not evaluated how endocranial bones (i.e., the ethmoid and sphenoid) play a role in postnatal craniofacial growth. Thus, while researchers have hypothesized that the long postnatal period of continued growth contributes to the high amount of variation observed in adult facial variation, this has yet to be shown empirically.

The presented research uses cranial data obtained from 299 computer tomographic (CT) scans of juvenile heads to document the growth changes that take place in the mid-face to establish adult human craniofacial variation. The growth trajectories of five developmentally independent regions of the face were studied: the frontonasal "module", the left and right maxillary "modules", the sphenoid "module", and the ethmoid "module". This study examined: 1) if developmental "modules" of the face remain proportional to each other throughout postnatal growth; 2) which "modules" of the face experience the most shape change during postnatal growth; and 3) if males and females have different growth trajectories of the five "modules" under study.

Results of analyses demonstrate clear distinctions between the sexes in growth patterns, as well as between the modules. Analyses within each module indicate that shape changes are occurring locally, while all of the units of the face, with the exception of the ethmoid, are remaining in relatively the same positions throughout growth. Results also reveal that males and females display different growth trajectories for the five "modules" under investigation.

This study applies current hypotheses of postnatal ontogeny to a human skeletal sample of known age and sex, providing support for the early onset of craniofacial variation and differential growth trajectories for males and females. The implications of this study provide important information for our current understanding of postnatal facial growth.

TABLE OF CONTENTS

LIST OF TABLES

LIST OF FIGURES

CHAPTER 1

INTRODUCTION

For over a century, research across multiple biological disciplines, especially biological anthropology, has focused on documenting patterns of human craniofacial variation (e.g., Boas 1912), as well as understanding the processes that shape this variation (Bastir et al. 2006; Sardi and Ramirez 2012; Sardi and Rozzi 2005; Vioarsdottir and Cobb 2004; Vioarsdottir et al. 2002). Researchers have analyzed craniofacial variation from genetic, evolutionary, biomechanical, and forensic perspectives. These studies have long established that craniofacial morphology varies between the sexes (Kimmerle et al. 2008; Rosas and Bastir 2002), as well as among adults in covariance with geography (Relethford 1994; Relethford 2004; Roseman 2004), presumably reflecting population structure as well as adaptation (Roseman and Weaver 2007; Roseman et al. 2011).

This variation is the product of functional and structural interactions that occur during ontogeny, overlying genetically controlled growth processes (Enlow and Hans 1996). Previous studies have established the processes and patterns of development, the covariance of morphological traits of the facial skeleton, and hypotheses of how these relate to adult craniofacial form and variation (Ackermann and Krovitz 2002; Mitteroecker et al. 2004; Sardi and Ramirez 2012; Sardi and Rozzi 2005; Vioarsdottir and Cobb 2004; Vioarsdottir et al. 2002). I review these studies further in Chapter 3. Yet, these studies have not clearly documented the exact anatomical processes that occur in the splanchnocranium (the facial region of the cranium) during postnatal development to establish ultimate adult morphologies. Particularly, previous research has not evaluated how endocranial bones lying at the junction of the neurocranium (the

portion of the cranium forming the brain case) and splanchnocranium (i.e., the ethmoid and sphenoid) play a role in postnatal craniofacial development. This dissertation addresses this gap in knowledge, examining the postnatal changes that take place in the mid-face of human juveniles (ages 7-17) by assessing the interactions of five developmental modules of the splanchnocranium. Modules in the cranium are independent or semi-independent regions that are the result of separate developmental processes, often perform a common anatomical function, and may be able to evolve independently (Mitteroecker and Bookstein 2008). This concept is discussed at greater length in Chapter 2.

Unlike the cranial base and vault, the face continues growth through adolescence (Lieberman 2011; see also Chapter 2). While numerous studies have documented the postnatal cranial ontogeny of non-human primates, hominins, and modern humans, these studies have primarily been concerned with assessing interspecific differences in growth of the cranium and/or documenting patterns of ontogeny within taxa (Ackerman and Krovitz 2002; Bookstein et al. 2003; Cobb 2001; Krovitz 2000; Leon and Zollikofer 2001; Lieberman et al. 2002; May and Sheffer 1999; Mitteroecker et al. 2004; Sardi and Rozzi 2012; Vioarsdottir 1999; Vioarsdottir et al. 2002). Of these researchers, only two groups have attempted to directly assess how developmental variance influences adult human craniofacial variation (Sardi and Rozzi 2012; Vioarsdottir et al. 2002). However, these papers were focused on the developmental origins of inter-population differences, rather than on assessing the patterns of change among regions of the face throughout ontogeny, or the relationship of these to known developmental processes. Thus, most studies of postnatal ontogeny have described patterns of craniofacial change throughout ontogeny to understand underlying processes, but do not directly evaluate questions about the anatomical processes that lead to variation.

This dissertation directly examines hypothetical models describing developmental and growth processes in the face, using an analysis of the conformity of developmental patterns as expected by these processes. Through the use of clinical data obtained from CT scans of human juveniles, this dissertation is, furthermore, unique from all previous studies, which have relied on archaeological or cadaveric samples, and so have mostly relied on relative dental aging instead of known chronological age; this is the first study to use clinical data to assess the ontogeny of facial dimorphism. The use of clinical data also offers a broader perspective of sex-specific ontogeny because it allows for endocranial analyses and a more precise assessment of sex-specific variation across age groups. Using three-dimensional landmark data, this dissertation tests specific hypotheses of craniofacial development.

Research Goals and Hypotheses

This study uses cross-sectional data from a sample of more than 250 juveniles to evaluate three questions:

1) Are proportions among the facial modules set early in ontogeny?

2) Which modules of the splanchnocranium experience the most change during postnatal growth and development?

3) How do males and females differ in the developmental trajectories of the five independent craniofacial modules under study?

These three research questions structure the basis of the two following hypotheses. Justifications for these questions and the research hypotheses are discussed in Chapters 2 and 3.

The first hypothesis tested in this study is that proportions of the face, as defined by the developmental modules under investigation, are set early during primary growth. There are

currently two opposing hypotheses concerning the ontogenetic origins of human craniofacial variation. The main source of disagreement between these hypotheses is how much postnatal growth contributes to adult morphological variation. The proposed models by these many researchers have two mutually exclusive theoretical commitments. The first argues that modules of the face grow proportionally during primary growth, meaning that shape differences are present prenatally (Ackermann and Krovitz 2002; Leon and Zollikofer 2001; Lieberman et al. 2002; Mitteroecker et al. 2004). The other argues that the facial skeleton grows at different rates and at different proportions (Cobb 2001; Sardi and Ramirez 2012; Vioarsdottir and Cobb 2004; Vioarsdottir et al. 2002). As previously stated, most of these studies focus on patterns of change (i.e., whether species or populations have different postnatal ontogenetic patterns), and not the specific processes leading to change (i.e., documenting which dimensions of the face portray the most variation throughout ontogeny, how these relate to known developmental processes, and whether the variance in these traits leads to adult variation). A study that establishes the developmental and growth trajectories of different modules of the face throughout ontogeny will reveal whether postnatal life influences craniofacial variation.

This dissertation will address the two opposing hypotheses concerning postnatal ontogeny through an assessment of the growth trajectories of five developmentally independent modules of the face: the frontonasal module, the left and right maxillary modules, the sphenoid module, and the ethmoid module (further defined in Chapter 2). A model of proportionality among these developmentally independent regions of the face is proposed to test this first hypothesis. This model makes two assumptions. First, that centroid size-scaled landmark distances within and among the five modules maintain relative distances regardless of age (as standardizing by centroid size should account for all shape change arising from increases in

cranial size only). Secondly, the model assumes that the centroids of the five developmental modules grow proportionally relative to the overall cranial centroid regardless of age. If my results fit the model, this indicates support for the hypothesis that facial proportions are set early in ontogeny (before age seven) and are further elaborated throughout postnatal life through parallel developmental processes. That is, each developmental region of the face, as defined by its size-scaled centroid, maintains an equal (proportional) distance from the overall centroid throughout ontogeny. If my results do not fit the model, this indicates that growth processes and epigenetic or environmental factors occurring during postnatal ontogeny play a role in producing adult craniofacial variation. A more detailed description of the current literature pertaining to this hypothesis and discussion of the five developmental modules under investigation are provided in the next chapter. A visual representation of this hypothesis is presented in Chapter 4.

The second hypothesis tested in this study is that males and females exhibit different growth trajectories of the five modules under investigation. As previously stated, many studies have documented patterns of ontogeny in primates to evaluate how postnatal ontogeny contributes to observed adult craniofacial variation. Documenting the patterns of adult facial size and shape variation due to sexual dimorphism has become a priority in recent years (Bulygina et al. 2006; Gkantidis and Halazonetis 2011; Kimmerle et al. 2008; Rosas and Bastir 2002; Vioarsdottir 1999; see also Chapter 3). Through this research, investigators have shown that sexual dimorphism in the adult craniofacial complex can be ascribed to differential growth and development between the sexes (Bastir and Rosas 2004; Gkantidis and Halazonetis 2011; Rosas and Bastir 2002; Ursi et al. 1992), despite few studies utilizing juveniles to directly investigate the ontogenies of specific regions of the face that produce sexually dimorphic features (Maddux 2011; Weston et al. 2007). Furthermore, it remains unclear *when* sexually dimorphic features

appear during postnatal ontogeny and which regions of the face experience the most change after puberty (Maddux 2011; Weston et al. 2007). Therefore, this study will assess the developmental trajectories of the five modules of the face to determine if males and females experience different growth patterns throughout ontogeny. A more detailed discussion of previous research on the ontogeny of facial dimorphism is presented in Chapter 3.

Organization of Chapters

In order to further explain and justify this project, an extensive review of previous research pertaining to craniofacial development is imperative. Therefore, Chapter 2 provides an overview of the growth and development of the facial skeleton. This overview will also include a detailed description and justification for the five developmental modules used in this research. Chapter 3 presents the current literature on postnatal ontogeny and provides a more detailed description of the two opposing hypotheses explaining the ontogenetic origins of craniofacial variation, in particular, those that relate to facial dimorphism. The remainder of this dissertation presents my original analyses. Chapter 4 presents the materials and methods of the research. The statistical results of the study are found in Chapter 5. Chapter 6 presents my results and how they can be interpreted in light of the proposed hypotheses discussed above, followed by my conclusions.

CHAPTER 2

CRANIOFACIAL GROWTH, DEVELOPMENT, AND MODULARITY

The main goal of this dissertation is to document and describe the developmental changes that take place throughout ontogeny in the mid-face of human juveniles to gain a better understanding of postnatal ontogenetic processes and to determine how developmental variance and covariance of the facial skeleton establish adult facial dimorphism. In order to do this, one must first understand the ontogenetic processes, both prenatal and postnatal, that shape midfacial morphology. Therefore, a brief overview of craniofacial growth and development is presented below, and then I relate this to craniofacial morphological integration and modularity.

The two latter concepts are explained more fully at the end of this chapter. In brief, integration refers to phenotypes that are genetically and developmentally covariant, and modules are the resulting developmentally integrated structures. Modules are therefore developmentally independent or semi-independent, though they will interact throughout growth as each module increases in size and changes shape.

Midface Growth and Development

The craniofacial complex of the skull is made up of developmentally independent and semi-independent regions. Prenatal and postnatal ontogeny establishes the independence of these regions, and also plays a role in the coordination of their growth. As explored in the next major section, the skull is comprised of three developmental modules: the chondrocranium (basicranium), the dermatocranium (cranial vault), and the splanchnocranium (the face)

(Lieberman 2011; Schoenwolf et al. 2015) (Figure 2.1). The chondrocranium is formed by endochondral ossification (in which a cartilage anlage is replaced by bone) and it serves as the connecting portion between the face and cranial vault. The dermatocranium is formed through intramembranous ossification (in which bone is formed without a cartilaginous precursor) and is influenced by its constant interaction with the brain. As the focus of this study, the splanchnocranium, which is comprised of approximately 20 bones that undergo either form of ossification, is unique in its development because it grows around various functional organs and spaces − arguably, its growth is shaped by interaction of bone with these organs and spaces (e.g., the functional matrix hypothesis as argues by Moss, 1960) − and continues growth after the vault and base have ceased. For these reasons, it portrays the most variation, and is therefore least constrained despite integration (i.e., developmental and functional covariance) in its developmental modules (Ackermann 2005; Bookstein et al. 2003; Lieberman et al. 2000; Lieberman 2011).

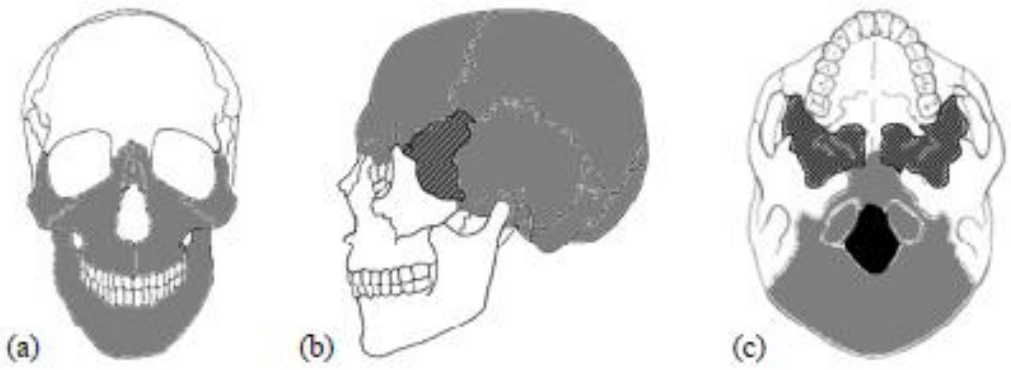

Figure 2.1. The three developmental modules of the cranium.
The shaded regions depict the (a) viscerocranium, (b) dermatocranium, and (c) chondrocranium. Note that the placement of the sphenoid bone (represented by diagonal lines) differs for researchers (i.e., some researchers place the sphenoid bone into the chondrocranium module while others place it into the dermatocranium module.

Prenatal Development of the Face

Development of the face begins in the third week *in utero*, and all of its components are established by the end of the embryonic period (week eight). The face is formed from three major developmental prominences: the frontonasal prominence, and bilateral maxillary and mandibular prominences (Figure 2.2). Two pairs of nasal plates that comprise the inferior nose and upper lip also develop from the frontonasal prominence. The prominences develop independently from each other, and can therefore be considered developmental modules. Through growth and development of the skull, the three modules become integrated (Bookstein et al. 2003; Lieberman et al. 2000; Lieberman 2011). The frontonasal prominence forms the upper face and surrounds the eyes and the nose. While the frontonasal prominence is growing inferiorly, the two other prominences expand from their lateral origins and grow medially around the sides of the face toward the midline. The midface inferior to the orbits and lateral to the nasal aperture is the end product of the maxillary prominence, while the mandibular prominence forms the lower jaw. During the fifth week of development, the paired maxillary prominences begin to grow ventrally and medially. This is also when the nasal plates form on the frontonasal prominence, and gradually enlarge, to become what is referred to as the frontonasal process. The nasal placodes develop between the medial and lateral nasal plate, which grow out to become processes. Since this study only focuses on midface morphology, the frontonasal, and the two maxillary prominences are viewed as independent developmental regions of the face. These regions comprise three of the five developmental modules under investigation. During the sixth and seventh weeks of development, the primary (premaxilla) and secondary palates form from the frontonasal process (specifically as outgrowths of the nasal processes) and maxillary prominences, respectively. The maxillary processes grow anteriorly and eventually fuse with the

medial and lateral nasal processes, fusing with the premaxilla and forming the nasolacrimal canal. The secondary palate begins its formation as the palatine processes appear from the maxillary swellings and grow out as transverse processes, ultimately separating the definitive nasal and oral cavities.

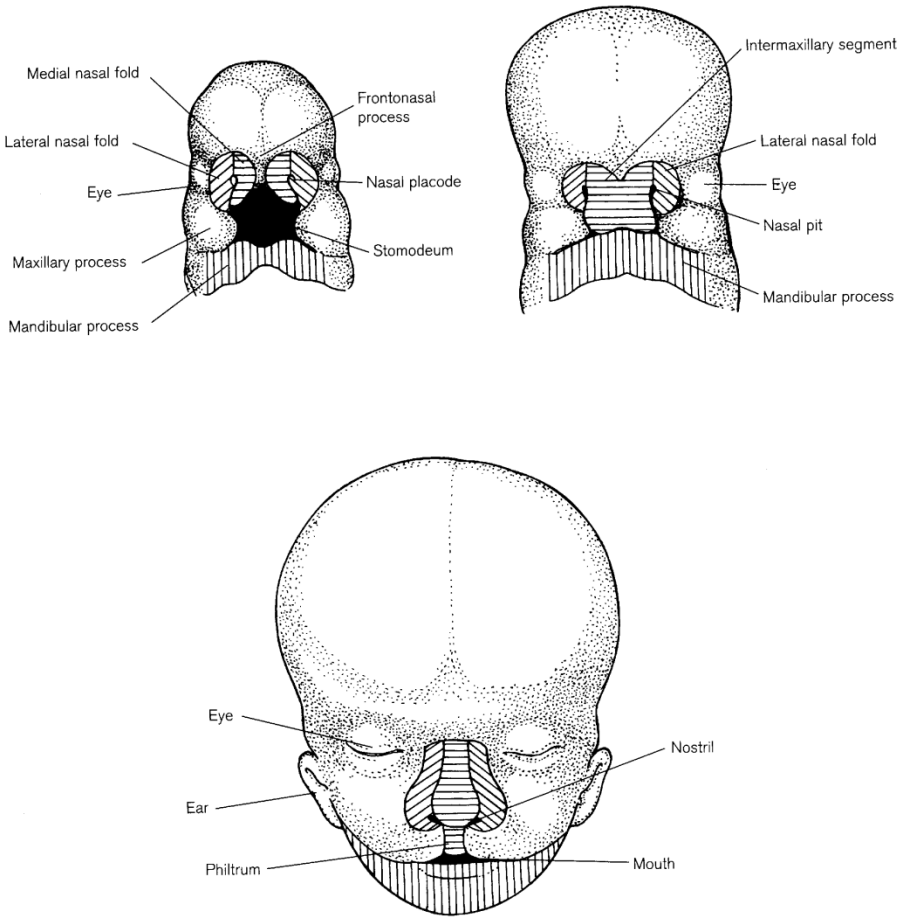

Figure 2.2. Developmental prominences of the face shown at 5 weeks, 7-8 weeks, and 10 weeks of development (adapted from Scheuer and Black 2000).

The bones of the face begin to ossify around the seventh week of development, marking the beginning of midfacial skeletal development (Dixon et al. 1997; Scheuer and Black 2000; Sperber et al. 2001). The nasolacrimal groove begins to close, and the lateral nasals and maxillary prominences begin to fuse. The frontonasal prominence drifts inferiorly between the nasal and lacrimal bones, fusing at the sphenofrontal suture. During the eighth week of gestation, intramembranous ossification centers appear in the frontonasal prominence, one for each of the nasal and lacrimal bones. A single ossification center appears for the two halves of the frontal bone around six to seven weeks of gestation. The maxilla fuses from four different ossification centers. Additionally, the premaxilla has two intramembranous ossification centers that appear during the seventh week of development. Eventually the maxilla and premaxilla fuse and form a horseshoe-shaped shelf bone around the roots of the teeth (referred to as the alveolar crest) (Lieberman 2011). During the eighth week of development the ossification center of the zygomatic bone creates the zygomatic arch, connecting the temporal bone to the face. Also during this time, intramembranous ossification centers located posterior to the maxilla contribute to bone formation of the greater wings and medial and lateral pterygoid plates of the sphenoid. The cranial vault and eye orbits undergo a faster pattern of development than the facial complex, resulting in a newborn skull with a large neurocranium and small face that is proportionally different when compared to an adolescent skull.

Two other bones interact with the midface during growth and development, the ethmoid and the sphenoid. The ethmoid interacts with the frontal, nasal, and maxillary bones while the sphenoid interacts with the ethmoid, frontal, zygomatic, and maxillary bones. Both of these bones develop through invaginations of the nasal cavity (Scheuer and Black 2000; Schoenwolf et al. 2015; Sperber et al. 2001) . The ethmoid appears during fetal life, forms as a result of

invaginations of the middle meatus of the nasal capsule, but doesn't complete its growth until puberty (see the next section for more detail about its postnatal growth). It is made up of four major parts: the horizontal cribriform plate, a midline perpendicular plate, and two lateral labyrinths (Scheuer and Black 2000; Sperber et al. 2001). Ossification of the ethmoid occurs in an inferior to superior and medial to lateral direction, with a number of ossification centers. Each labyrinth is completely ossified by the sixth month of fetal life. The cribiform plate does not ossify until after birth, during the first year of life.

The sphenoid has a similar developmental timeline as the ethmoid, and enlarges throughout ontogeny with the ethmoid. Unlike the ethmoid, the formation of the sphenoid is complex, is comprised initially of hypophyseal, trabecular, alisphenoid, and orbitosphenoid cartilages, which interact with each other, other ossification centers, and soft tissues, namely the developing meninges and brain (Scheuer and Black 2000; Schoenwolf et al. 2015). The ossifying sphenoid is typically divided into five regions: the body, the lesser wings, the greater wings, the pterygoid plates, and the sphenoidal conchae (Scheuer and Black 2000). These five regions consist of both intramembranous and endochondral ossification centers, of which there are a total of fourteen. Fusion of these five regions is variable, occurring as early as 17 weeks in utero and as late as after birth (Scheuer and Black 2000; Schoenwolf et al. 2015), though typically the sphenoid consists of three ossified but unfused parts at birth: the body with the lesser wings, and each of the greater wings separated. The sphenoid body is derived endochrondrally from two units: the presphenoid (anterior portion of the sphenoid body) and the postsphenoid (posterior portion of the sphenoid body). Fusion of these two units takes place at the tuberculum sellae. Three ossification centers of the presphenoid appear in the fourth month *in utero.* These centers fuse around 24 weeks. Two centers of ossification make up the postsphenoid bone, and are

located at the base of the sella turcica. These centers of ossification appear around 13 weeks of gestation and typically fuse around 16 weeks, becoming recognizable as a quadrilateral bone around the fifth month of fetal life. The two lesser wings also become recognizable as bone around five months of gestation, articulating with the presphenoid part of the body later in fetal life. The greater wings of the sphenoid experience both endochondral and intramembranous ossification, becoming recognizable around the fifth fetal month.

Much of the previous research on facial skeletal variation in juveniles has not included the ethmoid and sphenoid bones for analysis due to their location deep in the face and at the junction of the neurocranium; however, as they articulate and interact with the face throughout development, they are important elementsthat need to be included in studies of ontogeny. For this reason, in this research they are considered as independent regions of the midface and comprise two of the five developmental units under investigation. While no previous research has definitively shown the ethmoid and sphenoid to be modules − highly developmentally and evolutionarily internally integrated units that are independent from other such units (Klingenberg 2008; Mitteroecker and Bookstein 2008) − they are considered only as developmental modules for the current research, since it is known that these bones develop as independent regions of the cranium (separate from the face).

Postnatal Growth of the Face

Postnatal growth of the face is often described as a simple "forward and downward" growth process (Dixon et al. 1997; Enlow 1968; Enlow 1990; Lieberman 2011; Scheuer and Black 2000; Sperber et al. 2001). However, it is a much more complicated process that is characterized by an interplay of bone deposition and resorption (Enlow and Hans 1996). The facial skeleton is made up of fourteen intramembranous bones. Given the number of ossification

centers, it is helpful to approach postnatal ontogeny of the face by examining the separate craniofacial modules, keeping in mind that all bones are also bound by interactions with other bones, spaces, and organs of the face. Thus, for the purpose of clarity, the growth processes that occur during postnatal ontogeny are discussed in light of the five developmental modules under investigation: the frontonasal module, the left and right maxillary modules, the sphenoid, and the ethmoid.

The Frontonasal Module

The frontonasal prominence forms the upper part of the face. Developmentally, it is derived from the cranial neural crest mesenchyme (Scheuer and Black 2000; Sperber et al. 2001). Its adult components include the forehead, the bridge and midline of the nose, the alae of nose, and the philtrum of the upper lip. Of the five developmental modules under study, the frontonasal module contains the most bones. Given the amount of the face comprised by this region, as well as its central connections to all of the other modules, the most landmarks used for a module in this study were chosen to define the frontonasal module (15 landmarks, see Chapter 4). Thus, postnatal ontogeny of the frontonasal module is reviewed through a discussion of its various parts: the frontal region, the nasal region, the frontal processes of the maxilla, and the premaxilla.

The Inferior Frontal Region

The frontal bone articulates with the parietals, the greater wings of the sphenoid, the zygomatics, the frontal process of the maxillae, the lacrimals, the nasals, and the cribiform plate of the ethmoid (Scheuer and Black 2000; Sperber et al. 2001). The frontal bone plays an important role in connecting the face to the neurocranium, and therefore experiences shape

changes in response to growth of the brain (Scheuer and Black 2000). At birth, the frontal bone is composed of two halves, separated by the metopic suture. Closure of this suture normally takes place during the first year of life (Molleson and Cox 1993; Scheuer and Black 2000). An anterior fontanelle is also present at birth, and is located between the parietal bones and the frontal bone. This opening is typically closed by the age of two. In response to rapid brain development, the frontal bone becomes more arched in shape until the third year of life, after which, a deceleration in growth occurs and the bone begins to slowly flatten throughout ontogeny. The frontal air sinuses, which begin their formation as mucosal evaginations during fetal life, pneumatize with the frontal bone during postnatal growth (Lang 1989; Scheuer and Black 2000). However, the age at which this occurs has been shown to differ between males and females, with females portraying a visible sinus around four years of age and three years of age in males. The sinus continues growth throughout postnatal ontogeny, increasing in size with the frontal bone (Lang 1989). Bone deposition at the sphenofrontal suture also plays a major role in shaping the frontal bone during postnatal life (Enlow and Hans 1996). As the brain enlarges, the frontal bone is pushed outward. Deposition of bone at the sphenofrontal suture occurs as a response to brain growth as well as deposition on the ectocranial and endocranial sides of the frontal bone, increasing its overall thickness. In response to these changes, the midface is pushed in a forward and downward direction.

The Medial Orbital Region

The orbital region is made up of six bones. Three are unpaired: the frontal, sphenoid, and ethmoid; three are paired: the zygomatic, maxilla, and lacrimal (Dixon et al. 1997; Scheuer and Black 2000; Sperber et al. 2001). Generally, studies have long established that throughout postnatal growth the orbital region expands continuously through drift and displacement (Enlow

1968; Enlow and Hans 1996). Drift occurs when new bone tissue is added to one side of a bony surface (deposition) and taken away from the opposite side (resorption). Displacement occurs when deposition of new bone occurs on one side of an element but does not resorb on the other. Most postnatal expansion of the orbit occurs near its lower and outer rims and is seen as an inferior and lateral movement along with the maxilla. The sphenoid and parts of the zygomatic bone comprise the lateral margins of the eye orbit, which shows little growth throughout childhood (Waitzman et al. 1992), but experiences deposition on its lateral surface and resorption on its medial surface. This acts to widen the orbital region throughout postnatal ontogeny. Of the six bones comprising the bony orbit, the lacrimal bone, which is located at the anterior edge of the medial wall of the orbits, is most noteworthy due to its interaction with the frontal, ethmoid, maxillary, and sphenoid bones (Scheuer and Black 2000). Little is known about the postnatal growth of the lacrimal bone. It has been described as having two periods of growth, from seven months to three years and then again between 12 and 14 years of life. These two stages of growth are coincidental with the eruption of the deciduous dentition and the second permanent molars (Scheuer and Black 2000). Dixon et al. (1997) described the medial wall of the orbit as undergoing two major growth spurts during postnatal ontogeny, one during the first year of life followed by another growth spurt between six and eight years of age; note that the latter timing contrasts with studies cited above for growth of the lacrimal bone. The orbital floor remodels through deposition of bone on the superior surface and resorption on the inferior surface, which changes the position of the orbit relative to the nasal region throughout ontogeny. Thus, though the nasal and orbital floors are in close proximity early in ontogeny, this changes as the nasal floor is displaced downward throughout primary growth (Enlow and Hans 1996).

The Exterior Nasal Region

The nasal region is made up of the ethmoid, sphenoid, nasal, nasal conchae, maxilla, palatine, and vomer bones (Scheuer and Black 2000; Sperber et al. 2001). A great deal of shape change in the midface throughout postnatal ontogeny is due to the growth mechanisms occurring in the nasal region (Enlow 1968; Enlow and Bang 1965). For instance, the midface becomes taller and wider throughout postnatal life in response to two growth processes occurring in the nasal region. Resorption of the floor of the nasal cavity along with sutural growth occurring at the pterygopalatine, frontomaxillary, zygomaxillary, and zygotemporal sutures, act to increase the height of the midface. At the same time, lateral drift of the outer walls of the nasal cavity and resorption of the inner nasal surfaces contribute to an increase in midfacial width.

The nasal bones reflect this general ontogenetic trend in overall midface shape change. The nasal bones form the bridge of the nose and articulate with the ethmoid, the frontal bone, and the frontal processes of the maxillae (Enlow 1990; Enlow and Hans 1996; Scheuer and Black 2000). At birth, the length of the nasal bones is about twice their breadth (when taken across the lower inferior border of the bones). After the first year of life, these bones begin to increase in length at their inferior border, becoming approximately three times longer superioinferiorly than the inferior transverse breadth. The nasal bones show depository growth along their external surfaces, and are resorptive along their endosteal surfaces (Enlow 1990; Enlow and Hans 1996). This results in an anterior, lateral, and superior drift of the nasal region. The superior drift maintains the spatial position of the nasal region, while the lateral drift acts to slowly increase the width of the nasal bridge. Such patterns of growth occur in all of the bones forming the margins of the nasal region

The Frontal Process of the Maxillae and the Premaxilla

The frontal process of the maxilla is located between the nasal and lacrimal bones (Enlow and Hans 1996; Scheuer and Black 2000). Its lateral borders are defined by the zygomaxillary suture. At its most superior tip, it articulates with the frontal bone. Like the nasal bones, it has a depository external surface and a resorptive endosteal surface (Enlow and Bang 1965). As remodeling occurs, the frontal processes of the maxillae experience an anterior, lateral, and superior drift. The superior drift maintains the spatial position of the superior nasal region while the anterior and lateral drift lengthens and broadens the nasal cavity.

The premaxilla (also referred to as the incisive bone) is located posterior to the nasal opening and contains the incisor teeth (Enlow 1968; Enlow and Bang 1965; Scheuer and Black 2000). It possesses resorptive remodeling along its labial surface and depository remodeling along its lingual periosteal surface. The principle direction of deposition is inferior. This results in a downward drift of the premaxilla throughout postnatal ontogeny. The nasal spine is resorptive on its superior surface and depository along its inferior surface. This deposition results in an anterior drift of the nasal spine.

Summary of Growth in the Frontonasal Module

The frontonasal module undergoes significant shape change throughout postnatal ontogeny. Through a combination of various growth processes, the frontonasal module experiences an overall increase in width and height throughout ontogeny. An increase in the overall width of the frontonasal module can be contributed to lateral drift occurring at the lateral rims of the eye orbits and the nasal walls as well as a lateral drift of the frontal processes. An increase in the interorbital width, due to bone deposition occurring at the sphenofrontal suture

combined with growth of the medial orbital walls, also contribute to an overall increase in facial width. An increase in the height of the frontonasal module occurs due to the premaxilla drifting inferiorly, resorption occurring on the nasal floor, and sutural growth at the sphenofrontal suture pushing the entire midface downward. A visual representation of the frontonasal region, as defined in this research, is depicted in Figure 2.3. A description of the landmarks used to define the frontonasal module is provided in Chapter 4.

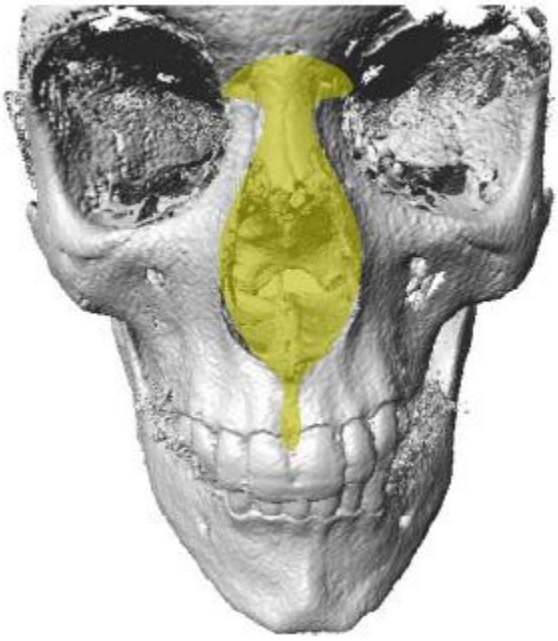

Figure 2.3. The region of the craniofacial complex captured in the frontonasal module.
The shaded area depicts the region of the face that is captured in the frontonasal module.

The Left and Right Maxillary Modules

Unlike the frontonasal module, the maxillary bones are comprised of only two definitive bones: the maxilla and zygomatic bones. While they are a bony bridge between the orbits, nasal cavity, and oral cavity, and thus articulate with a number of cranial bones, much of their later growth is influenced by the upper dentition and forces associated with mastication (Lieberman et al. 2004; Pearson and Lieberman 2004; Pinhasi et al. 2008; Sardi et al. 2006). Some variation in the growth and shape of the maxilla is due to dental variation in the alveolar bone. While this is informative, such variation arising from the alveolus may only be locally important for differences in patterns of craniofacial growth, and not indicative of the global patterns of midface development that are the concern of this study. The landmarks chosen to represent the shape of the maxilla (see Chapter 4), therefore, do not include the bone surrounding the upper dentition.

Developmentally, the left and right maxillary prominences are derived from the first pharyngeal arch neural crest mesenchyme (Scheuer and Black 2000). Their adult components include the cheeks and the lateral upper lip. The left and right maxillae join with each other at the midline of the hard palate and articulate with the zygomatics, frontal, nasals, lacrimals, inferior conchae, ethmoid, and palatine bones. Due to the articulation with the zygomatic bone, a portion of the zygomatic (up to the zygotemporale suture) is included in the left and right maxillary modules. The maxilla experiences rapid postnatal growth due to its interaction with a number of bones and spaces in the face. For instance, as described in the previous subsection, increases in the size of the eyes and nose directly influence the growth process of the maxillae. The need to accommodate an increasing number and size of teeth during ontogeny further drive an anterior, inferior, and lateral expansion of the maxilla . The zygomatic bone also rapidly increases in height and width, keeping pace with the fast growth of the maxilla. This interaction of growth

between the two bones shifts the infraorbital zygomaticomaxillary suture in a medial to lateral direction.

This growth is driven by incongruent bone removal and additions that occur both through modeling and remodeling. For example, the zygomatic process of the maxilla possesses both depository and resorptive remodeling (Enlow 1968; Enlow and Bang 1965). The infraorbital plate is resorptive along the anterior surface and depository along its posterior surface. The temporal fossa plate is depository along its posterior surface and resorptive along its anterior surface. Elongation of the zygomatic arch primarily occurs at the temporozygomatic suture. Throughout postnatal ontogeny the zygomatic process drifts posteriorly and slightly inferiorly, increasing the vertical dimensions of the entire process. A visual representation of the left and right maxillary modules, as defined in this research, is depicted in Figures 2.4 and 2.5.

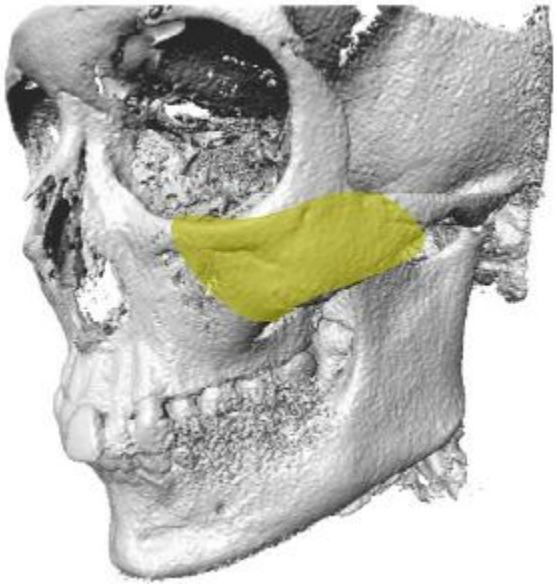

Figure 2.4. The region of the craniofacial complex captured in the left maxillary module.
The shaded area depicts the region of the face that is captured in the left maxillary module.

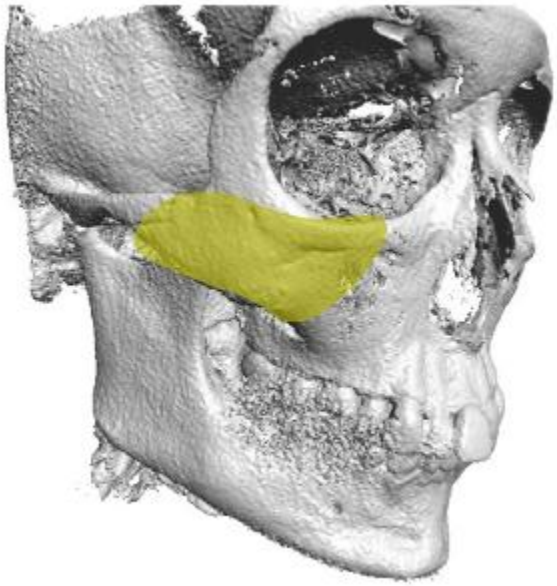

Figure 2.5. The region of the craniofacial complex captured in the right maxillary module.
The shaded area depicts the region of the face that is captured in the right maxillary module.

The Sphenoid Module

The sphenoid articulates with the ethmoid, frontal, zygomatics, partietals, squamous and petrous temporal, vomer, and occipital bones (Enlow and Hans 1996; Scheuer and Black 2000). As discussed in the previous section, it is typically composed of three parts at birth, and is fused into a single structure during the first year of life. Given its unique position, adjoining the orbits, the endocranial space, and the posterior nasal and oral cavities, the development of the sphenoid is potentially subject to influence from multiple factors (brain growth, as well as orbital, nasal, oral and pharyngeal growth). Yet, little research exists on the growth or ontogenetic integration of the sphenoid bone with the craniofacial complex. Much of the previous research on the postnatal growth of the sphenoid was conducted using radiographs, limiting the ability for any type of three-dimensional analyses (Acheson and Archer 1959; Chilton et al. 1983; Latham 1972; Scheuer and Black 2000; Underwood et al. 1976). These studies have shown that, unlike

most sutures of the face, the sphenoethmoidal suture experiences little growth after ten years of age. In addition, postnatal growth of the sella turcica ceases around seven years of age, while bone resorption of the hypophyseal fossa, during the first ten years of life, results in an upward and backward movement of the dorsum sellae. How any of these morphological patterns of growth reflect the unique position of the sphenoid relative to the bones of the three cranial regions remains unresolved. A description of the landmarks used to define the sphenoid module is provided in Chapter 4 along with figures depicting landmark placement.

The Ethmoid Module

Unlike the sphenoid, the growth of the ethmoid has been more readily observable and thus is better understood. The ethmoid is essentially part of the nasal cavity and the orbits, as well as forming the center of the anterior cranial fossa (Enlow and Hans 1996; Scheuer and Black 2000). It articulates with the frontal bone, the sphenoid, the vomer, maxillae, lacrimal and nasal bones. During the first year of life, the cribriform and upper portion of the perpendicular plate begins to ossify, which follow the ossification of the crista galli, which begins between the fourth through eighth postnatal months. The growth of the cribriform plate is complete by the age of two to three, at which time it fuses with the labyrinths (Scheuer and Black 2000). The lower perpendicular plate experiences a slow ossification with the vomer. It is not until between 20-30 years of age that the ethmoid and vomer fully fuse. Throughout postnatal ontogeny, the ethmoid experiences a downward and forward drift due to displacement (Enlow 1968; Enlow and Bang 1965), matching the general pattern of growth outlined for the orbital and nasal cavities. A description of the landmarks used to define the ethmoid module is provided in Chapter 4, along with figures depicting landmark placement.

Summary of Growth in the Maxillary, Sphenoid, and Ethmoid Modules

Similar to the frontonasal module, the maxillary, sphenoid, and ethmoid modules all contribute to an overall increase in the width and height of the face throughout postnatal ontogeny. The maxillary modules play a significant role in the lateral expansion of the face, with the zygomatic bones experiencing a posterior drift due to growth occurring at the zygomaticomaxillary suture. While the maxillary modules are contributing to an increase in the width of the face, the sphenoid and ethmoid push the face in an anterior and downward direction in response to the forward drift of the ethmoid and the anterior-posterior growth of the sphenoid. As previously mentioned, although growth processes of the ethmoid and sphenoid are known through radiographic studies, little research exist on the ontogenetic integration of these two bones with the craniofacial complex.

Synopsis of Global Craniofacial Growth

The postnatal growth of each independent region of the face as discussed above results in a gradual size and shape modification of the entire craniofacial complex (Enlow 1968; Enlow and Hans 1996; Ranly 1988) (Figure 2.6). As stated above, the postnatal ontogeny of the face is typically described as a "forward and downward" movement (Lieberman 2011; Scheuer and Black 2000). This movement is a product of the surface remodeling processes that each facial bone experiences throughout growth, as summarized in the preceding section. In addition, this "forward and downward" movement for the entire craniofacial skeleton is best discussed by examining changes in the height, length, and width of the face.

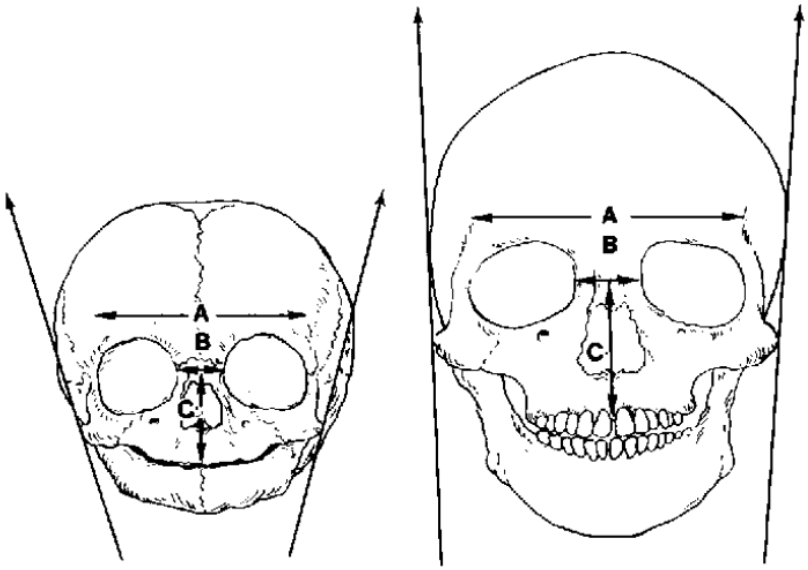

Figure 2.6. Changes in the size and shape of the craniofacial complex from newborn to adulthood (adapted from Ranly 1988).

Changes in the shape of the craniofacial complex throughout postnatal ontogeny can be seen as increases in width (A & B) and height (C).

Facial Mediolateral Width

Increases in facial width throughout postnatal ontogeny are a result of displacement and drift (Edwards et al. 2007; Enlow and Bang 1965; Enlow and Hans 1996; Ranly 1988). As noted above, the ethmoid completes fusion around the age of three. Due to the orbits' interaction with the ethmoid, interorbital breadth reaches its adult dimensions at or around this same time (Maddux 2011; Ranly 1988). Still, the orbits continue to grow in a lateral direction, which in turn drives the zygomatic and superior portions of the maxillary bones to broaden laterally. The midpalatal suture also contributes to an increase in facial width. While most sutures of the face fuse early in postnatal life, the midpalatal suture remains unfused until the adolescent growth period to permit increased space in the oral cavity for adult dentition (Bjork and Skieller 1976; Ranly 1988). This shifts the lateral extent of the inferior portions of the maxilla, increasing overall facial width.

Facial Anteroposterior Length

Increases in facial length are a result of growth primarily occurring along the zygomaticotemporal suture (Edwards et al. 2007; Enlow and Bang 1965; Enlow and Hans 1996; Ranly 1988). As the maxilla is being displaced anteriorly (in concert with the eruption of the permanent molars) the anterior-posterior dimensions of the maxilla increase in response to depositional growth. Thus, the midface is displaced anteriorly and surface deposition occurs posteriorly (Enlow and Hans 1996; Ranly 1988). Another notable component that contributes to an increased facial length is the relative position of the zygomatic bones. As the maxilla is displaced anteriorly, the zygomatic bones are prevented from moving proportionally anterior with the maxilla and nasal region of the midface, presumably due to anatomical constraints (primarily related to the muscles of mastication) (Enlow and Hunter 1966). In other words, the zygomatic process experiences a posterior drift while the maxilla and nasal complex is displaced anteriorly (Figure 2.7).

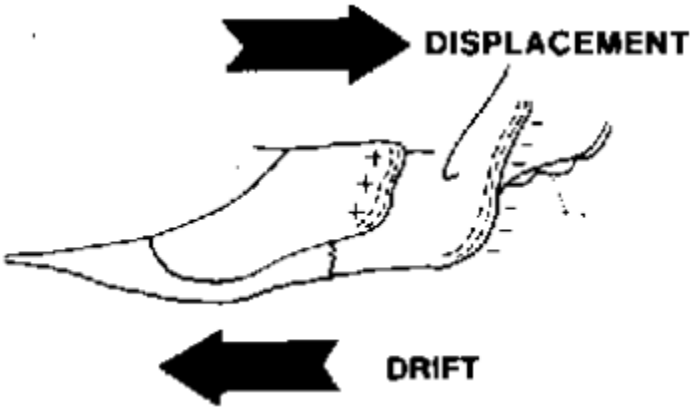

Figure 2.7. Depiction of displacement and drift of the zygomatic process that prevents its anterior movement with the maxilla and nasal complex (adapted from Ranly 1988).

Facial Superoinferior Height

An increase in facial height is the most significant dimensional change of postnatal ontogeny (Bastir and Rosas 2004; Dixon et al. 1997; Edwards et al. 2007; Maddux 2011; Ranly 1988). Increased dimensions in height of the face can primarily be contributed to an enlargement of the alveolar process and the nasal cavity. The floor of the nasal cavity is displaced inferiorly due to resorption of the nasal floor and deposition of the roof of the mouth (Dixon et al. 1997; Enlow 1968; Enlow and Hans 1996; Ranly 1988). As described above, the nasal bones experience a continuous lengthening throughout postnatal ontogeny, eventually becoming three times longer superioinferiorly than transversely. Increases in the length of the nasal bones along with sutural growth at the sphenofrontal suture push the nasomaxillary region in a downward direction. The inferior movement of the nasomaxillary region is also influenced by the movement of the orbital floor and nasal floor. The anterior drift of the orbital floor occurs at a slow rate while the frontal processes of the maxillae and the nasal bones undergo a more rapid anterior drift, moving the orbital floor and floor of the nasal aperture away from each other, resulting in an increase in facial height. Furthermore, the frontal processes of the maxillae experience an anterior drift that influences the superior movement of the infraorbital region, also contributing to an increase in facial height. In a longitudinal study of facial growth, Björk (1966) noted a slight increase in facial height during the pre-pubertal years (1-11.5 year). Beginning around 12 years of age, vertical dimensions of the face were shown to steadily increase (approximately 1.5 mm annually), ceasing around age 14. Interestingly, Björk (1966) found that completion of growth in facial height occurred 1.5 years earlier in females than males. As previously noted, increases in the height of the nasal bones during ontogeny also contribute to the increase in facial height.

Craniofacial Integration

It is evident that growth and development of the skull is very complex. Viewing cranial development in its entirety can be challenging, and for this reason, most researchers approach cranial growth through an evaluation of its parts as separate components. This allows researchers to capture the developmental independence of different regions of the face *and* the developmental interactions between these regions. Craniofacial growth, then, is best explained in the context of integration and modularity. While most researchers recognize the patterns indicative of craniofacial modularity, there are different theories for the specific processes that drive integration in the cranium throughout growth. Before discussing these theories, clear definitions of integration and modularity, as they relate to the purpose of this project, are necessary.

Modularity and Integration

The concepts of modularity and integration are complementary and it is difficult to discuss one without considering the other. While a complete review of the literature on these concepts is beyond the scope of this dissertation, a brief consideration of the current literature is necessary for the models set forth for examination. Various definitions and explanations have been proposed for modularity and integration, and these are often dependent upon the type of study being imposed (i.e., developmental, evolutionary, functional, or genetic); most researchers define traits within modules as being integrated due to functional or developmental processes, and cite coevolution through conditional selection as the process limiting the independence of those traits (Lande 1979; Rolian 2014). While integration and modularity are often viewed as complementary processes, some noteworthy theoretical differences exist between them.

Modularity is defined as the developmental and/or functional autonomy of groups of traits that form units. These units are modules, which are developmentally and evolutionarily integrated internally and are independent from other such units. While a number of definitions have been proposed (Klingenberg 2008; Mitteroecker and Bookstein 2008; Raff 1996; Wagner 1996), modularity is most simply a constrained area of integration. All organisms possess multiple levels of modularity. For instance, the genotype is defined by various modules including gene regulatory modules and *cis*-regulatory modules (Bolker 2000; Klingenberg 2008). The phenotype is also defined by various modules including skeletal modules, tissue modules, and organ modules (Gilbert 2006; Schlosser and Wagner 2004). For the current research, a module is best defined according to Bolker's (2000) three requisites:

(1) A module is a biological entity (a structure, a process, or a pathway) characterized by more internal than external integration.
(2) Modules are biological individuals that can be delineated from their surroundings or context, and whose behavior or function reflects the integration of their parts, not simply the arithmetical sum.
(3) A module can be delineated from other entities with which it interacts in some way (Bolker 2000: 773).

The human skull is typically defined as having two major modules, the neurocranium (which is often subdivided into the dermatocranium and chondrocranium) and the viscerocranium (Enlow and Hans 1996; Lieberman 2011; Lieberman et al. 2002). However, the viscerocranium (the

face) is usually further broken down into separate modules, delineated on the basis of functional or developmental integration.

As stated above, modularity is a concept that describes interdependence among developmentally or functionally related processes. It is typically studied through an evaluation of the patterns of variation and covariation among traits within modules, as well as among modules themselves, which is essentially integration (Lieberman et al. 2000; Mitteroecker and Bookstein 2008). The concept of morphological integration was first introduced by Olson and Miller (1958). At its most essential definition, it is the connectivity among parts (Ackermann 2005; Klingenberg 2008). Thus, integration provides a mathematical way to conceptualize the interdependence of morphological modules.

Like modularity, integration can be observed at various levels, but is typically described at the functional or developmental level (Cheverud 1996; Klingenberg 2008). Functional integration describes the interactions between modules that are anatomically and/or mechanically related (e.g., the mandible and basicranium are said to be functionally integrated due to their mechanical interactions during mastication). Developmental integration describes the interactions between modules that are related through processes of growth and development (e.g., the basicranium and face are said to be developmentally integrated due to their interactions during pre- and postnatal growth). The quantification of these interactions can differ depending on whether patterns of integration or processes of integration are being analyzed.

Patterns of morphological integration in the skull are often analyzed via statistical analyses of correlation and covariance matrices (Mitteroecker and Bookstein 2007; Olson and Miller 1958). These methods assess the strength of covariation among different developmental or functional modules. Strong integration among modules is indicated by high correlations among

measurements, with variation concentrated in one or a few dimensions. Weak integration among modules, therefore, is indicated when variation is equally distributed across all dimensions under study (Klingenberg 2008). The use of geometric morphometric techniques has gained increased interest in the assessment of morphological integration. Through the use of principal component analysis, the integration of various modules is assessed through an evaluation of three-dimensional landmarks and their correlated shifts in space. Using this approach, many studies have assessed patterns of correlation and covariation in the skull of human and non-human primates (Ackermann 2005; Cheverud 1982; Cheverud 1988; Cheverud 1995; Cheverud 1996; Marroig and Cheverud 2001; see also Chapter 3).

Theories of Craniofacial Integration

When assessing the *processes* of integration, there are two different frameworks under which integration of the craniofacial complex is viewed. Both frameworks are concerned with describing *how* modules become integrated. The functional matrix hypothesis (FMH) views cranial modules as independent matrices (Moss and Young 1960). The part-counterpart system (Enlow 1990) views cranial modules as interdependent units (Enlow 1990). Depending on the research questions being asked, each viewpoint offers a useful approach for the study of integration.

The functional matrix hypothesis (FMH) (Moss 1968; Moss and Young 1960) approaches craniofacial integration through an evaluation of functional matrices, defined by Moss as "genetically determined and functionally maintained" (Moss 1968:69). According to the FMH the skull is comprised of two components. The first component includes all soft tissues, muscles, tendons, organs, and spaces, which are referred to as functional matrices (FM). The second component refers to the skeletal capsules that surround the various FMs. The hypothesis

poses that interactions with the functional matrices determine the size and shape of the skeletal capsule. Under the FMH, therefore, craniofacial growth and development is completely dependent upon soft tissue growth. The FMH states that each cranial component (as comprised by the FM and its capsular unit) is an independent unit, but each indirectly interacts with other components (Moss 1968; Moss 1997). While the FMH provides a useful framework for the evaluation of cranial integration, there are some criticisms.

Parts of the FMH have been shown to have validity, but this mostly applies to the integration of the brain and neurocranium. For instance, a number of clinical studies have shown that the overall size and shape of the neurocranium is dependent upon the growth of the brain (Mooney and Siegel 2002; Moss and Young 1960). Yet, due to the very complex nature of the face, the FMH does not always hold true for craniofacial integration (Lieberman 2011; McCarthy 2004). For instance, many studies have indicated interactions between independent functional matrices of the face, showing that bones do not always interact with only one functional matrix (Cheverud 1982; McCarthy and Lieberman 2001; Ravosa and Shea 1994). Moreover, research has also indicated that capsular matrices are also influenced by interactions with other skeletal matrices and cartilage. This means that parts of the human skull are not always responsive to the FM to which each belongs. Research has shown that the nasal cartilage, for example, has a significant influence on the growth and development of the nasal bones and maxilla to the exclusion of soft tissues (Moss and Bromberg 1968; Moss and Salentijn 1969).

The other framework in which craniofacial integration is viewed is Enlow's (1990) part-counterpart principle. Researchers that view the skull as highly integrated, making independent modules non-existent, favor Enlow's framework (McCarthy 2004). The part-counterpart principle argues that growth of each part of the skull is dependent upon the growth of its

structural counterparts. Enlow viewed the skull as having an imaginary line of separation, referred to as the posterior maxillary plane (PM plane) (Figure 2.8). This line separates the anterior compartment of the skull (which includes the frontal lobes, the anterior cranial fossa, the nasomaxillary complex, and the mandibular corpus) from the posterior compartment (which includes the temporal lobe, middle cranial fossa, the naso-pharynx, and the mandibular ramus). Enlow argued that parts within each compartment were highly integrated, but the two compartments were independent from each other.

Few studies have evaluated the validity of Enlow's part-counterpart principle. In 2006, Bastir and Rosas investigated patterns of covariation between the face and the basicranium (Bastir et al. 2006). They found that the midline cranial base did not correlate with facial patterns of covariation. However, they did report that the lateral basicranium is significantly correlated with facial variation. Their paper concluded that midsagittal and lateral compartments exists, but not anterior and posterior compartments as Enlow argued. A similar conclusion was made by McCarthy (2004) in a study on patterns of constraint among primate species. McCarthy found a correlation in the widths (not lengths) of the parts and counterparts. The widths of the bony regions comprising the anterior compartments were isometrically scaled with their adjacent counterparts (McCarthy 2004), indicating some support for Enlow's principle.

Craniofacial integration is a complex phenomenon, and there is no unified view of how to assess the patterns and processes of integration throughout ontogeny. Therefore, the methods used to analyze integration will often depend upon the research questions being asked. Since the first paper concerning morphological integration was published in 1958 by Olson and Miller, there have been a number of papers investigating the ontogenetic patterns of integration in non-human primates, hominids, and humans. Chapter 3 reviews these studies in light of the current

research and discusses what is currently known about the postnatal ontogenetic patterns of the craniofacial complex in modern humans, particularly those that contribute to sexual dimorphism.

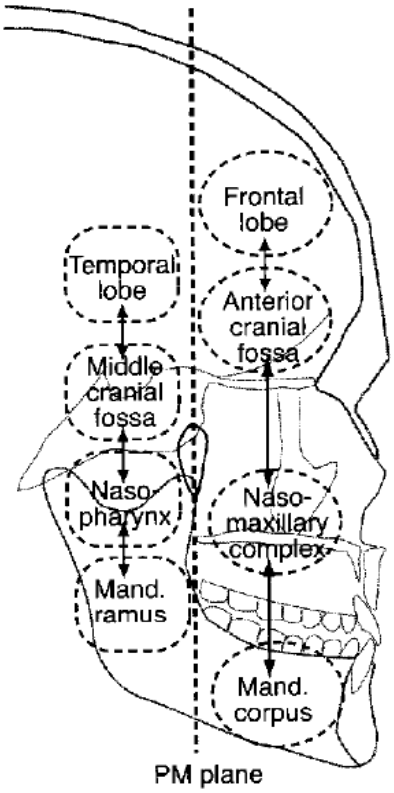

Figure 2.8. Depiction of Enlow's part-counterpart principle (adapted from Lieberman 2011).

CHAPTER 3

POSTNATAL ONTOGENY OF THE FACE

Understanding the processes that shape craniofacial variation has been a major focus within the field of biological anthropology (Kimmerle et al. 2008; Lieberman et al. 2002; Relethford 1994; Sardi and Rozzi 2012; Vioarsdottir 1999; Vioarsdottir et al. 2002). As noted in Chapter 2, the face continues growth through adolescence, unlike the rest of the cranium (Lieberman 2011). Researchers have hypothesized that the long postnatal period of continued growth contributes to the high amount of variation observed in adult facial variation (Ackerman and Krovitz 2002; Sardi and Rozzi 2005; Sardi and Rozzi 2012; Vioarsdottir 1999; Vioarsdottir and Cobb 2004; Vioarsdottir et al. 2002). Because this dissertation is focused on directly examining facial growth patterns and how these contribute to craniofacial variation, a background in the ontogenetic basis of craniofacial variation is necessary. This chapter reviews the current literature on the ontogeny of craniofacial variation, particularly sexually dimorphic variation, and provides an overview of the current hypotheses of the influence of postnatal ontogeny on craniofacial variation.

Postnatal Growth

Generally speaking, growth in the human skeleton is positively correlated with age. While there are variations in growth rate throughout postnatal ontogeny, research indicates that a generally constant rate of growth occurs after the second to third year, with periods of increased growth rate occurring between six to eight years of age and again during the adolescent growth

spurt (Bogin 1999; Bogin 2003; Cameron 2002). This general pattern of growth has been shown to differ between males and females, with distinctions in the timing and magnitude of the adolescent growth spurt between males and females (Bogin 1999; Cameron 2002) (Figure 3.1). Among human groups, males commonly enter the adolescent growth spurt approximately two years later than females, but experience a greater magnitude of height gain during that period of time (Bogin 1999). Thus, when viewing the overall height of adult males and females, males, on average, show increased height. Other changes occur in the skeleton that also reflect sexual differences in growth, including wider hips in females and larger crania in males. Among these skeletal changes, the timing for the appearance of sexually dimorphic traits in the cranium and whether or not these are accentuated through the adolescent growth spurt is still debated (Bogin 1999; Bulygina et al. 2006; Garvin and Ruff 2012; Gkantidis and Halazonetis 2011; Kimmerle et al. 2008; Rosas and Bastir 2002). Nonetheless, the two later periods of accelerated growth (between eight and nine years, and puberty) are of the greatest interest in this dissertation when assessing the establishment of proportionality and sexual dimorphism in craniofacial growth.

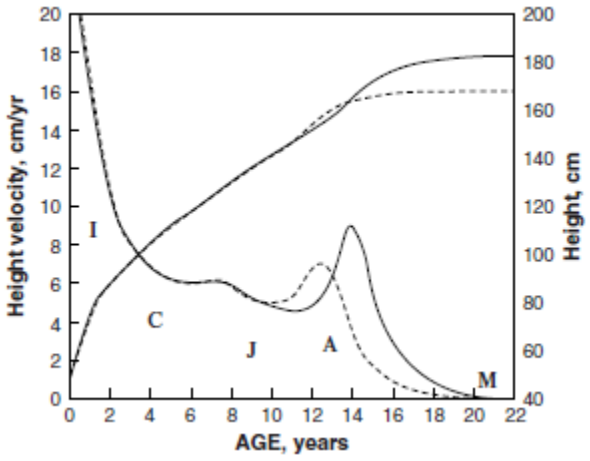

Figure 3.1. Amount and rate of growth (velocity) curves of growth in height for males (solid lines) and females (dashed lines).

The velocity curves for males and females show spurts in growth rate during late childhood and adolescence for both sexes. The stages of postnatal growth are abbreviated as follows: I, infancy; C: childhood; J: juvenile; A: adolescence; M: mature adult. (adapted from Bogin 1999).

Variation due to Sexual Dimorphism

Research into adult craniofacial variation falls into four broad categories: the genetic contribution to variation (Relethford 1998; Sherwood et al. 2008; Strauss and Hubbe 2010); variation due to adaptation and/or climatic influences (Roseman and Weaver 2007; Roseman 2004); variation due to sexual dimorphism (Garvin and Ruff 2012; Kimmerle et al. 2008; Rosas and Bastir 2002); and variation that is geographically patterned (Hubbe et al. 2009; Relethford 1994; Relethford 2004; Roseman 2004). Of these, variation due to sexual dimorphism has been extensively studied in both human and non-human primates (Bulygina et al. 2006; Ewing and Harris 2000; Gazi-Coklica et al. 1997; O'Higgins and Collard 2002; O'Higgins and Dryden 1993; Richtsmeier et al. 1993; Rosas and Bastir 2002; Ursi et al. 1992; Wood and Lynch 1996). Through this research, investigators have shown that sexual dimorphism in the adult craniofacial complex can be ascribed to differential growth patterns and timing between the sexes, despite few studies utilizing juveniles to directly investigate the ontogenies of specific regions of the cranium that produce sexually dimorphic features (Maddux 2011; Weston et al. 2007).

Many studies have found allometric differences (i.e., size-correlated shape change) in the midfacial morphology of males and females, including differences in the proportional size of the neurocranium to the face, the degree of midfacial vertical rotation, and the height of the alveolar region (Rosas and Bastir 2002). Other distinctions in the size related sex-specific shapes of males and females include differences in the height, width, and length of the midface, alveolar prognathism, and the shape of the browridges and chin (Bastir and Rosas 2004; Garvin and Ruff 2012; Rosas and Bastir 2002; Ursi et al. 1992). Overall, adult males have been shown to be 5-10% larger in the midface than females (Ursi et al. 1992). Thus, size is implicated to be a major factor in influencing sexually dimorphic differences (Rosas and Bastir 2002). Whether this is a

result of overall larger body size, effects of hormonal differences, differential growth periods, or a combination of these has not been demonstrated. Additionally, authors have had a tendency to make adaptationist claims for the emergence of this dimorphic trait without directly testing their evolutionary assumptions (Weaver et al. 2007). For example, males have longer and wider noses with larger, more flaring nostrils (Enlow and Hans 1996). The bony nasal opening is generally larger in males, as well as the naso-oropharyngeal cavity (Enlow and Hans 1996; Rosas and Bastir 2002). As observed laterally, a rotation of the lower face and a downward displacement of the nasal floor also occur as an effect of the increased nasal spaces. This pattern of morphological differences between the sexes was argued by Rosas and Bastir (2002) to signify increased demand for air intake in males. This is but one distinction between males and females, and even if the increased respiration does result in males (and reflects differences in activity levels), the evolutionary causes of these dimorphic patterns remain unexplored.

One important step in understanding the processes that shape the observed patterns of sexual dimorphism lies in understanding when the distinctions appear during growth. Some researchers have argued that sexually dimorphic features of the face do not appear until around thirteen years of age (at or around the adolescent growth spurt) at which time facial growth slows down in females but continues in males (Enlow 1990). Enlow was among the first to argue this, but it has been criticized (Bulygina et al. 2006; Ursi et al. 1992; see Enlow and Hans 1996a for a discussion) These researchers present evidence that some sexually dimorphic traits are present early in ontogeny (Bulygina et al. 2006; Ewing and Harris 2000; Ursi et al. 1992; Vioarsdottir 1999), and Bulygina and colleagues (2006) even suggest a prenatal origin for sexual dimorphism. As the majority of these studies, however, utilized traditional metric analyses, the ability to partition size from shape was limited. Therefore, there is still some uncertainty of *when*

sexually dimorphic traits that do not result from size differences alone appear during ontogeny(Jungers et al. 1995).

Regardless of the age when differences first appear, studies have implicated a combination of differential growth patterns and the age at which growth ceases as establishing sexual dimorphism in the face (Bulygina et al. 2006; Ewing and Harris 2000; Ursi et al. 1992; Vioarsdottir 1999). Ewing and Harris (2000) reported evidence for growth differences between males and females through an increase in dimorphism of facial dimensions from age six to seventeen. In a longitudinal study of 61 individuals, Gazi-Coklica et al. (1997) found similar results, reporting that craniofacial measurements of sexual dimorphism increased during the transition from deciduous to permanent dentition (4.7-7.5 years). Similar results have been found by a number of researchers (Bulygina et al. 2006; Cortella et al. 1997; Weston et al. 2007). Differences in growth rates also have been shown to occur after the onset of puberty – the timing of which itself is sexually dimorphic (see above) – with males maintaining a relatively accelerated rate (Bulygina et al. 2006; Enlow and Hans 1996; Ursi et al. 1992; Weston et al. 2007). A more notable result of these studies, as it directly relates to this dissertation, is that growth of the midface stopped between one and a half and two years earlier in females than in males (Maddux 2011). Males portray an extended period of growth and development, beyond what is documented in females, presumably in association with skeletal maturity associated with reproduction in the latter (Maddux 2011; Martin et al. 1994; Plavcan et al. 1995; Plavcan and Cope 2001).

Though this research argues for differential growth patterns between males and females as the source of definitive anatomical differences in the craniofacial skeleton; little research has documented the ontogenetic causes that lead to sexual dimorphism in the adult human facial

complex (Weston et al. 2007). The majority of the previously discussed studies utilized adult skeletons to make inferences about the development of sexually dimorphic traits (Hennessy and Stringer 2002; Rosas and Bastir 2002). Others utilized lateral radiographs, limiting analyses to landmarks located only in the midsagittal plane (Bulygina et al. 2006; Ursi et al. 1992). In order to better evaluate how growth of the face contributes to sexual dimorphism and to determine *when* sexually dimorphic features of the face appear during ontogeny, a sample that is comprised of juveniles of known age and sex should be utilized instead of the approaches taken in these papers. Even when juvenile skeletons are used in studies like those by Vioarsdottir (2009) or Krovitz (2000), they have relied on archaeological human remains, and so were subject to aging biases. Moreover, methods that capture the interactions of facial regions throughout ontogeny would provide a clearer picture of *how* postnatal growth contributes to establishing sexual differences and reveal which regions of the face experience the most change after puberty. This dissertation seeks to do this. As stated in the Introduction, this is the first study to use clinical data to assess the ontogenetic differences of facial growth between males and females, allowing for endocranial analyses and a more precise assessment of sex-specific variation across ages.

Variation due to Ancestry

Variation that is geographically patterned has also been a major topic of study in biological anthropology (Howells 1973; Hubbe et al. 2009; Relethford 1994; Relethford 2004; Roseman 2004). Cranial shape is geographically structured (Relethford 1994; Relethford 2004) and shows limited phenotypic plasticity (Sparks and Jantz 2002). An important emerging perspective from this body of research is that craniofacial differences among human populations have largely been shaped through neutral evolutionary processes (Ackermann and Cheverud

2004; Roseman and Weaver 2007), though regional selection pressures shaped some geographical variation in adult crania (Roseman 2004).

While a great deal of research has been conducted that documents the geographical patterning of craniofacial variation, very little of this research focuses on the ontogenetic basis of the geographical variation. In fact, only two published studies have attempted to directly assess the developmental origins of inter-population differences (Sardi and Ramirez 2012; Vioarsdottir et al. 2002). Both studies used geometric morphometric analyses postmortem and juvenile crania without known associated sex or age data.

Sardi and Ramirez (2012) analyzed craniofacial changes throughout ontogeny in western Europeans and southern Africans. Thirty-three three-dimensional landmarks located on the face and cranial vault were recorded from the two populations. Age, for both populations, was estimated using dental maturation, encompassing an age range of birth to 39 years. Generalized Procrustes analysis, principal component analysis, and transformation grids were used to examine differences between populations. An analysis of covariance (ANCOVA) was utilized to test for differences in growth trajectories (within population regression lines of size against age) between populations. These techniques were applied separately to the neurocranium and the face. Based upon the results of the ANCOVAs, the authors concluded that differences in adult morphology between the two populations arise from both pre- and postnatal processes. Differences throughout ontogeny in nasal shape and midfacial shape were the most notable; however, these differences were only based on principle component loadings (in other words, no statistical analysis was conducted to assess statistical significance of these shape differences). The authors did not note which of the landmarks could be contributing to the shape disparities and/or the specific anatomical changes that take place in the face to yield the two group growth

patterns observed in postnatal ontogeny. Furthermore, they assess shape variation of the face as one unit and do not evaluate how the various developmental regions of the face interact with each other throughout postnatal ontogeny.

The other study that assessed inter-population variation using juvenile skeletal remains was published in 2002 by Vioarsdottir and colleagues. They utilized crania from ten geographically distinct human populations (N=334) to investigate the timing of the appearance of population-distinct features found among adults. They also examined how differences in growth trajectories contributed to populational facial shapes. Twenty-six landmarks were recorded for each individual and analyzed using generalized Procrustes analysis (GPA) and principal component analysis (PCA). The authors concluded that facial shape differences existed across all ages. Even the youngest individuals in their study (those in the first year of life) portrayed population-specific morphologies. Moreover, their study indicated that differences in facial morphology, for some populations, were due to differences in growth trajectories throughout postnatal life. The authors concluded that population-specific morphologies are present early in postnatal life, possibly even present during prenatal ontogeny, and that populations exhibit different growth trajectories during ontogeny.

Even though Vioarsdottir and colleagues (2002) indicated clear differences in postnatal ontogeny between human populations, their research did not offer any information about the specific anatomical changes that take place in the face to create those differences. For example, when describing facial shape variations, Vioarsdottir et al. (2002) noted reductions in the size of skeletal traits, and increases in heights of features, but did not discuss the interactions of particular craniofacial regions throughout ontogeny that ultimately achieve the observed patterns of differences. While there is evidence supporting population-based differences in craniofacial

shape, one would assume that all humans have similar modularity and integration in the cranium, and that group differences are therefore relatively minor. Interpreting the results of Vioarsdottir et al. is complicated by the fact that the use of archaeological samples presents issues with age and sex estimations. For their study, age was estimated using dental standards (though eruption timing relative to chronological age differs between human populations), and sex cannot reliably be estimated from juvenile human remains. Therefore, it is unclear if sex-specific ontogenetic shape trajectories played a role in the results of their study. A study that investigates the ontogeny of specific, developmentally distinct regions of the face, and that uses individuals of known age and sex will provide a better understanding of the postnatal processes that contribute to facial variation.

Assessing Growth using Craniofacial Modules

Despite the lack of research on the ontogenetic factors that contribute to craniofacial variation, there has been a great deal of published research on craniofacial growth and development using juvenile skeletal samples or radiographs of living children (Buschang et al. 1983; Krieg 1987; Little et al. 2006; Sardi and Rozzi 2005; Vioarsdottir et al. 2002; Waitzman et al. 1992). Each of these studies have contributed to our understanding of the patterns of postnatal growth and development in the face. Yet surprisingly, only one of them assessed facial ontogeny through an evaluation of growth and development of specific facial regions (Sardi and Rozzi 2005).

Sardi and Rozzi (2005) assessed the growth trajectories of individual cranial modules, referred to by the authors as functional cranial components (FCCs) (Moss and Young 1960; Sardi and Rozzi 2005). Their study was based on Moss' Functional Matrix Hypothesis, and it

investigates the ontogenetic growth of the cranium through an assessment of the amount of growth attained in each FCC at different ages. The study utilized skulls housed at the Museu Antropologico of Coimbra, Portugal, and the Musée de l'Homme of Paris, France (Sardi and Rozzi 2005). Two-hundred twenty eight of the skulls were aged from birth to 20 years (again using dental methods), and 121 skulls were aged from 21-39 years and used as the adult reference. Individuals of unknown sex were between the ages of birth and five years of age; older individuals had either known sex or could have sex estimated. The neurocranium was divided into four FCCs: anteroneural, midneural, posteroneural and otic. The face was also divided into four FCCs: the optic, respiratory, masticatory, and alveolar. The length, breadth, and height of each FCC were recorded and a volumetric index (a geometric mean of the three dimensions) was calculated and used for comparing variation across ages. Using a non-parametric smoothing spline, growth trajectories of each FCC were calculated. The amount of growth for each FCC and its growth rate (calculated as a percentage) was measured at birth, 7, 14, and 20 years of age.

The authors found two distinct groups of FCCs, distinguished by similar growth trajectories within each group. Most of the FCCs were 50-60% of adult size at birth. The first group included the anteroneural, midneural, posteroneural and optic FCCs. This group portrayed a rapid growth period up to 3-5 years of age, followed by a slower rate of growth. The second group included the respiratory, masticatory, and otic FCCs. This group experienced a less rapid growth rate during this early period than the first group. The alveolar FCC portrayed a unique growth trajectory, different from all other FCCs; like overall growth trends, the alveolar FCC exhibited two separate periods of fast growth: birth to 4 years, and after 14 years of age. Early in ontogeny, at ages 7 and 14, the FCCs with the greatest growth rates were the otic, respiratory,

masticatory, and alveolar FCCs. The alveolar and masticatory FCCs showed the greatest growth rate later in ontogeny (from 14-20 years).

This study is unique. Unlike the research reviewed in the previous section, Sardi and Rozzi (2005) assessed the ontogeny of individual cranial modules, though their modules were assigned based on perceived functional groupings, and not based on developmentally separate modules. There are also some inherent issues that may be affecting the results of their study. For instance, the researchers pooled all individuals in the study, regardless of sex. Therefore, it is still unclear how the associations among cranial regions differ between males and females. Also, due to the particular methodology used in their study, it is still unclear whether particular modules proportionally grow with age (i.e., maintain an equal variance throughout ontogeny). While their research provides an excellent start to evaluating *how* and *which* modules change with age, it is still unclear how the *interactions* of the modules differ between males and females and throughout ontogeny (i.e., which landmarks play a significant role in ontogenetic shape changes).

This dissertation aims to address this latter point. As the first study to approach ontogenetic questions with the use of clinical data obtained from CT scans of human juveniles, this dissertation will assess the developmental processes that contribute to shape differences among individuals and between the sexes. It will also determine if craniofacial regions grow at proportional rates throughout ontogeny during the two growth rate increases occurring after early childhood. More importantly, this study has the potential to contribute crucial data toward resolving the ongoing debates summarized above about the importance of postnatal growth in influencing the appearance of craniofacial shape differences among humans. One important assumption made in this study is that, despite documented variation between human groups in

the ontogenetic establishment of population-specific craniofacial traits, the overall patterns of integration should be similar among all human groups, especially when compared to other taxa.

Current Hypotheses of the Influence of Postnatal Ontogeny on Craniofacial Variation

Researchers have conducted multiple studies that evaluate how postnatal changes in shape relate to interspecific differences amongst adult human and non-human primates (Ackermann and Krovitz 2002; Bastir and Rosas 2004; Bookstein et al. 2003; Cobb 2001; Leon and Zollikofer 2001; Lieberman et al. 2002; May and Sheffer 1999; Mitteroecker et al. 2004; Sardi and Ramirez 2012; Vioarsdottir and Cobb 2004). From this research, two hypotheses with mutually exclusive theoretical commitments have emerged concerning the ontogenetic origins of human craniofacial variation. The main source of disagreement between these hypotheses is how much postnatal growth contributes to adult morphological variation. The first argues that modules of the face grow proportionally during primary growth, meaning that shape differences are present prenatally (Ackermann and Krovitz 2002; Leon and Zollikofer 2001; Lieberman et al. 2002; Mitteroecker et al. 2004). The other argues that portions of the facial skeleton grow at different rates and at different proportions (Bastir and Rosas 2004; Cobb 2001; Sardi and Ramirez 2012; Vioarsdottir and Cobb 2004; Vioarsdottir et al. 2002).

Ackerman and Krovitz (2002) used Euclidean distance matrix analysis (EDMA) (Richtsmeier and Lele 1993) to assess facial ontogeny in fossil and extant hominins, including *Australopithecus africanus* (1 adult and 1 juvenile), modern humans (141 adults and 21 juveniles), chimpanzees (65 adults and 13 juveniles), bonobos (23 adults and 27 juveniles), and gorillas (15 adults and 11 juveniles). Eight unilateral and midline three-dimensional facial

landmarks were recorded, creating 36 Euclidean distances, analyzed with EDMA and used to compare growth patterns among species. The authors concluded that morphological differences between species are the result of early ontogenetic processes. These differences are further accentuated throughout postnatal ontogeny through parallel ontogenetic trajectories. The only exception to this was the variation observed in *G. gorilla*, where postnatal trajectories differ throughout ontogeny.

Another study came to similar conclusions about shape changes in Neandertals and modern humans (Leon and Zollikofer 2001). The sample under investigation included adult and subadult Neandertals (n=16), fossil modern humans (n=3), and extant modern humans from five different geographic populations (n=22). Fifty one cranial and 22 mandibular three-dimensional landmarks were recorded on the specimens. A generalized least-squares (GLS) superimposition was applied to the data and a relative warp analysis was used to assess statistical differences in shape. The researchers determined that Neandertals and modern humans have parallel ontogenetic trajectories, and suggest a prenatal origin for the divergence of facial shapes (also note there is evidence for different patterns of cranial integration in these groups, as argued by Roseman and colleagues in 2011).

Mitteroecker et al. (2004) provided additional evidence to support the findings of the other two studies. They assessed the ontogenetic trajectories of modern humans, *P. paniscus, P. troglodytes, G. gorilla,* and *P. pygmaeus*. In this study, 96 three-dimensional landmarks and semilandmarks of the face and basicranium were collected from 268 adult and sub-adult crania. Using relative warp analysis, the authors found that shape differences exist very early in ontogeny, around birth. However, this was shown to differ between humans and great apes. Differences in shape between modern humans and other great apes appear very early in ontogeny

while differences separating non-human great apes among themselves appear later in ontogeny. This study, like the other two discussed (Ackermann and Krovitz 2002; Leon and Zollikofer 2001), suggests a prenatal origin for morphological shape differences between species. These three studies, along with Lieberman et al. 2002, argue for a prenatal origin of craniofacial variation that is further elaborated through parallel postnatal ontogenetic trajectories. While no attempt has been made to assess the growth trajectories of individual craniofacial modules, if this collective hypothesis is true, modules of the face should proportionally grow throughout ontogeny.

Contrary to the three previously discussed studies, other research has concluded that divergent trajectories exist among species or within a single hominin species (Bastir and Rosas 2004; Cobb 2001; Sardi and Ramirez 2012; Vioarsdottir and Cobb 2004; Vioarsdottir et al. 2002). In a study using four species of hominins, the hypothesis of parallel postnatal ontogenies was tested. Three distinct populations of modern humans, *G. gorilla*, *P. troglodytes* and *P. paniscus* were the four species under investigation (Vioarsdottir and Cobb 2004). Eighteen unilateral three-dimensional landmarks defining the facial skeleton were collected from 349 sub-adult crania. Age was assessed on the basis of dental development. Principal component analysis (PCA) and discriminant function analysis (using Mahalanobis distances) were used to statistically assess differences in facial shape across ages. Significant differences in facial form between the three species of non-human great apes were shown to be present in early ontogeny, prior to the onset of the eruption of the permanent dentition. The same results were found for intra-population differences in the three populations of modern humans. Furthermore, the authors found that all taxa showed statistically significant differences in their ontogenetic trajectories,

indicating that the species began with different ontogenies that are further accentuated throughout postnatal life through distinct growth trajectories.

Other studies have found similar results. O'Higgins and Collard (2002) reported significant divergences in the postnatal facial shape trajectories of the papionin Old World monkeys. In 2001, Collard and O'Higgins used facial landmarks to assess the ontogenetic trajectories of macaques (*Macaca*), mangabeys (*Cercocebus* and *Lophocebus*), and baboons (*Mandrillus* and *Papio*) (Collard and O'Higgins 2001). Thirty-one three-dimensional landmarks defining the facial shape of the five species were recorded and compared across primary growth using principal component analysis (PCA) with permutation tests. The authors concluded that postnatal ontogenetic shape trajectories for the five species are not parallel. Bastir and Rosas (2004) found interspecific differences in the ontogenetic trajectories of facial height in modern humans and chimpanzees. They argue the results of their study indicate support for early determination of facial patterns. Vidarsdottir et al. (2002) and Sardi et al. (2012), as previously discussed, both revealed divergent trajectories within modern humans, arguing that population-specific morphologies are the result of distinctions already present at birth which are further modified, through varying degrees of divergent shape trajectories, throughout postnatal ontogeny. All of these studies, unlike those discussed above, reveal that differences in adult facial shape arise due to distinct ontogenetic shape trajectories.

The conflicting results that arise from the studies of facial ontogeny could be due to a number of factors (Cobb and O'Higgins 2004). First, methodological differences exist between the various studies. For instance, Ackerman and Krovitz (2002) utilized EDMA while other researchers utilized Procrustes-based methods (Collard and O'Higgins 2001; Leon and Zollikofer 2001; Vioarsdottir et al. 2002). Secondly, dissimilar areas of the cranium were used to evaluate

differences in ontogenetic shape. Some authors only assessed facial shape (Collard and O'Higgins 2001; Vioarsdottir and Cobb 2004) while others evaluated the cranium globally, utilizing landmarks that define the basicranium, vault, and face (Cobb and O'Higgins 2004). Lastly, differences in sample size may be affecting differences in results. Smaller sample sizes, often the case for studies of subadult hominids, could lead to a failure to produce significant divergences (Cobb and O'Higgins 2004).

As previously stated, most of these studies focus solely on patterns of change (i.e, whether species or populations have different postnatal ontogenetic patterns), and not in conjunction with the specific processes leading to change (i.e., documenting which dimensions of the face portray the most variation throughout ontogeny, how these relate to known developmental processes, and whether the variance in these traits leads to adult variation). A study that establishes the developmental trajectories of different modules of the face throughout ontogeny will reveal whether or how postnatal life influences craniofacial variation. Furthermore, none of the previous research investigating postnatal ontogeny assesses the developmental trajectories of separate regions of the face. Determining if individual facial units grow proportionally would contribute important information for evaluating hypotheses of postnatal ontogeny.

This dissertation, then, will address the two opposing hypotheses concerning postnatal ontogeny by documenting the specific ontogenetic patterns that lead to the variance seen in adults, through an assessment of five developmentally independent regions of the face (Lieberman et al. 2000; Lieberman 2011). As discussed in Chapter 2, these include the frontonasal module, the left and right maxillary modules, the sphenoid module, and the ethmoid module. To address the two opposing hypotheses related to the influence of postnatal ontogeny, a

model of proportionality among the five modules under investigation is proposed: once scaled to the main centroid, the distances of the centroids for each module should change equally throughout primary growth. If my results fit this model, this indicates support for the hypothesis that facial proportions are set prenatally and are further elaborated throughout postnatal life through parallel developmental processes. If my results do not fit the model, this indicates that facial proportions change throughout ontogeny, and further suggests that developmental processes and epigenetic or environmental factors occurring during postnatal ontogeny play a role in producing adult craniofacial variation.

Utilizing Morphometric Analyses to Study Growth

Based on the previously reviewed literature, it is clear that the majority of studies on craniofacial growth and development utilize geometric morphometric methods of analysis (Cobb and O'Higgins 2004; Lieberman et al. 2000; O'Higgins and Collard 2002; Sardi and Ramirez 2012; Vioarsdottir et al. 2002). This methodology allows researchers to not only assess growth of the craniofacial complex, but it also reveals changes in shape and overall spatial relationships between regions of the face. Euclidean distance matrix analysis (EDMA) and Procrustes based methods are the most commonly used methods (Rolf and Marcus 1993), though the latter is far more common.

Geometric morphometric methods are useful for studying growth and development because they allow for the statistical analysis of shape, represented visually as deformations in shape from a mean shape. These approaches also permit researchers to separate "shape" from "size," a useful tool for the assessment of changes in shape throughout ontogeny (O'Higgins and Vioarsdottir 1999). However, it should be realized that "shape" is effectively shape- and size-

data, as variations in shape are still the product of size variance. In order to capture the geometric shape of the structures under study, two- or three-dimensional coordinates (i.e., landmarks defining particular sutural intersections, maximum/minimum points of reference) are recorded. A representation of shape is then obtained by scaling, rotating, and reflecting these coordinates using a reference (e.g., Procrustes superimposition, generalized least squares, and generalized Procrustes analysis). Geometric morphometric techniques, including EDMA and generalized Procrustes analysis, will be utilized in the present study. Details of these methods and their application to the data under investigation are outlined in the next chapter, Materials and Methods.

CHAPTER 4

MATERIALS AND METHODS

This chapter provides details about the sample, data collection methods, and analytical approaches taken in this dissertation. A detailed description of the skeletal sample used in this study is discussed first, along with descriptions of the distribution of the data set according to age. This is followed by an explanation of the use of individual cross-sectional data, rather than longitudinal data, for the purpose of evaluating hypotheses about ontogenetic processes. Finally, the methods for obtaining three-dimensional data from CT scans are described, followed by an explanation of the statistical analyses used in this research.

Materials

Clinical Sample

In the past, as reviewed in Chapter 3, most research concerning juvenile craniofacial growth and development has utilized archaeological skeletal samples (Bulygina et al. 2006; Krovitz 2000; Sardi and Ramirez 2012; Vioarsdottir et al. 2002). Because juvenile crania obtained from archaeological contexts are not fused and are subject to taphonomic damage, obtaining sufficient sample sizes − even under the best circumstances − is difficult. Preservation biases, furthermore, limit the possibility of studying how endocranial growth influences developmental trajectories. In addition to these potential restrictions to sampling, both known chronological age and sex are not reliably ascertainable in archaeological contexts.

The use of clinical data offers a broader perspective of ontogeny because it allows for full analyses of the complete cranium and for more precise assessments across ages, as well as

between sexes. Therefore, this study used computed tomography (CT) scans of living individuals that are associated with demographic information (sex and age). These scans come from the Diagnostic Digital Imaging Center (DDI) in Sacramento, California. DDI is an imaging center used by local dentists, orthodontists, and craniofacial surgeons to obtain three-dimensional cone beam imaging of their patients. These scans are HIPPA-compliant and an IRB review with the University of Tennessee was completed before obtaining the scans (See Appendix A). In March of 2014, I traveled to Sacramento to access the scans, 531 of which I de-identified and downloaded. Some of these scans were excluded based on selection criteria explained below.

One limitation of these data is the lack of ancestral information available in association with each individual. DDI does not collect any self-identified ancestral information from their patients, and therefore, associated ancestral information for all individuals was not an option for this research. Some researchers have argued that the juvenile splanchnocranium is not diagnostic among individuals of different ancestry (Scheuer and Black 2000), however, many studies (especially in forensic anthropology) have argued that facial morphology shows diagnostic characteristics of ancestry early in postnatal life (Buck and Vidarsdottir 2004; Harris et al. 2001; Vidarsdottir 2003; Vioarsdottir and Cobb 2004; Vioarsdottir et al. 2002; Weinberg et al. 2002). Regardless, understanding and establishing how males and females differ in their postnatal ontogenetic trajectories of their face, regardless of ancestry, is essential before defining craniofacial traits and/or dimensions that are indicative of ancestry in juvenile remains. Also, as explained in Chapters 2 and 3, the patterns of modularity and integration in the cranium are not different among human populations, and thus any differences between populations should only affect variation within modules. For these reasons, this study seeks to contribute to the literature concerning postnatal growth of the craniofacial skeleton in relation to sexual differences alone.

However, due to a lack of geographic origins informaion for the individuals in this study, all results will be cautiously interpreted, considering that ancestry could be playing a role in the establishment of particular patterns of variation. This issue will be further discussed in Chapter 6.

Use of Cross-Sectional Data

The available CT scan data from the DDI is cross-sectional; individuals were only scanned once and not longitudinally over a course of years. Thus, growth patterns of individuals cannot be assessed. However, the average growth patterns, calculated by sex, may be assessed to make inferences about growth trends within the population. Most studies of growth using these types of data have utilized mean measurements for age groups to assess growth trends (Sardi and Rozzi 2012; Vioarsdottir et al. 2002). The limitation of this approach is that it ignores variance among individuals within the group, especially the unequal variance that likely exists between different age categories (due to different rates of growth within each group). Restricting contrasts to mean comparisons reduces the amount of information that may be gleaned from a sample. As this study is focused on assessing growth trends between sexes and not analyzing growth patterns of each individual, the use of cross sectional data is justified.

Selection Criteria and Final Sample

The individuals used in this study possess no facial anomalies. Scans were only used if they included the entire head (and not just the face) and were aged between seven and seventeen years of age. The total sample is comprised of 299 juveniles (155 females and 144 males). Individuals were assigned to age groups based upon the whole number of their age, regardless of the amount of months encompassed in their age according to their birthdates. For example, an individual was aged as “7” even if their age was seven years, 11 months, and 28 days. Sample

sizes for each of the resulting eleven age categories are listed in Table 4.1. There are a limited number of individuals at the extremes of the age range in the sample (Table 4.1). Most patients are sent to DDI by their dentist or orthodontist for CT scans before the patient receives orthodontic work, which typically occurs during early adolescence. Thus, fewer individuals are sent before age eight or after age sixteen. For this reason, groups of ages were created and used for analyses in an attempt to avoid issues of unequal sample sizes. This is discussed in further detail in the Methods section of this chapter.

Table 4.1. Age and sex of the sample used for study

Age Groups	Sex	Total N
7	Male	2
	Female	6
8	Male	5
	Female	14
9	Male	10
	Female	19
10	Male	11
	Female	16
11	Male	33
	Female	19
12	Male	21
	Female	20
13	Male	20
	Female	20
14	Male	20
	Female	20
15	Male	10
	Female	11
16	Male	9
	Female	8
17	Male	3
	Female	2

Computed Tomography Scan Data

All of the individuals whose crania are used in this study had craniofacial CT scans. These scans were acquired using three-dimensional cone beam imaging, which uses a filmless digital x-ray iCat (classic or platinum) scanner. The scanner rotates 360 degrees around each individual's head, producing images that may be presented both as two- and three-dimensional volumes. Each scan results in a DICOM image stack with .25 mm voxels, consisting of an average number of 520 slices, and capturing a 13 centimeter field of view.

Three-dimensional surface reconstructions were produced from the CT images using the morphometric software Stratovan Checkpoint, which is available for purchase at http://www.stratovan.com/index.php. Landmarks were placed on the virtual reconstructions of the scanned crania in this software. An isosurfacing tool in the Checkpoint program was used to segment the CT scans. This tool allows the user to select tissue density values that will segment the CT scan to display only bone and no soft tissue. The specific anthropometric landmarks used in this study as well as data collection techniques are described in the next section.

Methods

Landmarks

Landmark data may potentially limit analyses due to its ability to capture only a partial representation of shape; representations of complex three-dimensional shapes by linear distances among pre-determined landmarks loses much of the shape variation and are subject to pre-determined biases of the observer. That is, it is possible that important shape data are not collected because the researcher did not choose to include it or could not reliably quantify it.

Nevertheless, landmark data are used in this study because they have been used in most studies of the growth processes in the cranium (see Chapter 3), provide a clear geometric representation of form, and allow for differences in shape to be localized within the modules under investigation (Richtsmeier et al. 1992; Richtsmeier et al. 1995).

Thirty-eight landmarks that define the five developmentally independent modules of interest were recorded as coordinates in three-dimensional space. Landmarks were chosen that defined each module independently but also capture integration between modules. In addition, because of the use of CT scans, landmarks that were pertinent to the definition of modules but not obtainable on a dry skull due to their placement (i.e., between bones) may be included (such as those on the sphenoid and ethmoid). A justification for the landmarks used to define the regions of each module, as discussed in Chapter 2, follows in the sections below. Landmark definitions and abbreviations for each module are defined in Tables 4.2- 4.6, and landmark placement is shown in Figures 4.1- 4.12. The landmarks on the sphenoid and ethmoid bones were located by using the coronal, sagittal, or axial slices of the bone, which were visualized in Stratovan Checkpoint. These landmark placements can be seen in Figures 4.8- 4.12.

The Frontonasal Module

The frontonasal module is comprised of various bones and facial regions, as reviewed in Chapter 2. Therefore, a justification of the landmarks defining each of these regions is necessary. In this research, three landmarks define the frontal region and its interactions with other modules (see Table 4.2): nasion and nasale superius (left and right) (Martin 1956) (Figure 4.1). These three landmarks are located along the sphenofrontal suture. Nasion (landmark one in Figure 4.1 and Table 4.2) captures the intersection between the sphenofrontal suture and the median plane of the nasal bones. Left and right nasale superius (landmarks 4 and 5 respectively) capture the

interactions that occur between the sphenofrontal and naso-maxillary sutures, and will therefore demarcate sutural growth occurring in the frontal region.

Table 4.2. Landmarks defining the frontonasal module with definitions & abbreviations

Landmark Number	Landmark Abbreviation	Landmark Name	Definition
1	NAS	Nasion	The intersection of the frontonasal suture and the median plane
2/3	L/ R DAC	Dacryon	Point at which the lacrimal, maxilla, and frontal bones/sutures intersect
4/5	L/R NSU	Nasale Superius	Point at the intersection of the nasofrontal suture and the nasomaxillary suture
6/7	L/R SPI	Nasomaxillary Suture Pinch	Deepest point along suture where nasal bone meets maxilla
8/9	L/R NIN	Left Nasale Inferius	Lowest point where the nasal bone meets the nasal aperture
10	RHI	Rhinion	The midline point at free end of internasal suture
11/12	L/R ALA	Left Alare	Widest point on side of nasal aperture
13	NSP	Nasospinale	Most anterior point on the nasal spine
14	SSP	Subspinale	The deepest point seen in the profile below the anterior nasal spine
15	PRO	Prosthion	The most anteriorly prominent point, in the midline, on the alveolar border, above the septum, between the central incisors.

Definitions adapted from Howells (1973) and Martin (1956).

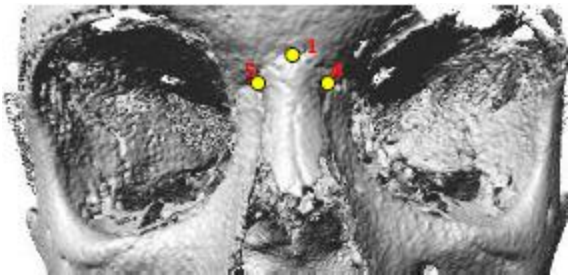

Figure 4.1 Landmarks capturing the growth and development of the frontal region.

The orbital region is defined by four landmarks: dacryon (left and right), and cheek height-superior (left and right) (Howells 1973) (Figure 4.2). Dacryon (landmarks 2 and 3) is important due to its location of intersection between three bones: the lacrimal, maxilla, and frontal bones. Cheek-height superior (landmarks 22 and 23) is located on the lower border of the orbit and will therefore capture the orbital expansion occurring at the lower lateral rim of the eye orbits.

Nine landmarks are used to capture growth in the nasal region: nasale superius (left and right), nasomaxillary pinch (left and right), nasale inferius (left and right), rhinion, and alare (left and right) (Howells 1973) (Figure 4.3). As stated above, nasale superius (landmarks 4 and 5) captures the interaction of the nasal bones with the frontal bone and the frontal processes of the maxilla. Nasale inferius (landmarks 8 and 9) defines the lower point of the nasal bones at the opening of the nasal aperture and captures changes in the length of the nasal bones. Rhinion (landmark 10) also captures any increases or decreases in the length of the nasal bones. Nasomaxillary pinch (landmarks 6 and 7) is located at the deepest point along the suture intersection of the nasal bones and the frontal process of the maxilla. This landmark captures changes in the width of the nasal bones across the nasal bridge area. Left and right alare (landmarks 11 and 12) are located at the widest points of the nasal aperture and will therefore capture changes in the width of the nasal opening.

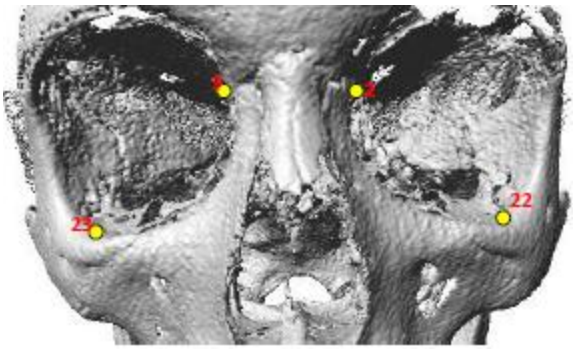

Figure 4.2. Landmarks capturing the growth and development of the orbital region.

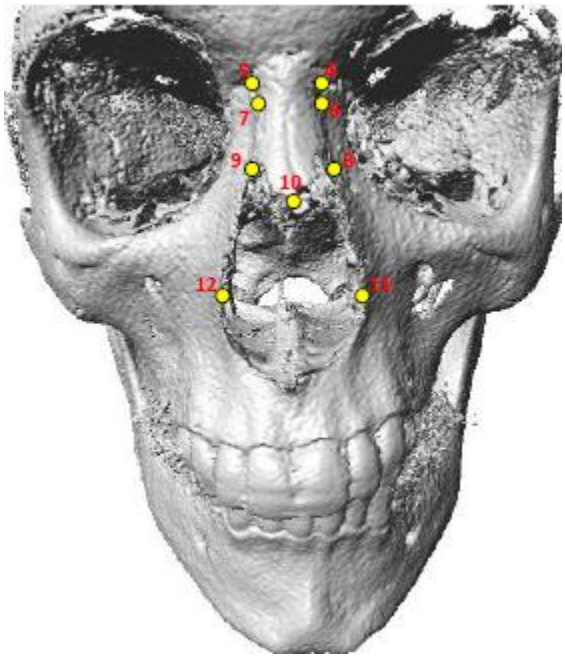

Figure 4.3. Landmarks capturing the growth and development of the nasal region.

The frontal processes of the maxilla are defined by twelve landmarks: nasale superius (left and right), nasomaxillary pinch (left and right), nasale inferius (left and right), left and right alare, zygomaxilare (left and right), and zygoorbitale (left and right) (Howells 1973) (Figure 4.4). As stated above, nasale superius (landmarks 4 and 5) and nasale inferius (landmarks 8 and 9) capture the interaction of the nasal bone (at its most superior and inferior border) with the frontal process. The nasomaxillary pinch (landmarks 6 and 7) delineates the superior portion of the frontal process, capturing increases or decreases in the width of its most superior tip. The zygomaxillary suture of the frontal process is defined by zygomaxilare (landmarks 16 and 17) and zygoorbitale (landmarks 18 and 19). These two pairs of landmarks define the most inferior and superior portions of the suture and will therefore capture any increases or decreases in length as well as any directional movements of the suture.

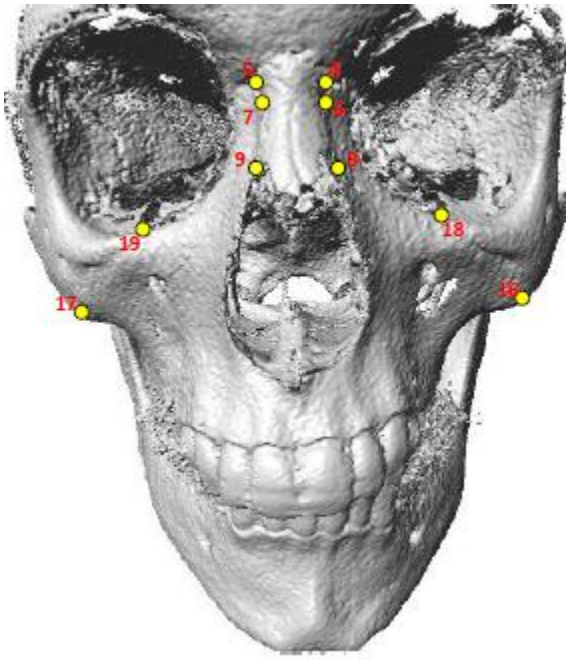

Figure 4.4. Landmarks capturing the growth and development of the frontal processes of the maxilla.

Three landmarks define the premaxilla region of the frontonasal module: nasospinale, subspinale, and prosthion (Howells 1973) (Figure 4.5). Nasospinale (landmark 13) is located at the most anterior point of the nasal spine and will therefore capture its anterior or posterior directional changes. Subspinale (landmark 14) is the deepest point below the nasal spine. This landmark will capture any labial surface remodeling. Prosthion (landmark 15) is located in the midline of the alveolar border between the central incisors. This landmark will capture increases or decreases in the height of the premaxilla.

It is important to note that the landmarks described above define two developmental modules: the frontonasal as well as the maxillary. Figure 4.6 presents only those landmarks that form the frontonasal module. Cheek height-superior and the zygomaxillary suture landmarks are part of the maxillary module, though they are also functionally part of the orbit.

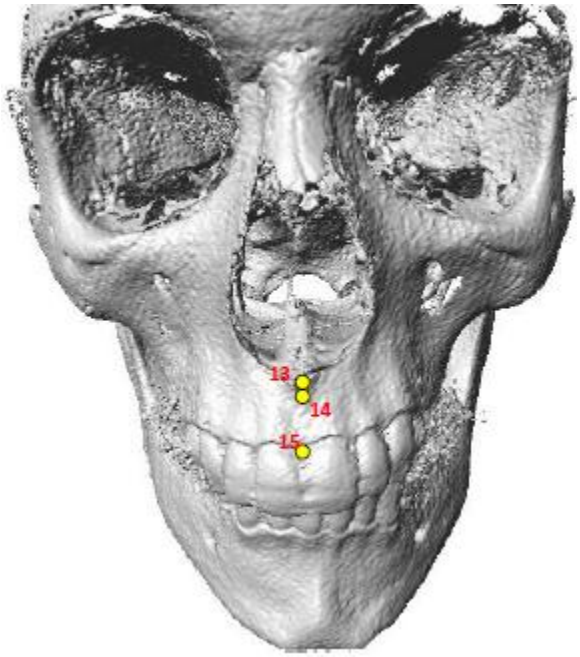

Figure 4.5. Landmarks capturing the growth and development of the premaxilla.

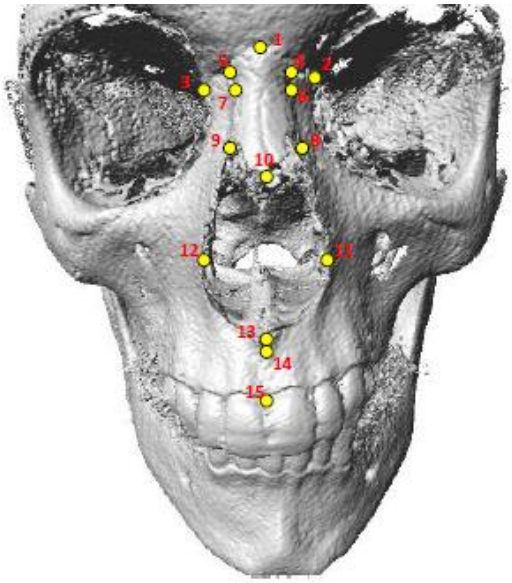

Figure 4.6. Example of landmark placement for all 15 landmarks that define the frontonasal module.

The Left and Right Maxillary Modules

For the current research, the left and right maxillary modules are each defined by six landmarks (left and right): zygomaxilare, zygoorbitale, cheek height-inferior, cheek height-superior, zygotemporale inferior, zygotemporale-superior (Howells 1973) (Figure 4.7; Tables 4.3 and 4.4). The zygomaxilare (landmarks 16 and 17) and zygoorbitale landmarks (landmarks 18 and 19) define the inferior and superior points of the zygomaxillary suture and define points of intersection between the maxilla and zygomatic bones. These landmarks capture growth occurring at the suture as well as shape changes that take place in the height of the cheek area. The cheek height-inferior (landmarks 20 and 21) and superior landmarks (22 and 23) capture changes in the dimension of the cheek region. The zygotemporale landmarks (inferior and superior) (landmarks 24-27) define the height of the zygomatic process. These landmarks are used to capture sutural changes as well as directional movement of the zygomatic process in relation to the maxilla bone.

Table 4.3. Landmarks defining the left maxillary module with definitions & abbreviations

Landmark Number	Landmark Abbreviation	Landmark Name	Definition
16	LZYM	Left Zygomaxilare	The intersection of the zygomaxillary suture and the limit of the attachment of the masseter muscle
18	LZYO	Left Zygoorbitale	Point at intersection of zygomaxillary suture and the lower orbital border
20	LCHI	Left Cheek Height-Inferior	The point of minimum distance from the lower border of the orbit to the lower margin of the maxilla
22	LCHS	Left Cheek Height-Superior	The point of minimum distance from the lower border of the orbit to the lower margin of the maxilla
24	LZTI	Left Zygotemporale Inferior	Lower point at suture where zygomatic and temporal bones intersect
25	LZTS	Left Zygotemporale Superior	Upper point at suture where zygomatic and temporal bones intersect

Definitions adapted from Howells (1973), Martin (1956), and Trevor (1950).

Table 4.4. Landmarks defining the right maxillary module with definitions & abbreviations

Landmark Number	Landmark Abbreviation	Landmark Name	Definition
17	RZYM	Right Zygomaxilare	The intersection of the zygomaxillary suture and the limit of the attachment of the masseter muscle
19	RZYO	Right Zygoorbitale	Point at intersection of zygomaxillary suture and the lower orbital border
21	RCHI	Right Cheek Height-Inferior	The point of minimum distance from the lower border of the orbit to the lower margin of the maxilla
23	RCHS	Right Cheek Height-Superior	The point of minimum distance from the lower border of the orbit to the lower margin of the maxilla
26	RZTI	Right Zygotemporale Inferior	Lower point at suture where zygomatic and temporal bones intersect
27	RZTS	Right Zygotemporale Superior	Upper point at suture where zygomatic and temporal bones intersect

Definitions adapted from Howells (1973), Martin (1956), and Trevor (1950).

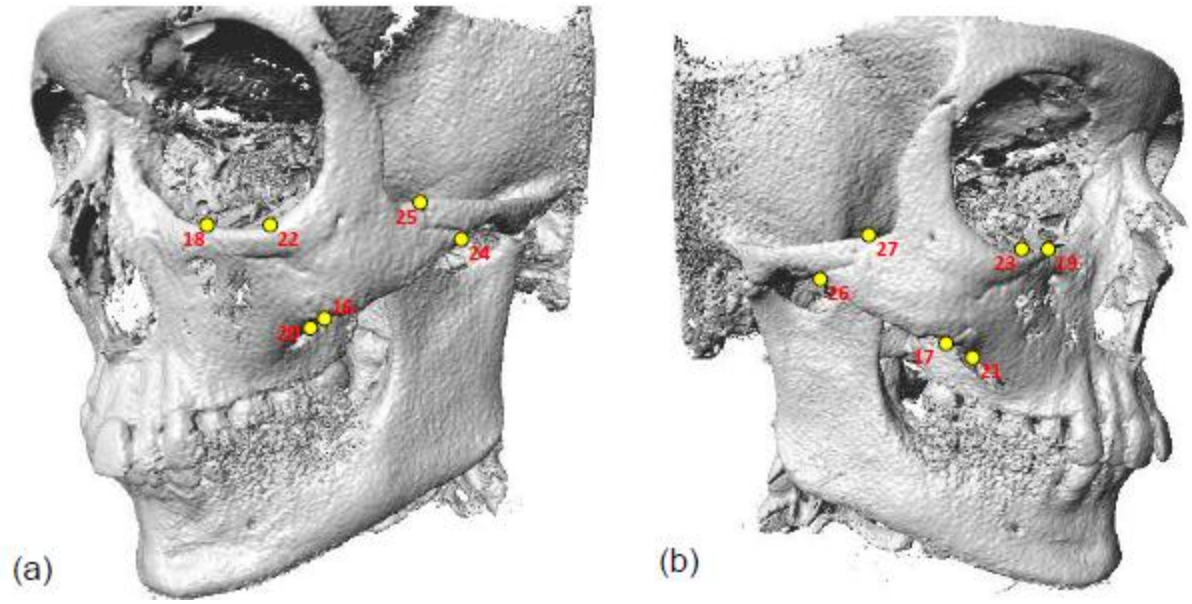

Figure 4.7. Example of landmark placement for the left (a) and right (b) maxillary modules.

The Sphenoid Module

Seven landmarks in this study define the sphenoid module: dorsum of sella, sella, left and right clinoidale, sphenoethmoidal, sphenoidale, and superior sella (Cobb and O'Higgins 2004; Lieberman et al. 2007) (Figures 4.8 and 4.9; Table 4.5). All of these landmarks were identified both from a superior perspective and in a sagittal section of the CT scan. Four of these landmarks, dorsum of sella, sella, sphenoidale, and superior sella (landmarks 28, 29, 33, and 34 respectively) are located on and define the structure of the sella turcica. These landmarks will capture any directional movement of the region. The left and right clinoidale (landmarks 30 and 31) are located on the most superior points of the anterior clinoid. These delineate the lesser wings of the sphenoid. Finally, the sphenoethmoidal point (landmark 32) captures the interaction between the greater wings of the sphenoid and the anterior cranial base.

Table 4.5. Landmarks defining the sphenoid module with definitions & abbreviations

Landmark Number	Landmark Abbreviation	Landmark Name	Definition
28	DOS	Dorsum of Sella	Most superior and posterior midline point on the dorsum sellae
29	SEL	Sella	Midline point at the center of the sella turcica
30	LCLI	Left Clinoidale	The most superior point on the left anterior of the contour of the clinoid
31	RCLI	Right Clinoidale	The most superior point on the right anterior of the contour of the clinoid
32	SPE	Sphenoethmoidal Point	The point of intersection between the greater wings of the sphenoid and the anterior cranial base
33	SPH	Sphenoidale	Most superior and posterior midline point on the tuberculum sellae
34	SSE	Superior Sella	The most superior midline point on the dorsum sellae

Definitions adapted from Cobb & O'Higgins (2004) and Lieberman et al. (2007).

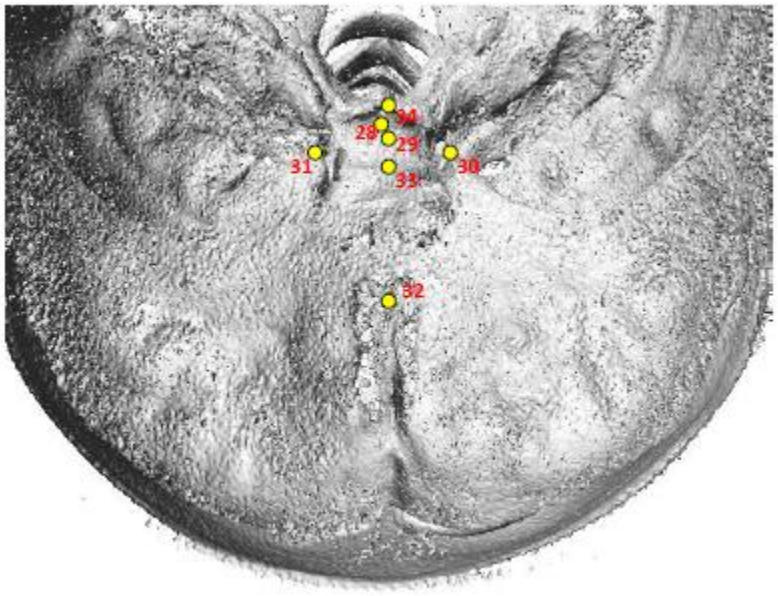

Figure 4.8. Landmarks defining the growth and development of the sphenoid module.

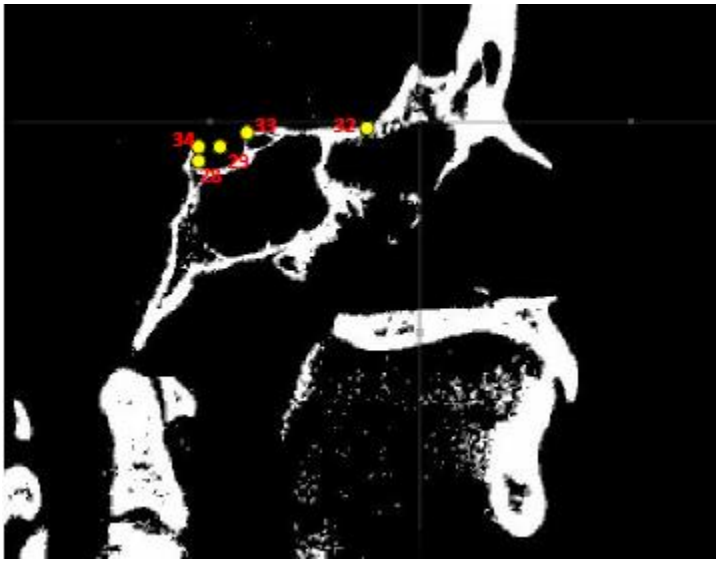

Figure 4.9. Landmarks 28, 29, 32, 33, and 34 of the sphenoid module shown on a sagittal slice.

The Ethmoid Module

For this research, four landmarks define the ethmoid module: neck of crista galli, left and right medio-orbitale, and ethmoidale (Phulari 2013) (Figures 4.10 - 4.12; Table 4.6). Like the sphenoid landmarks, these landmarks were identified using sagittal and coronal cross-sectional slices through the cranium. Ethmoidale (landmark 38) captures the interaction between the anterior cranial fossa and the cribriform plate of the ethmoid. The left and right medio-orbitale landmarks (landmarks 36 and 37) define the most medial points of the wall of the eye orbit, delineating the ethmoidal region of the eye orbit. Finally, neck of crista galli (landmark 35) delineates projection of the ethmoid at the most constricted point of the perpendicular lamina.

Table 4.6. Landmarks defining the ethmoid module with definitions & abbreviations

Landmark Number	Landmark Abbreviation	Landmark Name	Definition
35	NCRG	Neck of Crista Galli	The most constricted point of the projection of the perpendicular lamina of the ethmoid
36	LMO	Left Medio-Orbitale	The point on the left medial orbital margin that is closest to the median plane
37	RMO	Right Medio-Orbitale	The point on the right medial orbital margin that is closest to the median plane
38	ETH	Ethmoidale	The deepest median point of the anterior cranial fossa, corresponding to the cribriform plate of the ethmoid bone

Definitions adapted from Phulari (2013).

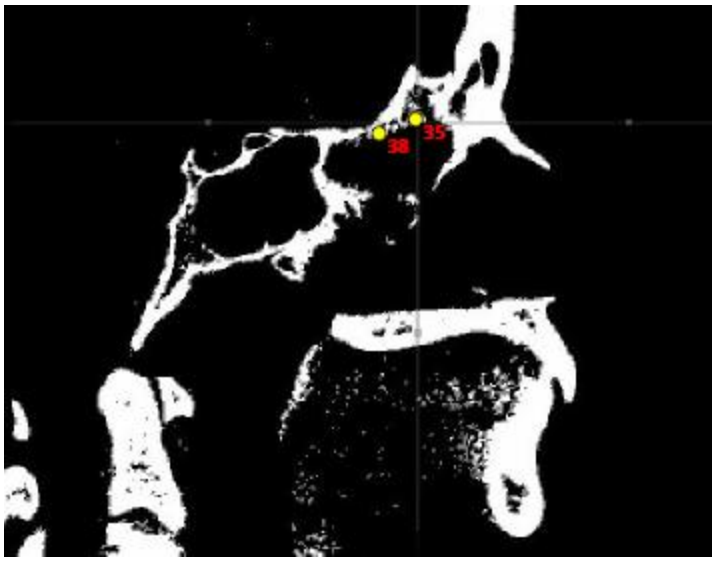

Figure 4.10. Landmarks 35 and 38 capturing the growth and development of the ethmoid module shown on a sagittal slice.

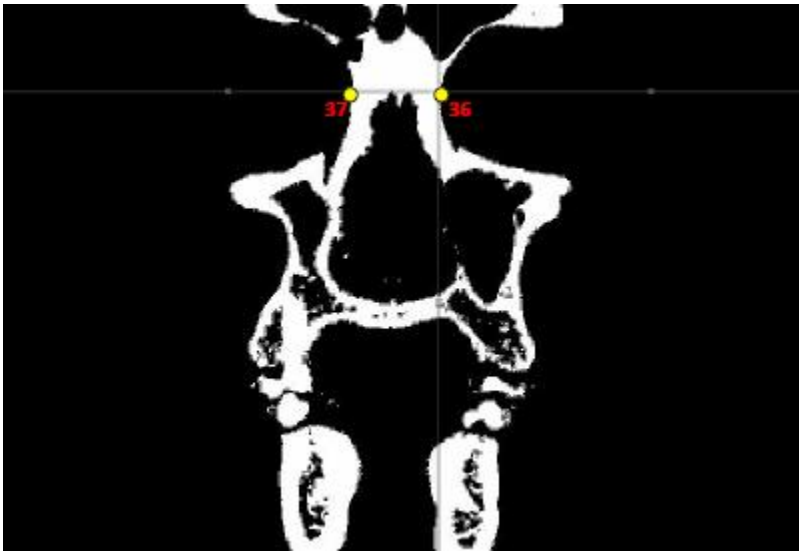

Figure 4.11. Landmarks 37 and 38 capturing the growth and development of the ethmoid module shown on a coronal slice.

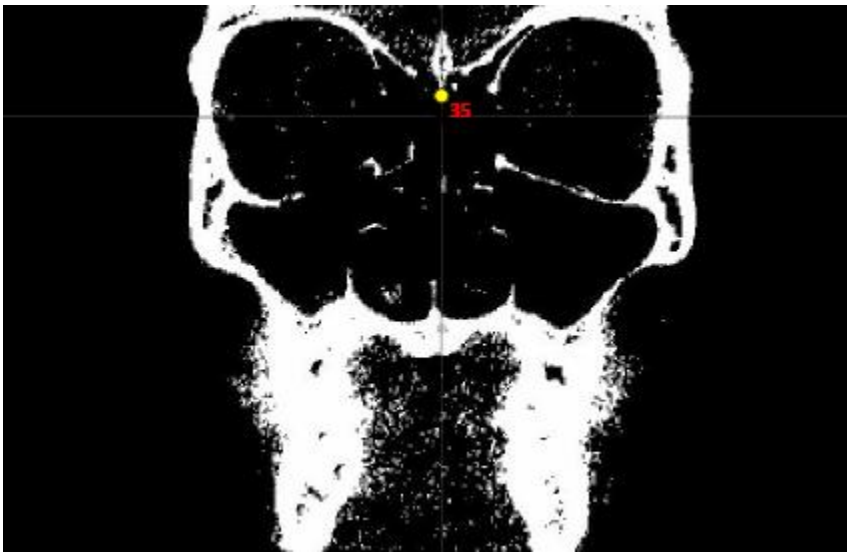

Figure 4.12. Landmark 35 capturing the growth and development of the ethmoid module shown on a sagittal slice.

Outlier Analysis

Using the Stratovan Checkpoint program, landmarks were placed on the three-dimensional surface reconstructions over a period of three months. Before any analyses were carried out an editing process took place to rectify any problems with landmark placement. An outlier analysis was conducted in MorphoJ, which allows the user to visualize the deviation of each individual from the average shape. Individuals may be selected to examine which landmarks deviate from the average shape. If an individual displayed deviations on particular landmarks instead of an overall deviation from the average shape, then the individual's three-dimensional reconstruction file was re-opened in Stratovan Checkpoint to visually evaluate the placement of each of the 38 landmarks. If the individual had landmarks that were not appropriately placed (that is, I misplaced them on the CT scan), the landmarks were fixed and the

three-dimensional coordinates for that individual were re-saved. Using this process, approximately 36 different individuals required a landmark adjustment.

Measurement Error

Before analyses could be conducted, I needed to determine the amount of error attributable to non repeatability of landmark placement. Two tests of intra-observer error were conducted. In both tests, in three separate bouts, landmarks were placed on three-dimensional surface reconstructions for ten individuals. A period of two weeks separated each trial of landmark recording. In order to test for the precision of landmark placement on the three-dimensional models, standard deviations of the raw coordinates along each of the three dimensions among the three landmark placement trials were calculated following Sholts et al. (2011). The standard deviations for each of the landmarks are listed in Table 5.1 in Chapter 5, along with the results of this test.

The second error test used the Procrustes ANOVA method outlined in Klingenberg and McIntrye (1998). This test only utilized the first two landmark placement trials. The Procrustes ANOVA determines if landmark placement error is influencing mean shape deviations away from the expected measurement of ontogenetic variation (Aldridge et al. 2005; Klingenberg and McIntyre 1998). The Procrustes ANOVA involves two steps: quantification of among individual shape variation in the dataset (individual) and the quantification of the variation among replicates (Error 1). If the mean sum of squares estimated from the second landmark placement trial is less than the mean sum of squares in the initial landmark placement trial then the placement of landmarks in the second trial did not counteract the shape differences identified in the first trial (Klingenberg and McIntyre 1998). Results for this ANOVA are, likewise, reported in Table 5.2 in Chapter 5.

Analytical Methods

Three separate analyses were conducted to assess the expectations described in the hypotheses in Chapter 1. Because this research is concerned with evaluating hypotheses concerning the ontogenetic basis of sexual dimorphism in the craniofacial complex (see Chapters 1 and 3), males and females were treated separately for all analyses. The first analyses assessed whether each of the five developmentally independent modules grow proportionally; that is, do the centroid size-scaled landmark distances within and among the modules maintain their relative distances, or do they change with age? Relatedly, do the centroids of the five modules grow proportionally relative to the overall cranial centroid, or do their distance from the overall centroid shift with age? The second and third analyses assess the variation in growth patterns between males and females. These tests used two geometric morphometric methods: Generalized Procrustes Analysis (GPA) and Euclidean Distance Matrix Analysis (EDMA).

Test of Proportionality

To test for proportionality between the five modules under study, the scaled Euclidean distances of all thirty-eight landmarks and of each individual module were calculated using the steps below:

1. Calculate the overall centroid location (x,y,z) for each individual by taking the mean of all the x coordinates, all of the y coordinates, and all of the z coordinates (i.e., standard unweighted calculations of mean centroid location).

2. Calculate the centroid location (x,y,z) of each module for each individual by taking the mean of all the x coordinates, all of the y coordinates, and all of the z coordinates using the landmarks that comprise the module (e.g., for the frontonasal module, take the mean of all the x coordinates, all of the y coordinates, and all of the z coordinates for landmarks 1-15).
3. Calculate the Euclidean distance of each landmark from the overall centroid location (calculated in step 1).
4. Calculate overall centroid size by taking the square root of the summation of the squared Euclidean distances (calculated in step 3) (Bookstein 1991). This is a measure of overall size that is uncorrelated with shape.
5. Divide the Euclidean distance of each landmark (calculated in step 3) by the overall centroid size (calculated in step 4). This provides a scaled distance, eliminating any size differences between individuals.
6. Calculate the Euclidean distance of each module centroid from the overall centroid (calculated in step 1).
7. Calculate the scaled module distances by dividing the Euclidean distance of each module (calculated in step 6) by overall centroid size (calculated in step 4).

To determine if the centroid size-scaled landmark distances maintained a relatively equal distance from the overall centroid regardless of age, a two-factor ANOVA was conducted using the scaled Euclidean distances of each module centroid (calculated in step seven). Age group and module type were used as factors. Individuals were combined into three separate age groups for males and females and defined using the following nominal variables: 1 = 7-9 year olds (early

childhood), 2 = 10-13 year olds (late childhood), and 3 = 14-17 year olds (adolescence). While three age groups were formed, as noted above, the extremes of the sample are smaller in sample size. Therefore, the younger age group is primarily comprised of nine year olds, and the older age group is mostly 14 to 15 year olds. Module type was defined using the following nominal variables: 1 = frontonasal module, 2 = left maxillary module, 3 = right maxillary module, 4 = sphenoid module, 5 = ethmoid module. If there is a significant main effect for module type, this indicates that the size-scaled landmark distances differ according to module type (e.g., the distance between the module centroid and overall centroid for the ethmoid module differs from the distance for the sphenoid module); even with scaling, the distances of each module centroid are expected to be significantly different. To test the hypothesis that modules are growing proportionately with age, I expect no significant main effect for age group. A significant main effect indicates that the size-scaled landmark distances for at least one of the modules is changing disproportionally with age, indicating non-proportionality among the five developmental modules. Furthermore, a significant interaction effect indicates that the five modules are not consistently growing relative to each other or with age. In other words, at least one of the modules is changing with age, but it is not the same module. Proportionality, therefore, is indicated by a non-significant main effect of age and a non-significant interaction effect (Figure 4.13). One-way ANOVAs were also conducted as *post-hoc* tests for both males and females to assess which modules changed with age. Because multiple comparisons are taking place and the five modules under investigation are not completely independent from one another, a Holm's adjustment for serial comparisons was applied to the p-values of the one-way ANOVA results.

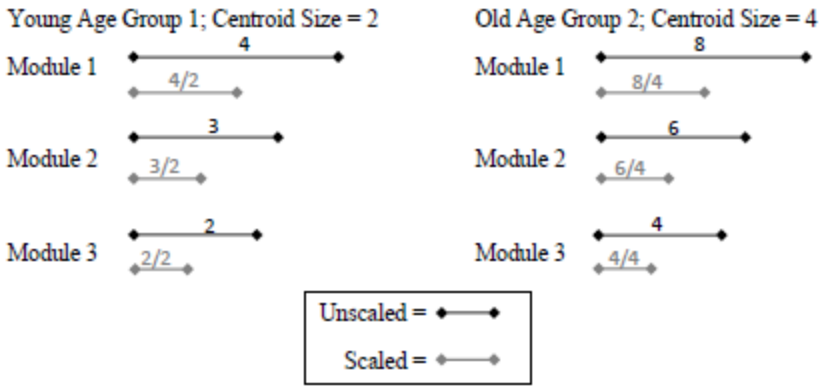

Figure 4.13. Example of proportionality among two age groups.
This figure is a depiction of proportionality, which would be represented by a significant main effect for module number, but no significant main effect for age and no significant interaction effect. The scaled and unscaled Euclidean distances for three modules are shown for each age group. For example, the unscaled Euclidean distance for module 1 for the younger age group is 4. The scaled Euclidean distance is divided by the centroid size. Although the modules are clearly changing throughout ontogeny, the three modules are proportionally changing from age group 1 to age group 2 (no significant age effect). Also, the three modules, in relationship to one another, are changing in the same way (no significant interaction effect).

Geometric Morphometric Analyses

Two different approaches were used to tests the hypotheses of shape variation: a generalized Procrustes analysis (GPA) and Euclidean distance matrix analysis (EDMA). The advantages and disadvantages to both procedures and an explanation of how each was used in this study are discussed below. Recent studies (Richtsmeier et al. 2002; Rohlf 2000) have discussed the merits and limitations of both approaches. Because each method offers a unique approach to the analysis of biological shape, however, many researchers have argued for the use of both approaches (Hallgrimsson et al. 2004; Weinberg et al. 2009). Following their arguments, and in order to provide the most complete picture of shape variation, both methods were employed in this study.

Generalized Procrustes Analysis

Generalized Procrustes Analysis (GPA) (Bookstein 1991; Chapman 1990; Goodall 1991) is one of many geometric morphometric methods used to analyze landmark data, and is the most common approach used in anthropological skeletal biology studies (Bastir and Rosas 2005; Bookstein et al. 2003; Cobb and O'Higgins 2004; Martinez-Abadia et al. 2009; Mitteroecker et al. 2004). GPA is a least-squares procedure that optimizes shape differences by scaling, rotating, and translating data into a common coordinate system. Average landmark positions among all individuals are generated from scaled and rotated scatter plots of individual landmarks, effectively showing the mean morphological shape represented by all of the landmarks. By showing the deviations of landmarks from this mean, groups of individuals may be compared to ascertain what shape aspects represented by the landmarks vary.

An advantage of Procrustes-based methods is that they provide a way to quantify and visualize overall shape differences. However, there are some noteworthy disadvantages. By scaling all landmark distances to centroid size, the method removes the source of most individual variance − size − even though size-driven shape change is maintained for analysis. Additionally, this method does not reveal how much variation (or movement) occurs at each individual landmark since the variation in each landmark is measured relative to all other landmarks (Figure 4.14). Since this dissertation is concerned with describing the variation of developmental modules throughout ontogeny, knowing the variance that occurs at each landmark and how this changes according to age is important information. Furthermore, Procrustes-based methods also mask extreme variation in particular landmarks by re-distributing the variance across all landmarks (known as the ‘Pinocchio effect’) (Chapman 1990; Cramon-Taubadel et al. 2007; Rohlf and Slice 1990). The Pinocchio effect occurs when large variances in one or a few of the

landmarks under study are "smeared out" over many landmarks. This is an effect of the least-squares rotation, which assumes equal variance at all landmarks. This is typically not true for most three-dimensional data sets (Webster and Sheets 2010).

Using GPA, shape variation in modules across the sample was analyzed using a three-step process. First, the raw landmark data was subjected to a generalized Procrustes analysis (GPA). This was conducted separately for each sex and for each module using the morphometrics package MorphoJ (Klingenberg 2011). The variance/covariance matrices of the GPA-scaled and transformed coordinate distances were analyzed through a principal component analysis (PCA). A PCA reduces the shape data for each module into components that maximize the orthogonal (i.e., uncorrelated) variances with the variance/covariance matrix. In doing this, the PCA emphasizes the linear relationships among distances within modules with high covariances and variances. Finally, using the principal component (PC) scores, a multivariate analysis of variance (MANOVA) was performed in IBM SPSS Statistics software (v. 22.0) to test for significant differences in shape for each of the five modules among age groups (using an alpha level of 0.05). Since MorphoJ does not produce a scree plot of the PC scores, the Procrustes coordinates were imported into SPSS and a scree plot was produced. Inflection points were used to determine the number of PC scores to keep for each MANOVA (Cattell 1966). As stated above, because multiple comparisons are made and each of the five modules interact with one another (i.e., they are not complete independent units), a Holm's adjustment for serial comparisons was applied to the p-values of the MANOVA results.

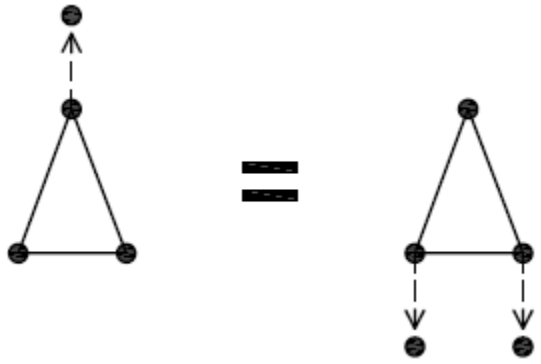

Figure 4.14. The variation in generalized Procrustes analysis is relative.
Moving one landmark in the superior direction is equal to moving the other two landmarks in the inferior direction (Polly 2012) .

There are four assumptions of a MANOVA: independence of observations, random sampling, multivariate normality, and homogeneity of covariance matrices. Observations from this research are statistically independent from one another and have been randomly sampled from the population. Since PC scores were being used in the MANOVAs and not coordinate data, multivariate normality of the PC scores for each module for both sexes was tested using the Royston's Multivariate Normality test. This test is an extension of the univariate normality test, the Shapiro-Wilk's W test, and it uses the W statistic for significance (Royston 1983; Royston 1995). This test was performed using the MVN package in R(Korkmaz and Goksuluk 2014). Homogeneity of covariance matrices was tested using the Box's M test in SPSS.

The GPA and MANOVA are useful methods for determining if shape differences exist between age groups. However, this approach does not provide any information on which landmarks are driving the shape differences or when these differences occur during ontogeny (the only reliable *post-hoc* analysis for a MANOVA is discriminant function analysis, a procedure that still cannot ascertain which landmarks are responsible for observed variance). For this reason, a second analysis was conducted using EDMA.

Euclidean Distance Matrix Analysis

Euclidean distance matrix analysis (EDMA) is a quantitative morphometric method that compares shapes of organisms that have been measured using two- or three-dimensional coordinates of anatomical landmarks (Lele and Richtsmeier 1991; Lele and Richtsmeier 1995; Richtsmeier and Lele 1993). Unlike most other morphometric methods, EDMA is coordinate-system invariant (Lele and Richtsmeier 1991). Unlike GPA, EDMA-based methods are not affected by the distribution of variance across landmarks, since it is an approach that is invariant to the parameters of translation, rotation, and reflection (Figure 4.15). Therefore, it provides a measure of the displacement of each landmark relative to all others. Because this research is concerned with analyzing the variation within and among five developmental modules, comparing the variation that occurs at each individual landmark provides a useful way to determine which modules experience the most change throughout ontogeny. A visual representation of the analytical differences between GPA and EDMA is presented in Figure 4.15. GPA is beneficial for this research as it provides a way to visualize shape changes throughout ontogeny. This is useful for assessing and describing how the developmental modules interact with each other. As an example, GPA can visually show how the left and right maxillary modules move (described as anterior, posterior, medial, or lateral movements) in relation to the frontonasal module. While GPA is useful for describing the overall shape differences between modules and their interactions with each other, EDMA provides a measure of the displacement of each landmark relative to all others, describing the variation that occurs at each individual landmark. Therefore, as stated above, each method offers a unique way to evaluate three-dimensional data, but are both useful, here, for answering different questions posed in this research.

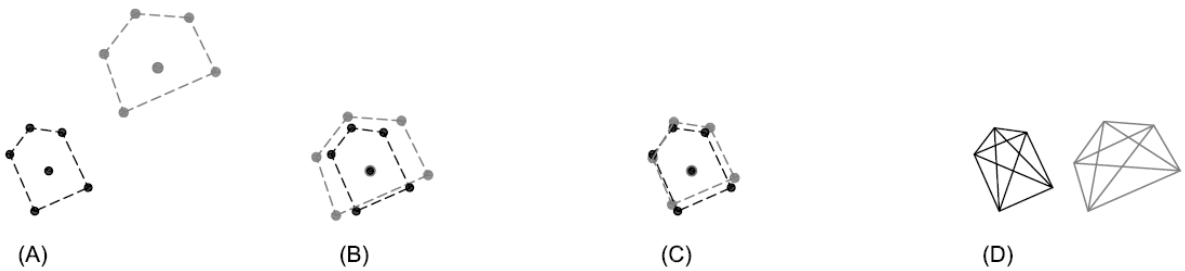

Figure 4.15. Comparison of generilized Procrustes analysis (A-C) and Euclidean distance matrix analysis (D).

(A) Raw coordinates for 2 individuals and their centroids; (B) Rotated and reflected coordinates; (C) Rotated, reflected and scaled coordinates; (D) EDMA is invariant to the parameters of translation, rotation, and reflection. Instead, it compares a matrix of linear distances between individuals (shapes).

EDMA describes the size and shape of a subject using the set of all linear distances among its landmarks. For a given subject, the raw landmark coordinate data (as they are digitized) are contained in a *K x D* matrix, where *K* defines the number of landmarks and *D* defines the number of dimensions (two or three). The set of all possible Euclidean distances between the subject's landmarks are placed into a *K x K* matrix called a form matrix: FM(*i*). FM(*i*), therefore, describes the size and shape of an individual without reference to a coordinate system, and FM is reliably calculated regardless of the orientation of a subject. For a sample, all of the individuals' form matrices are used to compute a mean form matrix. In the original description of EDMA (Lele and Richtsmeier 1991), the mean form was simply computed as the elementwise means of all the distances, taken across the sample. Lele and Richtsmeier (1991) noted that this estimate of the mean form is biased, so that the means are slightly overestimated. Lele (1993) published an algorithm to correct this bias, but it can produce unstable results when samples are relatively small, when samples are produced with a bootstrap, or when some landmarks are very close together. However, Lele and Richtsmeier (1991) argued that their original, biased estimates can produce valid results if the coefficients of variation for

corresponding measurements are comparable in the two samples. This is probably a reasonable assumption for the samples studied here, so the original algorithm is used.

To determine if age groups differ in shape, form difference matrices (FDMs) are calculated for consecutive age groups. Like the form matrices, FDM is *K x K.* Suppose there are two samples, *A* and *B,* with form matrices FM(*A*) and FM(*B*), respectively. For two landmarks, *i* and *j,* the mean distance between them is d_{ij}. For each *i* and *j* where *i* </> *j,* we define $FDM(A,B)_{ij} = FM(A)_{ij}/ FM(B)_{ij.}$ The diagonal elements of the FDM where *i* = *j* are equal to zero. Importantly, as FDM is calculated from FM(*i*), it is also coordinate-system invariant (unlike generalized Procrustes analysis, where the subjects must be fit together to allow comparisons).

The elements of FDM describe how *A* and *B* differ in size and shape. If the means for a distance are identical in *A* and *B,* the corresponding off-diagonal element of FDM will equal one. If an element of FDM is greater than one, the corresponding mean distance will be greater in *A.* In contrast, if an element of FDM is less than one, the mean distance will be greater in *B.* In an overall sense, if the form (size and shape) of *A* and *B* are identical, all of the elements of FDM will equal one. If the off-diagonals are all equal, but differ from one, the samples have the same mean shape, but different sizes. Finally, if there is heterogeneity in the off-diagonal elements of FDM, the samples will differ in shape (and perhaps size). For this research, age groups are compared. The ratios of each FDM, therefore, represent changes occurring due to shape during the age intervals being considered. Since the older sample is used as the numerator, ratios larger than one indicates linear distances that are larger in the numerator (the older sample) and vice versa.

EDMA has two ways of statistically evaluating differences between samples: a test for overall differences in shape between two samples (in this case age groups), and the calculation of

confidence intervals for element of each FDM. To test for significant differences in shape, a max/min statistic is used ($T_{obs)}$. This is calculated by dividing the maximum value in FDM by the minimum value. If T_{obs} is close to one, this indicates the two samples are similar in shape. As with each FM and FDM, the T_{obs} statistic is coordinate-system invariant. Because it is computed as a ratio of ratios, it is also scale invariant. After the T_{obs} has been calculated, the probability of obtaining the observed T statistic is calculated through a non-parametric bootstrapping procedure, which can be described as a ten-step process, taken directly from Krovitz (2000):

1. Let A and B be the two samples under study, with sample sizes *m* and *n*, respectively.
2. Calculate the mean FMs for samples A and B.
3. Calculate FDM(B,A), and sort the vector of ratios in ascending order.
4. Calculate T_{obs} from the maximum and minimum ratios in FDM(B,A).
5. Choose one sample, B for this example (usually the one with the larger sample size), as the reference sample.
6. Select *m* individuals randomly and with replacement from sample B, and call this sample A_1*.
7. Select *n* individuals randomly and with replacement from sample B, and call this sample B_1*.
8. Repeat steps 2, 3, and 4 using A_1* and B_1*.
9. Repeat steps 6, 7, and 8 a large (>100) number of times.
10. Plot the distribution of T values produced in step 9 as a histogram. If T_{obs} falls outside this distribution, the null hypothesis of similarity in shape between the two samples is rejected (Krovitz 2000: 86).

This is a one-way test, meaning it only tests if the mean form of one sample is similar to the reference sample. See Lele and Richtsmeier (1991; 2000) for more details concerning this particular statistical test.

Calculation of confidence intervals using a non-parametric sampling procedure provides more biologically meaningful information since it will determine which linear distances are statistically different between samples. Taken directly from Krovitz (2000), this procedure requires six steps:

1. Let A and B be the two samples under study, with sample sizes *m* and *n*, respectively.
2. Select *m* individuals randomly and with replacement from sample A, and select *n* individuals randomly and with replacement from sample B.
3. Calculate the FDM for the samples created in step 2.
4. Repeat steps 2 and 3 *C* times, where *C* is sufficiently large (>500 times).
5. This collection of bootstrapped samples is then written as a matrix with *C* columns and K(K-1)/2 rows. In the matrix, each column is a FDM obtained in step 3, and each row represents a ratio for each interlandmark distance within the bootstrapped FDM.
6. A confidence interval for each linear distance is obtained by sorting the ratios in each row in ascending order (Krovitz 2000: 87-88).

Because a 90% confidence interval is sought (a=0.10), the first 5% and last 5% of the entries in each row are removed, with the remaining entries representing the lower and upper confidence limits for that particular linear distance. If the confidence interval for a linear distance does not contain the value of one, this means the null hypothesis of similarity in shape can be rejected. If the lower bound of the confidence interval exceeds one, this means that particular linear distance

is significantly larger in the numerator variable (the older age sample). Again, Lele and Richtsmeier (1995; 2000) provide more information on this particular statistical method.

For this research, two comparisons were conducted using different age groupings. In the first age comparison, individuals were combined into three separate age groups for males and females: 7-9 (early childhood), 10-13(late childhood), and 14-17 (adolescence). In the second comparison, individuals were combined to produce age groupings that would encompass a smaller range of ages: 10-11 (late childhood), 12-13, (early adolescence), 14-15 (late adolescence). Two comparisons were made to ensure that changes taking place during adolescence were being captured and to provide the most detailed picture of these changes. To evaluate shape differences in each of the five modules independently, subsets of landmarks were created. This allowed for better interpretation of results since it decreases the number of distances represented in the FDM. The five modules under study contain a range of four to fifteen landmarks. Therefore, the FDMs reported in this study contain between six and 105 linear distances. Shape differences were compared between consecutive age groups for males and females separately. For example, the early childhood group was compared to the late childhood group and the late childhood group was compared to the adolescence group. All EDMA analyses were carried out using EDMAware software (Cole, 2014).

CHAPTER 5

RESULTS

This chapter presents the results for the analyses described in Chapter 4. Measurement error results are presented first. The two-factor ANOVA results for hypotheses of proportionality are presented next. The MANOVA results for tests of age differences are then reported, followed by the EDMA results for differences in shape between age groups. An in-depth discussion of the results presented here is found in the subsequent chapter. Summary statistics (mean inter-landmark distances by age and sex) are presented in Appendices B through G at the end of this dissertation.

Measurement Error

Intra-observer error and landmark precision was determined using two separate tests. Following Sholts et al. (2011), the first test measured landmark placement precision by calculating the mean standard deviations of the raw coordinates along each of the three trials. A value of 0.5 mm or greater was used to identify landmarks that have low precision (Cramon-Taubadel et al. 2007). The mean standard deviations of the 38 landmarks for the three replicates are listed in Table 5.1. Four out of 38 landmarks have a standard deviation of 0.5 or above, with only one over 0.6 standard deviations (ethmoidale). Notably, three of these landmarks are located on the sphenoid and ethmoid. Locating landmarks on these two modules is typically done using all three slice windows in the Stratovan Checkpoint program. Using three planes of reference to locate a landmark increases the difficulty and potential variability in landmark placement, as

opposed to directly placing a landmark on the surface of the skull. All 38 landmarks were retained for additional assessment using the Procrustes ANOVA error study.

Table 5.1. Standard deviations for thirty-eight landmarks used in study

Landmark	Module	Standard Deviation
Nasion	FN	0.13
Left Dacryon	FN	0.34
Right Dacryon	FN	0.29
Left Nasale Superius	FN	0.13
Left Nasomaxillary Suture Pinch	FN	0.19
Right Nasomaxillary Suture Pinch	FN	0.16
Left Nasale Inferius	FN	0.40
Right Nasale Inferius	FN	0.32
Rhinion	FN	0.08
Left Alare*	FN	0.53
Right Alare	FN	0.31
Nasospinale	FN	0.11
Subspinale	FN	0.19
Prosthion	FN	0.26
Left Zygomaxilare	LM	0.11
Right Zygomaxilare	RM	0.19
Left Zygoorbitale	LM	0.28
Right Zygoorbitale	RM	0.25
Left Cheek Height- Inferior	LM	0.16
Right Cheek Height-Inferior	RM	0.29
Left Cheek Height-Superior	LM	0.41
Right Cheek Height-Superior	RM	0.33
Left Zygotemporale Inferior	LM	0.08
Left Zygotemporale Superior	RM	0.25
Right Zygotemporale Inferior	LM	0.12
Right Zygotemporale Superior	RM	0.16
Dorsum of Sella	SP	0.19
Sella	SP	0.22
Left Clinoidale	SP	0.25
Right Clinoidale	SP	0.37
Sphenoethmoidal Point*	SP	0.53
Sphenoidale	SP	0.26
Superior Sella	SP	0.25
Neck of Crista Galli*	EM	0.56
Left Medio-Orbitale	EM	0.34
Right Medio-Orbitale	EM	0.44
Ethmoidale*	EM	0.79

*Standard deviation is greater than 0.5 mm.

[1]Abbreviations for modules: FN: frontonasal; LM, left maxillary; RM, right maxillary; SP, sphenoid; EM, ethmoid.

The second test of measurement error was the Procrustes ANOVA. This test was used to assess intra-observer variation. Error is considered to be minimal if the mean sum of squares measurement of Error 1 (the replicates) does not exceed the magnitude of the mean sum of squares for the individual data (Klingenberg et al. 2002). The mean sum of squares for the replicates was small compared to the individual specimen data (see Table 5.2). This suggests that error in landmark placement is small (Klingenberg et al. 2002). The parametric *F* statistic indicates there is significantly more shape variance among individuals shape than there are between the two trials of landmark placement (Aldridge et al. 2005).

Based on these two error studies, the landmarks were deemed to be reliable enough for all of them to be retained in the analysis. The low precision of the three landmarks located on the sphenoid and ethmoid modules was taken into consideration when interpreting results. Regardless, the majority of the variance in the data is attributable to individual differences.

Table 5.2. Procrustes ANOVA for intra-observer error for centroid size and shape

Centroid Size					
Effect	**Sum of Squares**	**Mean Sum of Squares**	**df**	**F**	**P value**
Individual	4725.13	525.01	9	2010.93	<0.0001*
Error 1	2.61	0.26	10		
Shape					
Effect	**Sum of Squares**	**Mean Sum of Squares**	**df**	**F**	**P value**
Individual	0.09	9.72×10^{-5}	963	5.70	<0.0001*
Error 1	0.02	1.71×10^{-5}	1070		

*Values significant at the 0.05 alpha level.

Test of Proportionality

A two-factor ANOVA was used to test whether or not there were differences in the size-scaled centroid distances of the five modules among age groups. Age group and module type were used as factors. This test was conducted separately for males and females and results are presented in Table 5.3. Among males, there was a non-significant interaction effect between modules and age groups, indicating that the effect of age on the distance measure is the same for all five modules. In other words, the module distances, relative to each other, are changing consistently across age. However, a significant interaction effect was found for females ($p<0.001$). This indicates that one or more of the modules are changing disproportionally with age, and this change is not constant across age groups (i.e., there is not consistency in the type of module that is changing with age). Because of the significant interaction effect, the main effects for females were not considered. As expected, a significant main effect for module type ($p<0.001$) was found for males; module centroids are not the same distance from the centroid. There was no significant main effect for age group among males ($p=0.54$). This indicates that module distances for males do not differ among age groups, indicating proportional growth among modules relative to the centroid. Though single-factor post-hoc tests may be misleading when significant interaction results are found in a two-factor ANOVA, such post-hoc tests may still be informative about general trends. Thus, post-hoc tests were performed for distances among modules and among age groups for females. Due to unequal variance of the dependent variable and non-normality of data, *Gabriel's* pairwise test was utilized due to its ability to cope with data that have violated assumptions (Field 2013). The results for module type show that all modules, with the exception of the two maxillary modules ($p=0.92$), significantly differ from each other ($p<0.001$). This finding is not surprising, as the maxilla should portray similar

centroid distance means. The results of the univariate post-hoc test of age group for females are presented in Table 5.4. The only age group comparison that shows significant difference in mean centroid distance is the comparison of age group one and three (7-9 year olds versus 14-17 year olds). To determine which modules are producing an interaction effect, the mean scaled module centroid to overall centroid distances were calculated for each module within each age group (Table 5.5). Only the ethmoid module shows change among age groups. It portrays a very slight decrease in mean centroid distance (i.e., the module centroid is moving closer to the overall centroid) from the 10-13 year old group to the 14-17 year old group, while the other four modules remain the same.

Table 5.3. Two-factor ANOVA results for females and males

Factor	Females			Males		
	df	**F**	***p***	**df**	**F**	***p***
Age	2	4.39	< 0.05*	2	0.61	0.55
Module Number	4	124470.71	< 0.05*	4	13597.51	< 0.05*
Age*Module Number	8	2.52	< 0.05*	8	1.32	0.23

*statistical significance $p < 0.05$

Table 5.4. Post-hoc results for two-factor ANOVA for main effect of age in females

Age Group Comparisons	***p***
1 versus 2	0.09
2 versus 3	0.51
1 versus 3	<0.05*

*statistical significance $p<0.05$

Table 5.5. Mean scaled module centroid distance per module and age group for females

Module	Mean Distances for 7-9 Year Old Group	Mean Distances for 10-13 Year Old Group	Mean Distances for 14-17 Year Old Group
Frontonasal	0.08	0.08	0.08
Left Maxillary	0.18	0.18	0.18
Right Maxillary	0.18	0.18	0.18
Sphenoid	0.17	0.17	0.17
Ethmoid*	0.06	0.06	0.05

*Module centroid distance shows change throughout ontogeny.

One-way ANOVAs, for both males and females, were conducted as a follow-up to the two-factor ANOVAs. These tests were conducted to determine which scaled module distances from the overall centroids, when analyzed separately, change among age groups. The results of the one-way ANOVAs for both males and females can be found in Table 5.6. The only module that showed a significant difference between age groups, for both males and females, was the ethmoid module ($p<0.05$). For males, significance at alpha 0.05 is lost for the ethmoid module after correcting for multiple comparisons (Table 5.6). This result matches the patterns observed in the two-factor ANOVA for females reported above, though the test also reveals a similar pattern among males.

To further visualize module variation throughout ontogeny, scatterplots were created for each module for males and females (Figures 5.1-5.5). Centroid size was placed on the x-axis and centroid distance (the size-scaled module centroid distance) was placed on the y-axis. Centroid size shows a correlation with age for both males ($r(145)=.53$, $p < 0.01$) and females ($r(155)=.55$, $p < 0.01$) when calculated for each individual module. Therefore, when interpreting the scatterplots, centroid size can be thought of as a representative measure of age (i.e., as age increases, centroid size should increase due to growth in the size of the skull). The scatterplots, then, are a visual way to assess proportionality. Proportionality is represented in the scatterplots

by the regression line. A line with little to no slope indicates that as centroid size increases (i.e, age increases), the module centroid distance neither increases nor decreases. This indicates equal proportionality of module distances with growth. A sloping line, therefore, indicates that module centroid distances are not proportionally constant with growth in overall cranial size.

It is important to point out that there is a lot of individual variation across age, as represented by the overall centroid size. That is, there is effectively no statistical relationship between centroid size and the scale distances of any of the modules from the overall centroid (most *r* values are effectively zero). Thus, the regression slopes through these scatterplots are at best, representative of a general trend between age and module distances; this variance reflects the idiosyncrasies of individual growth and indicates that, within individuals, it is likely that growth is not proportional, even if it statistically is across the sample averages for most modules.

Table 5.6. Results of one-way ANOVAs of scaled module distances among age groups for males and females

Module	Females				Males			
	df	**F**	***P* value (uncorrected)**	**Holm adjustment**	**df**	**F**	***P* value (uncorrected)**	**Holm adjustment**
Frontonasal	2	1.46	0.24	0.94	2	0.07	0.93	1.0
Left Maxillary	2	0.16	0.85	1.0	2	0.71	0.49	1.0
Right Maxillary	2	0.39	0.68	1.0	2	0.39	0.68	1.0
Sphenoid	2	0.58	0.56	1.0	2	0.32	0.73	1.0
Ethmoid	2	9.50	< 0.05*	< 0.05*	2	3.68	< 0.01*	0.14

*statistical significance $p < 0.05$

[1]A Holm's correction was applied to all p-values in R.

Despite the low correlations in these plots, general trends may be observed between scaled module distances. The frontonasal module shows a slight negative slope for both males and females (Figure 5.1). This indicates that as centroid size increases, module distance slightly (and non-significantly) decreases. The regression line for the left maxillary module differs between males and females (Figure 5.2). The females show a slight positive slope, indicating that as centroid size increases, module distance increases. Males show the opposite interaction in a negative slope, indicating that as centroid size increases, module distance decreases.

The right maxillary module shows a positive slope for both males and females, with females showing a stronger relationship between centroid size and distance (Figure 5.3). Statistically, these trends are no different from a slope of zero, and so the discrepancies in male left and right maxillary centroid distance change with age should not be interpreted as more than statistical artifacts. While not significant, it is noteworthy that the sphenoid module, for both males and females, portrays a negative slope (Figure 5.4). This likely means that growth and/or movement of the sphenoid bone slows down throughout ontogeny. The ethmoid module, for both males and females, portrays the greatest amount of change in its module centroid distance throughout ontogeny (Figure 5.5). As centroid size increases for the ethmoid module, the module distance decreases. This means one of two things: either the ethmoid experiences little growth and/or movement throughout postnatal ontogeny or the decrease in module distance for the ethmoid module is actually a by-product of the module being pulled closer to the overall centroid (decreasing the centroid distance). In other words, the growth and/or movement of the other four modules are affecting the location of the ethmoid's in relation to the overall centroid.

The results for the statistical tests of proportionality along with the visual scatterplot representations present some difficulties for interpretation. For instance, based upon the results

of the two-factor ANOVA alone, it seems that females do not portray proportionality among age groups. However, when the scatterplots are considered along with the similarities in results (between males and females) for the one-way ANOVAs, it becomes clear that the interaction effect found in the two-factor ANOVA for females is a reflection of the differences in how the module centroids are moving in relation to the overall centroid, and not a reflection of non-proportional growth among ages. Thus, each of these analyses cannot be interpreted alone, and must be considered in conjunction with one another. While the results of one analysis may indicate non-proportionality, this does not necessarily mean this is this case. A more detailed interpretation of the results for the test of proportionality will be discussed in the next chapter.

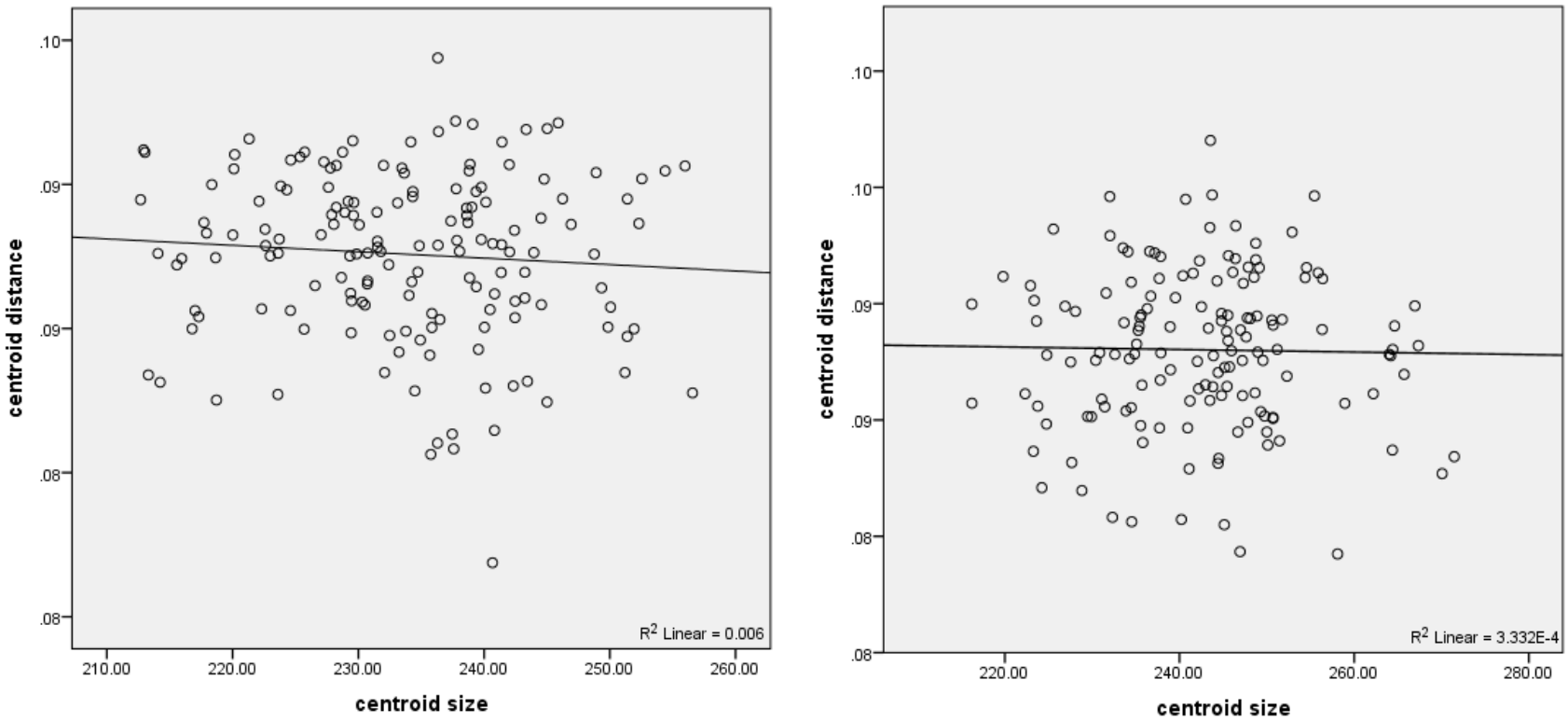

Figure 5.1. Scatterplots of frontonasal module for females (left) and males (right).

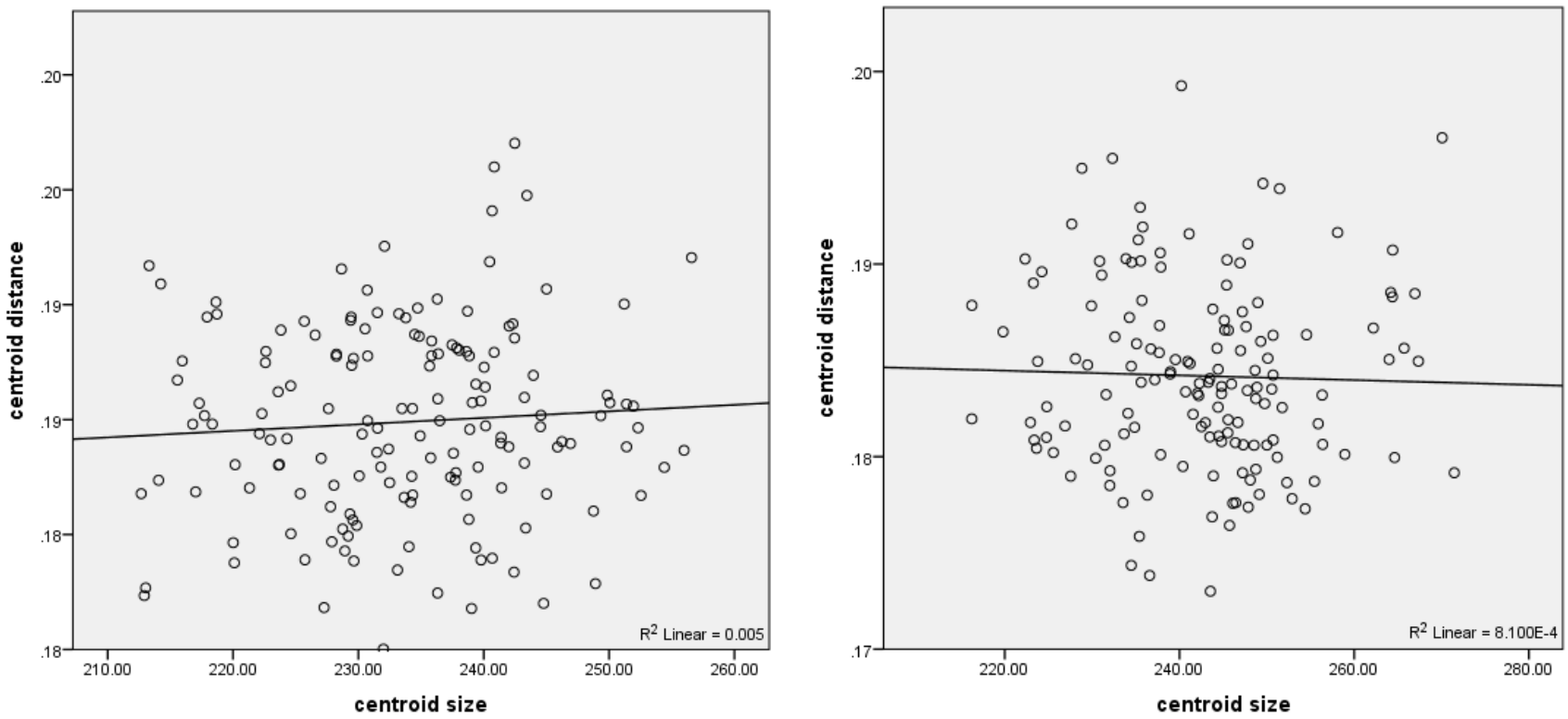

Figure 5.2. Scatterplots of left maxillary module for females (left) and males (right).

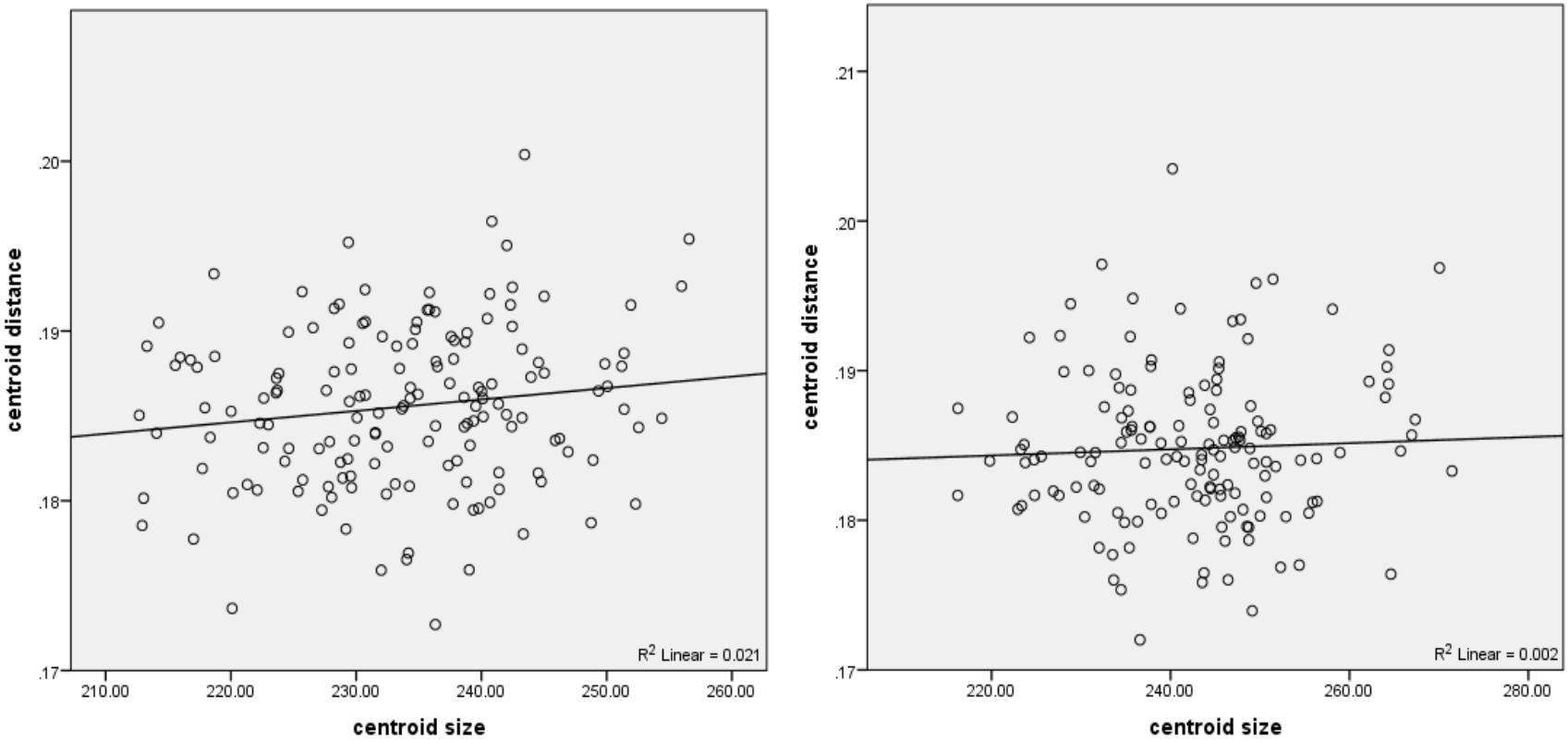

Figure 5.3 Scatterplots for right maxillary modules for females (left) and males (right).

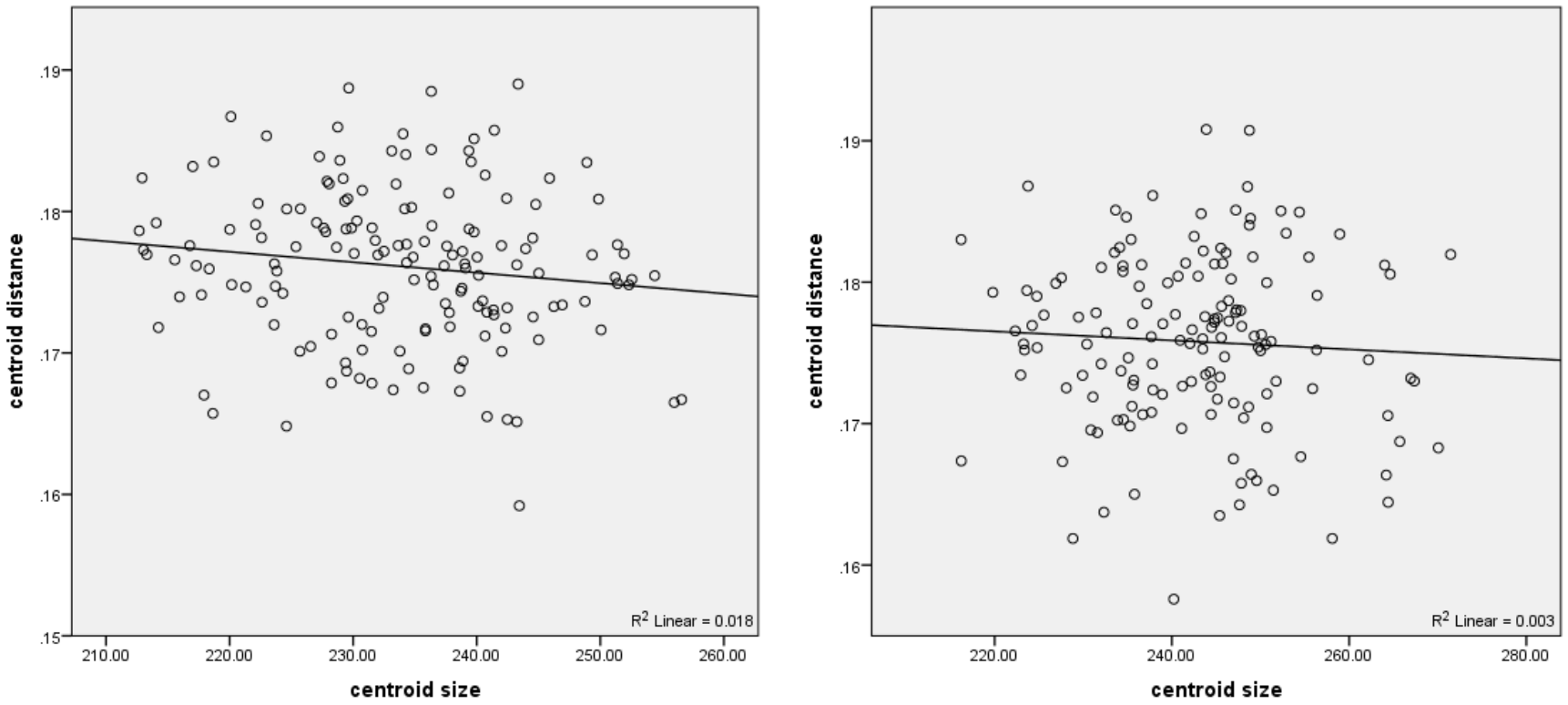

Figure 5.4. Scatterplots for sphenoid modules for females (left) and males (right).

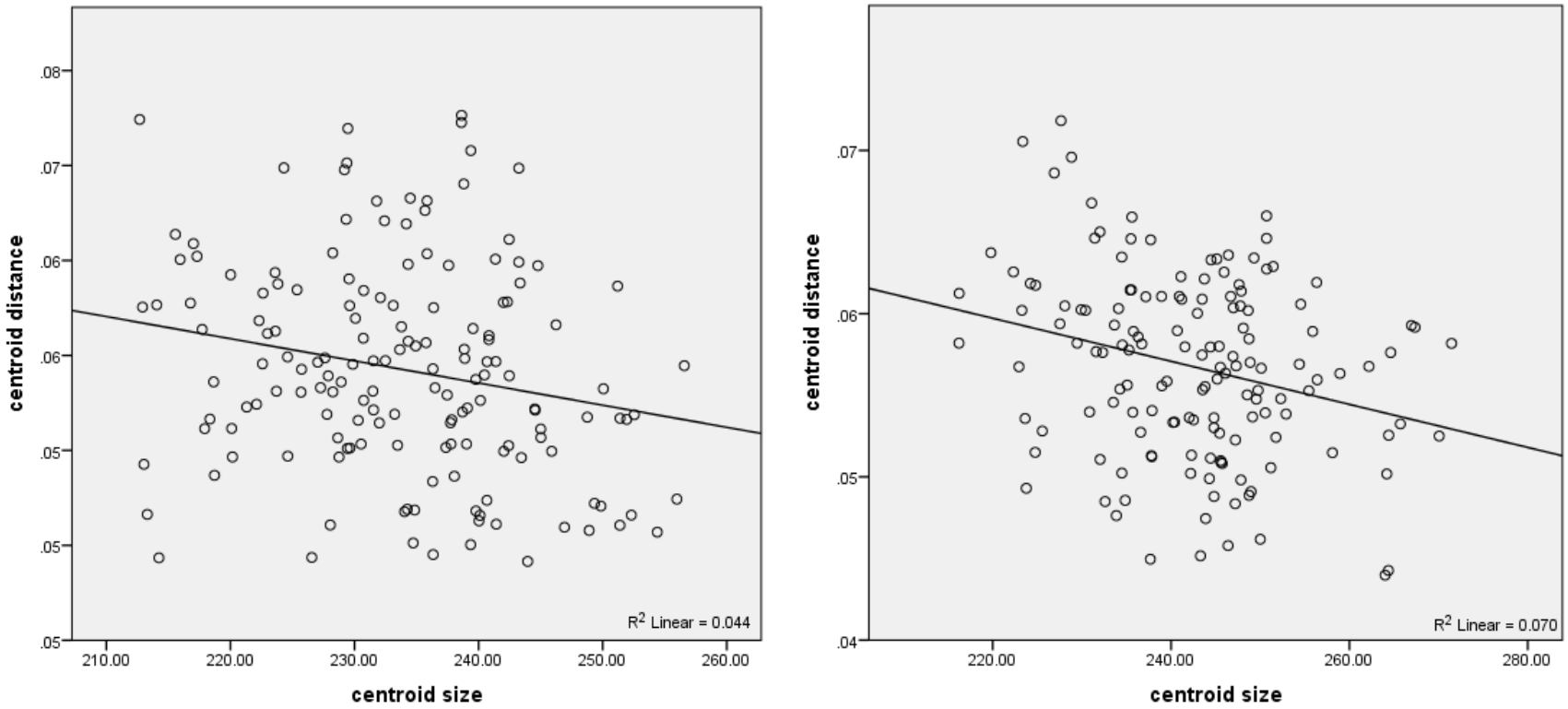

Figure 5.5. Scatterplots for ethmoid module for females (left) and males (right).

General Procrustes Analysis MANOVA results

As discussed in Chapter 4, the proportionality test only evaluates if the centroid size scaled landmark distances within and among the five developmental modules under study proportionally change with age. In order to assess the growth trajectories of the five modules between sexes and throughout ontogeny, another analysis was needed. Two geometric morphometric methods, generalized Procrustes analysis (GPA) and Euclidian distance matrix analysis (EDMA), were used to assess hypotheses of shape variation among males and females and age groups. In order to evaluate shape variation among the modules throughout ontogeny, the variance/covariance matrices of the GPA-scaled and transformed coordinate distances were analyzed through principal component analysis (PCA). The principal component (PC) scores were then used in a MANOVA to test for significant differences in shape for each of the five modules among age groups. The principal components and corresponding eigenvalues for each module for females and males are reported in Appendices H and I.

Tests of MANOVA Assumptions

Prior to conducting the MANOVA, multivariate normality of the PC scores for each module was tested for males and females using the Royston's test of normality in R (see Tables 5.7 and5.8). Only four out of the ten modules showed multivariate normality. A Box's M test was also conducted in SPSS to test for homogeneity of covariance of matrices. Two out of the ten modules did not meet this assumption (see Tables 5.9 and 5.10). The Pillai's Trace was chosen as the MANOVA test statistic because it is considered to be most robust for data that violate assumptions (Field 2013). For each MANOVA, scree plots were created and inflection

points were used to determine the number of PCs to retain for analysis (Cattell 1966) (see Appendix J).

MANOVA results

The MANOVA results are consistent with the proportionality results presented previously across age groups, males and females show different patterns of shape variation. However, unlike the tests for proportionality, the results for females indicate significant differences in module shape among age groups for more than just the ethmoid. For the females, Pillai's Trace tests of overall differences among age groups were significant for the frontonasal module (Pillai's Trace=1.02, $F_{(120,1420)=}1.34$, p=0.01), the left maxillary module (Pillai's Trace=0.61, $F_{(60,864)=}1.62$, p=0.00), the right maxillary module (Pillai's Trace=0.52, $F_{(50,720)=}1.68$, p=0.00), and the ethmoid module (Pillai's Trace=0.39, $F_{(40,576)=}1.56$, p=0.01). No significant difference in age groups was found for the sphenoid module (Table 5.11). For the males, significant differences between age groups were only detected for the ethmoid module (Pillai's Trace=0.42, $F_{(40,532)=}1.56$, p=0.01) (Table 5.11). However, significance at alpha 0.05 is lost after correcting for multiple comparisons. Plots of PC1 versus PC2 for each of the modules for females and males can be found in Appendices K and L.

Table 5.7. Royston's multivariate normality tests for females

Module	H	P value
Frontonasal*	100.93	< 0.05
Left Maxillary	12.35	0.34
Right Maxillary	15.49	0.16
Sphenoid*	86.76	< 0.05
Ethmoid	8.66	0.12

*Module is not multivariate normal

Table 5.8. Royston's multivariate normality tests for males

Module	H	P value
Frontonasal*	77.67	< 0.05
Left Maxillary	14.44	0.21
Right Maxillary*	52.63	< 0.05
Sphenoid*	91.97	< 0.05
Ethmoid*	23.66	< 0.05

*Module is not multivariate normal

Table 5.9. Box's M results for females

Module	Box's M	F	df1	df2	P value
Frontonasal*	828.69	1.23	468	16717.20	< 0.05
Left Maxillary	218.92	1.06	168	10290.40	0.29
Right Maxillary	183.52	1.10	135	6439.10	0.20
Sphenoid	169.95	1.02	135	6439.10	0.42
Ethmoid	96.92	.92	90	6827.02	0.70

*Module fails to meet assumption of equal covariance matrices

Table 5.10. Box's M results for males

Module	Box's M	F	df1	df 2	P value
Frontonasal	335.56	1.11	220	8044.87	0.12
Left Maxillary	183.07	0.98	147	7247.34	0.53
Right Maxillary	133.17	1.05	105	7506.80	0.35
Sphenoid	143.07	1.13	105	7506.80	0.18
Ethmoid*	148.50	1.53	80	3899.29	< 0.05

*Module fails to meet assumption of equal covariance matrices

Table 5.11. MANOVA results for males and females

Module	Sex	Pillai's Trace	F	Hypothesis df	Error df	P value (uncorrected)	Holm Adjustment
Frontonasal	Female	1.02	1.34	120	1420	< 0.05*	< 0.05*
	Male	0.86	1.25	100	1330	0.42	0.27
Left Maxillary	Female	0.61	1.62	60	864	< 0.05*	< 0.05*
	Male	0.45	1.08	60	798	0.32	0.32
Right Maxillary	Female	0.52	1.68	50	720	< 0.05*	< 0.05*
	Male	0.44	1.29	50	665	0.09	0.27
Sphenoid	Female	0.37	1.14	50	720	0.24	0.24
	Male	0.45	1.32	50	665	0.07	0.27
Ethmoid	Female	0.39	1.56	40	576	< 0.05*	< 0.05*
	Male	0.42	1.56	40	532	< 0.05*	0.08

*Significant difference between age groups at the 0.05 alpha level.
[1]A Holm's correction was applied to all p-values in R.

EDMA Results

The Generalized Procrustes analysis (GPA) and MANOVA evaluated if shape differences exist between age groups; however, these analyses do not provide any information about which landmarks are driving the shape differences. Furthermore, the results of the GPA and MANOVA do not indicate between which age groups differences occur during ontogeny. To further evaluate shape changes in the modules under study, Euclidean distance matrix analysis (EDMA) was conducted to assess the displacement of each landmark relative to all others and to describe the variation that occurs at each landmark.

Age Comparisons Tests

The same age groups used in the proportionality analysis were first used to compare shape changes within each module by EDMA in two comparisons; the age groups were: 7-9 year

olds (early childhood), 10-13 year olds (late childhood), and 14-17 year olds (adolescence). In the results reported below, the two comparisons are referred to as age comparison one (a comparison of the 7-9 year old group to the 10-13 year old group), and age comparison two (a comparison of the 10-13 year old group to the 14-17 year old group). For each comparison, the group with the largest sample size was used as the reference sample for the non-parametric bootstrapping procedure.

Results of the EDMA analysis are largely consistent with the results of the prior analyses using a Procrustes approach (both the proportionality test and the MANOVA of principal components). Females showed significant differences in overall shape in age comparison two for all modules except the ethmoid module (see Table 5.12). A significant shape difference was found between age comparison one for the ethmoid, but not for the later age group comparison (late childhood to adolescence). This finding relates to the proportionality results of females showing no significant difference in module centroid distance for age comparison one. The only significant shape difference in males was found in age comparison one for the ethmoid module (See Table 5.12). The fact that both males and females portray the same age related differences for the ethmoid module reveals its important role in early postnatal development. The relevance of this finding as it relates to postnatal growth and development will be further discussed in the next chapter.

The second test compared groups that encompassed a smaller age range: 10-11 year olds, 12-13 year olds, and 14-15 year olds. These comparisons are referred to as age comparison three (a comparison of the 10-11 year old group to the 12-13 year old group) and age comparison four (a comparison of the 12-13 year old group to the 14-15 year old group). Again, the group with the largest sample size was used as the reference group for the non-parametric bootstrapping

procedure. This test produced similar results to age comparisons one and two. Females showed a significant shape difference in the frontonasal, left and right maxillary, and the sphenoid for age comparison four (12-13 year olds compared to 14-15 year olds) (See Table 5.13). Males did not portray any significant shape differences between age groups for each of the five modules. Unlike age comparisons one and two, the ethmoid did not portray any significant shape differences for age comparisons three and four for both males and females. This indicates that the seven to nine year old group in age comparison one was likely driving the significant differences seen in the ethmoid module for both males and females.

Table 5.12. EDMA results for age comparisons one and two

Module	Sex	Age Comparison	T statistic	P value
Frontonasal	Female	1	1.26	0.12
		2	1.35	< 0.05*
	Male	1	1.27	0.32
		2	1.12	0.80
Left Maxillary	Female	1	1.15	0.23
		2	1.41	< 0.05*
	Male	1	1.09	0.64
		2	1.07	0.59
Right Maxillary	Female	1	1.13	0.32
		2	1.23	< 0.05*
	Male	1	1.09	0.68
		2	1.11	0.29
Sphenoid	Female	1	1.11	0.21
		2	1.25	< 0.05*
	Male	1	1.09	0.74
		2	1.09	0.37
Ethmoid	Female	1	1.14	< 0.05*
		2	1.06	0.34
	Male	1	1.31	< 0.05*
		2	1.03	0.85

*Significant difference in shape at the 0.05 alpha level.

Table 5.13. EDMA results for age comparisons three and four

Module	Sex	Age Comparison	T statistic	P value
Frontonasal	Female	3	1.16	0.75
		4	1.52	< 0.05*
	Male	3	1.19	0.38
		4	1.13	0.87
Left Maxillary	Female	3	1.08	0.69
		4	1.49	< 0.05*
	Male	3	1.05	0.88
		4	1.04	0.94
Right Maxillary	Female	3	1.11	0.52
		4	1.29	< 0.05*
	Male	3	1.09	0.57
		4	1.08	0.68
Sphenoid	Female	3	1.17	0.06
		4	1.33	< 0.05*
	Male	3	1.09	0.52
		4	1.12	0.49
Ethmoid	Female	3	1.07	0.45
		4	1.06	0.58
	Male	3	1.04	0.56
		4	1.07	0.62

*Significant difference in shape at the 0.05 alpha level.

Confidence Interval Testing

Although significant differences in overall shape were found in the EDMA (as well as MANOVA) results, there were no confidence intervals that indicated significant differences in the linear distances among any landmarks for any of the four age group comparisons. This indicates that the linear distances *collectively* produced an overall shape difference, but not *individually*. This makes sense in light of the proportionality results. The landmarks (as defined by their distances from each other as well as their distances from the overall centroid) are shifting relative to each other throughout ontogeny, and so do create shape changes within modules, but the shape differences produced are not detectable in terms of analyzing individual

linear distances. Even still, the maximum and minimum ends of the sorted FDM represent some of the largest differences in shape between the two age groups being compared and are therefore useful in determining how the modules change in relation to ontogeny.

Since none of the confidence intervals for each of the linear distances were significant, the maximum and minimum extremes of the FDM for each of the modules that showed a significant shape difference for age comparisons one and two are listed below. Ratios greater than one indicate a linear distance that is larger in the numerator sample (the older group), while ratios less than one indicate a linear distance that is larger in the younger sample. Ratios close to one indicate linear distances that are similar between the two age groups being compared. Only the ratios less than one and greater than one are listed in Tables 5.14-5.19. A graphic display of the EDMA results is not currently possible. Therefore, to illustrate the EDMA results, the inter-landmark distances (ILD) at the maximum and minimum extremes of the sorted FDM are indicated on a picture of the skeletal module (as done by Lele and III 1996; Richtsmeier et al. 1998). Since age comparisons three and four (which compared 10-11 year olds, 12-13 year olds, and 14-15 year olds) produced results very similar to age comparisons one and two (which compared 7-9 year olds, 10-13 year olds, and 14-17 year olds) only the results of age comparisons one and two are shown (see Figures 5.6-5.10). Only the confidence intervals for age comparisons that showed significance in the EDMA analysis are shown. The next chapter discusses the implications for these results in interpreting craniofacial shape change in the sample of juveniles.

Table 5.14. Maximum and minimum linear distances for female age comparison two for the frontonasal module

Landmarks	ILD ratio
ILD ratios below 1.0	
LNIN-RHI	0.98
RDAC- LNSU	0.98
RHI-NSP	0.98
LNIN- NSP	0.98
LNIN-SSP	0.99
RHI- SSP	0.99
RNSU-LSPI	0.99
RHI- LALA	0.99
ILD ratios above 1.0	
LNSU- LSPI	1.11
RSPI-LNIN	1.11
LSPI-RSP	1.11
NAS-LDAC	1.12
NSP SSP	1.12
LDAC-LNSU	1.12
LNSU-LNIN	1.13
LDAC-LSPI	1.13
RDAC-RSPI	1.13
NAS-RDAC	1.14
LSPI-LNIN	1.14
LDAC-LNIN	1.15
NAS-RHI	1.16
NAS RNIN	1.18
NAS-LNIN	1.19
RSPI-RNIN	1.19
RNSU-RSPI	1.24
NAS-LNSU	1.26
NAS-LSPI	1.26
NAS-RSPI	1.32
NAS- RNSU	1.32

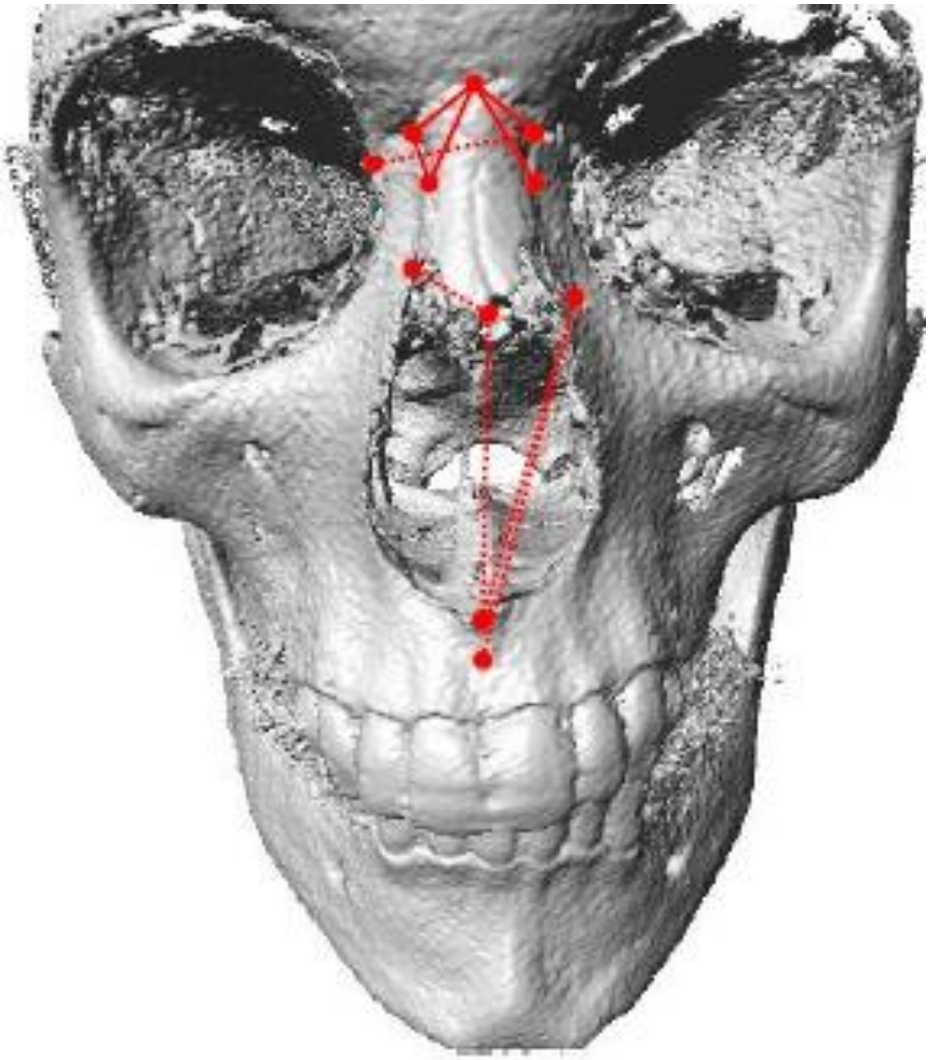

Figure 5.6. Illustration of distances listed in Table 5.14 for the older age group (14-17 year olds)

Only the highest five maximum and lowest five minimum distances are displayed. Solid lines represent distances that are larger in the 14-17 year old group when compared to the 11-13 year old group. Dotted lines represent distances that are smaller in the 14-17 year old group when compared to the 11-13 year old group

Table 5.15. Maximum and minimum linear distances for female age comparison two for the left maxillary module

Landmarks	ILD ratio
LCHS- LZTS	1.12
LZYM- LZTS	1.15
LZTI- LZTS	1.19
LZYM- LCHI	1.43

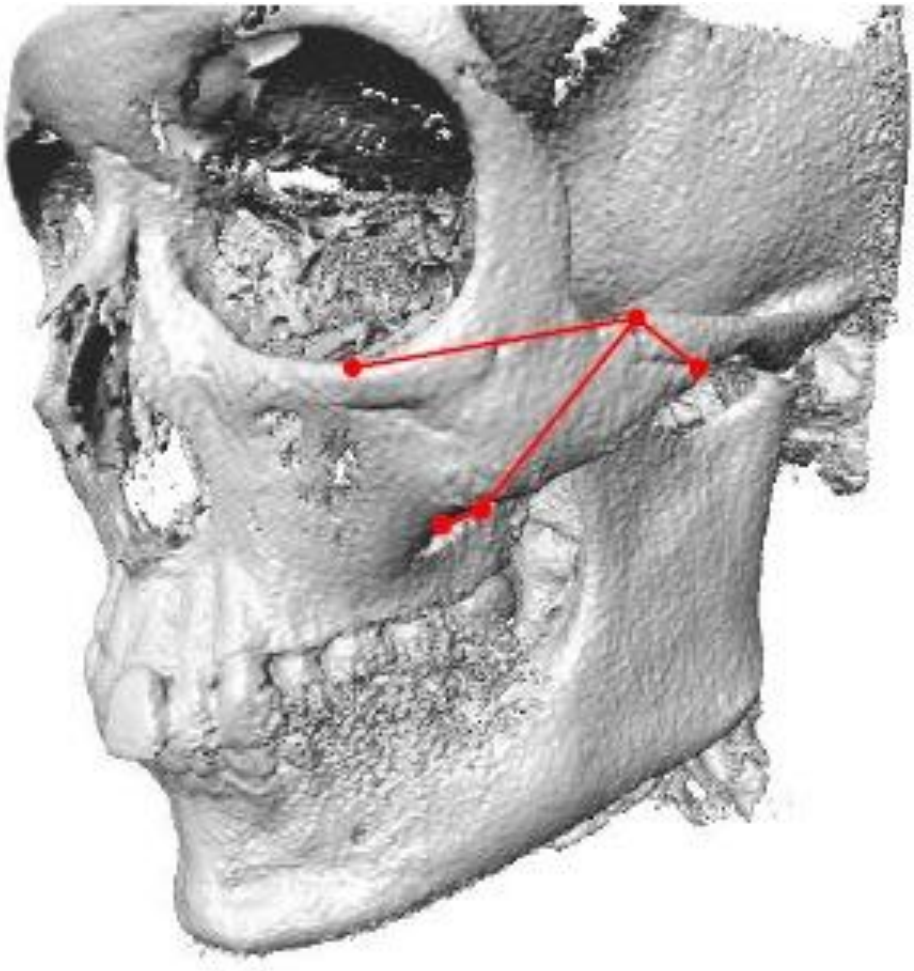

Figure 5.7. Illustration of distances listed in Table 5.15 for the older age group (14-17 year olds)

Solid lines represent distances that are larger in the 14-17 year old group when compared to the 11-13 year old group.

Table 5.16. Maximum and minimum linear distances for female age comparison two for the right maxillary module

Landmarks	ILD ratio
RCHS-RZTI	0.99
RCHI-RZTS	1.10
RZYM-RZTS	1.13
RZYO-RCHS	1.18
RZTI-RZTS	1.22

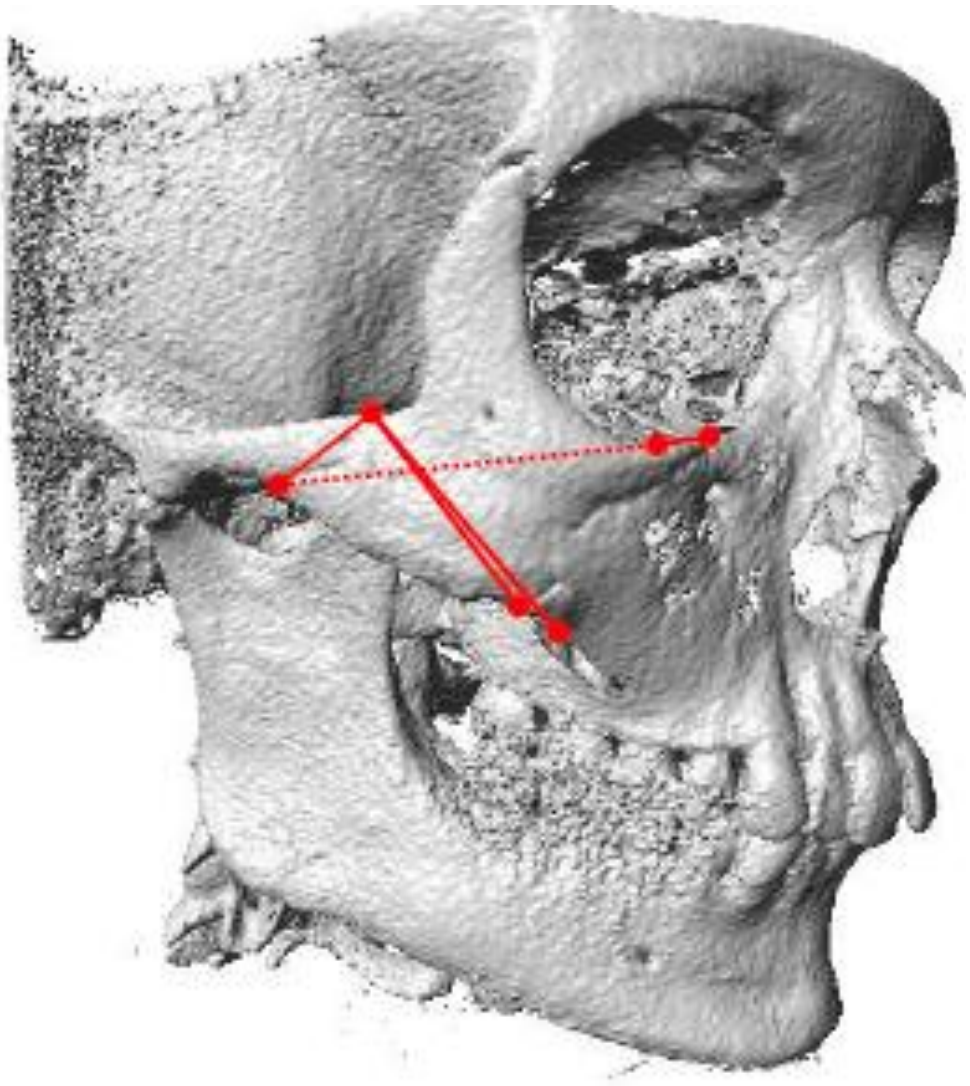

Figure 5.8. Illustration of distances listed in Table 5.16 for the older age group (14-17 year olds)

Solid lines represent distances that are larger in the 14-17 year old group when compared to the 11-13 year old group. Dotted lines represent distances that are smaller in the 14-17 year old group when compared to the 11-13 year old group.

Table 5.17. Maximum and minimum linear distances for female age comparison two for the sphenoid module

Landmarks	ILD ratio
SEL-LCLI	0.98
DOS-SPH	1.12
DOS-SEL	1.13
SEL-SPH	1.18
SEL-SSE	1.22
DOS-SSE	1.23

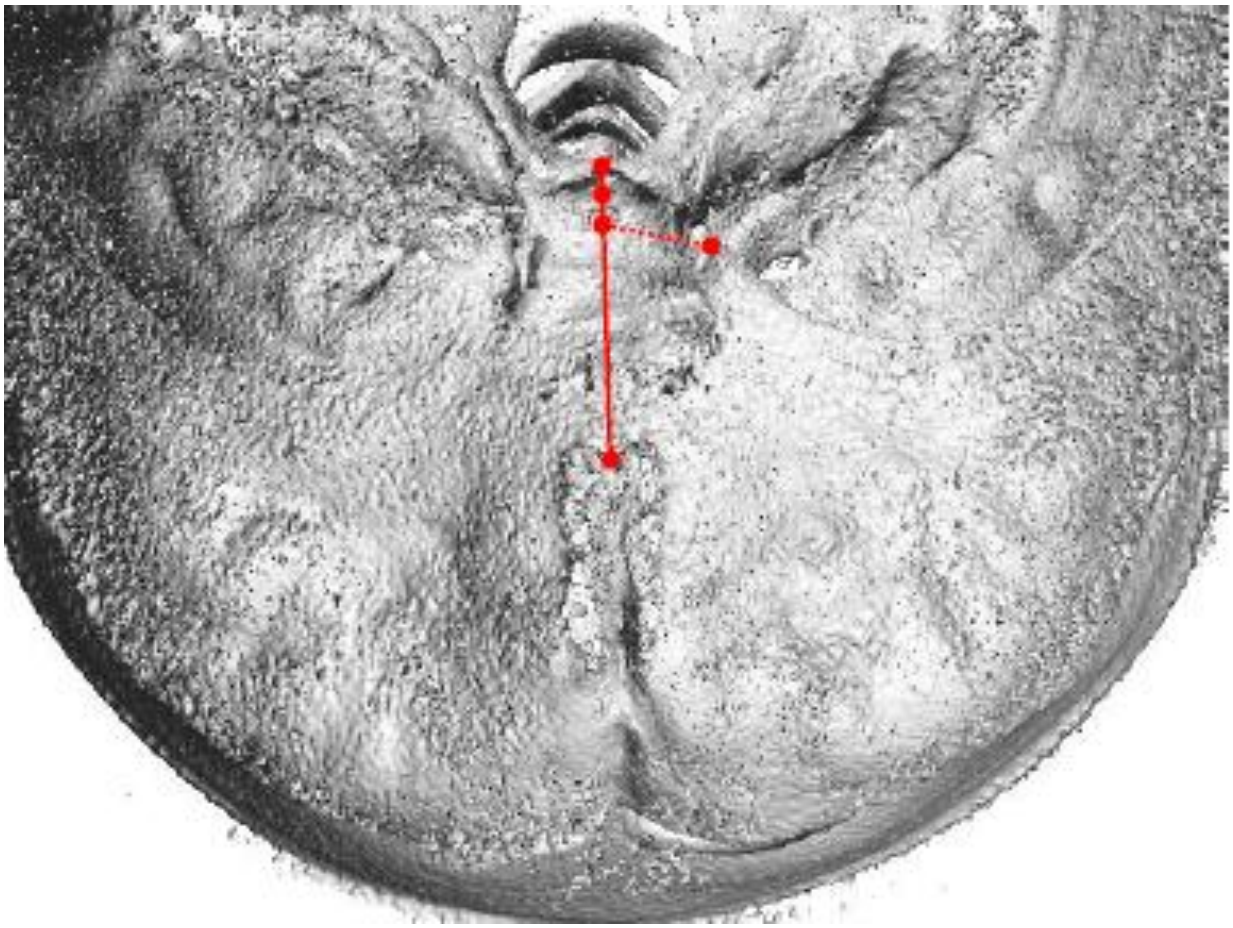

Figure 5.9. Illustration of distances listed in Table 5.17 for the older age group (14-17 year olds)

Solid lines represent distances that are larger in the 14-17 year old group when compared to the 11-13 year old group. Dotted lines represent distances that are smaller in the 14-17 year old group when compared to the 11-13 year old group.

Table 5.18. Maximum and minimum linear distances for female age comparison one for the ethmoid module

Landmarks	ILD ratio
LMO-ETH	1.09
RMO-ETH	1.10
NCRG-ETH	1.15

Table 5.19. Maximum and minimum linear distances for male age comparison one for the ethmoid module

Landmarks	ILD ratio
LMO-ETH	1.13
RMO-ETH	1.14
NCRG-ETH	1.31

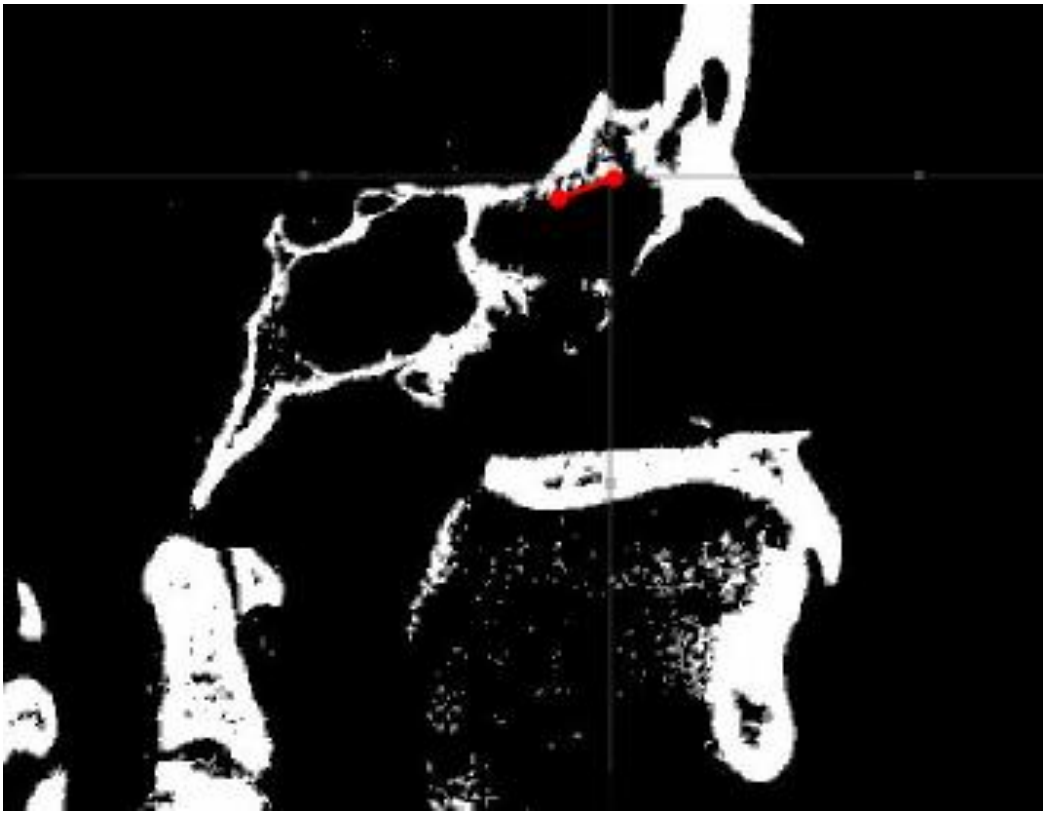

Figure 5.10. Illustration of NCRG-ETH distance listed in Tables 5.18 and 5.19 for the older age group (11-13 year olds) for males and females

Solid lines represent distances that are larger in the 11-13 year old group when compared to the 7-9 year old group. Due to the nature of landmark placement for the ethmoid module, the RMO/LMO-ETH distances could not be illustrated.

CHAPTER 6

DISCUSSION AND CONCLUSIONS

This dissertation had two main research goals. The first research goal was to assess proportionality among five developmentally independent modules of the facial skeleton, and, in turn, the contributions of shape change in each module to overall craniofacial growth. Secondly, this study set out to determine if males and females experience different growth trajectories of the five modules under investigation. This chapter reviews the results of these two research goals as they relate to the background and hypotheses presented in Chapters 1-3. The results of this study reveal as a whole that, while postnatal craniofacial growth is a complex process, it is better understood through an evaluation of the ontogenetic changes that occur within individual developmental modules. As this is the first study to use this approach, the results of this research have many implications to improve the understanding of postnatal facial growth.

Summary of Principal Findings

Analyses reported in Chapter 5 successfully examined the proposed hypotheses, and the general results are reported here before more fully discussing their implications. The first hypothesis is that proportions of the face, as defined by the five developmental modules under investigation, are established early during ontogeny. Assessing proportionality among modules will help to elucidate which of the current two models of postnatal ontogeny, as outlined in Chapter 3, is most probable. To assess this hypothesis, males and females were analyzed separately. The results for Hypothesis One can be summarized into two main conclusions:

1) Males and females have proportional growth throughout ontogeny for four of the five modules studied: the frontonasal, left and right maxillary, and the sphenoid modules.
2) The ethmoid module does not grow proportionally throughout ontogeny for either males or females.

The second hypothesis tested in this study is that males and females experience different growth trajectories of the five modules under investigation. This hypothesis was tested in an attempt to contribute information to our current understanding of the etiology of sexual dimorphism in the adult face. Four main conclusions may be drawn from the analyses:

1) Males and females have a similar growth trajectory for the ethmoid module.
2) For females, significant shape differences exist throughout ontogeny for all five developmental modules. However, the timing of these differences varies among modules. The ethmoid shows a significant shape difference early in postnatal ontogeny (from 7-9 years of age), but not in late ontogeny (14-17 years of age). The other four modules only show significant shape differences late in ontogeny (14-17 years of age).
3) For males, the only module to exhibit significant shape differences is the ethmoid module. This module shows a significant shape difference early in postnatal ontogeny (from 7-9 years of age), but not in late ontogeny (14-17 years of age).
4) No significant differences in the linear distances between all landmarks were found in either sex when compared among age groups. This suggests that, while individual

portions of each craniofacial unit do change shape ontogenetically, it is their global change (and not individual landmarks) that drive sexual dimorphism.

The combination of the two hypotheses analyzed in this study offers a unique opportunity to examine the postnatal growth processes that contribute to adult craniofacial variation in modern humans. The following two sections provide a synthesis of the results for each of the hypotheses along with explanations for how the results inform our current knowledge of the etiology of adult craniofacial variation. As with any research, there are limitations to this study. These are considered and discussed in a later section of this chapter.

Synthesis of Hypothesis One Results

Hypothesis 1: Proportions of the face, as defined by the five developmental modules under study, are set early in ontogeny.

As discussed in Chapter 3, within the current literature, two mutually exclusive hypotheses have emerged concerning the ontogenetic origins of human craniofacial variation. The first argues that shape variation is established prenatally and further elaborated throughout postnatal ontogeny through parallel ontogenetic trajectories (Ackermann and Krovitz 2002; Leon and Zollikofer 2001; Lieberman et al. 2002; Mitteroecker et al. 2004). The second argues that shape variation is established throughout postnatal growth due to divergent trajectories among and within species (Cobb 2001; Sardi and Ramirez 2012; Vioarsdottir and Cobb 2004; Vioarsdottir et al. 2002). These studies have essentially focused on global cranial patterns of change and not the contributions of specific components that drive those patterns. One way to

assess which of these hypotheses applies to the human craniofacial complex is to evaluate the proportionality of growth between and within modules.

As discussed in Chapter 5, the results of the proportionality tests do not present a clear conclusion about the two models. While the females statistically show an interaction between differences in module centroid distances from the overall centroid and age, this alone does not imply that the five modules are growing disproportionally. However, the slightly dissimilar one-way ANOVA that compared individual module distances among ages makes it clear that the ethmoid module is the only one that significantly differs among age groups. This results also appears in males (although more so as a trend since significance was lost after correcting for multiple comparisons), who did not have an interaction effect in the two-way ANOVA. In fact, only the ethmoid shows either an increase or decrease in scaled distance from the overall centroid across age groups among males. Furthermore, in the scatterplots presented in Figures 5.1 through 5.5, one can see that the modules exhibit similar ontogenetic patterns between the sexes despite the lack of correlation between module distance and centroid size (more about this will be discussed below). Collectively, we may conclude that males and females both share proportional growth in the facial skeleton throughout ontogeny, in all modules except for the ethmoid. There is shape change within each module, however, as the EDMA results indicate, none of the landmarks used are individually driving the ontogenetic shifts in shape within each craniofacial unit. Thus, while shape changes are occurring locally, with the exception of the ethmoid, all of the units of the face are remaining in relatively the same positions ontogenetically. These results are considered within each module below, and special attention is given to the position and shape change that occurs in the ethmoid. I will then return to the

discussion of how these results relate to the two developmental models that have been proposed about the origins of adult craniofacial variation.

Before considering growth within each of the facial units, some consideration should be given to the lack of correlation between scaled module centroid distances from the overall centroid and centroid size. Perhaps the most obvious conclusion to draw from the scatterplots presented in Chapter 5 is that growth is inherently idiosyncratic, and that individual facial differences may, in part, result from distinct growth trajectories for craniofacial modules; hence, there is considerable variance among individuals. However, there are two additional considerations to be made here. First, while the centroid size should closely match age of the individual, these are not going to be tied to the same point on a developmental trajectory among all individuals; that is, two individuals may have the same centroid size, but they may slightly be at different stages of primary growth. There is no way to correct for these differences; growth matches chronological age within a range of variation. For example, adult teeth erupt within increasingly greater age ranges (Scheuer and Black 2000), and using teeth as a gauge for a point in growth makes assumptions about the relationship of dental development to craniofacial development, when the relationship may only be local (e.g., affecting the alveolar bone and palate shape). Second, the lack of correlation between module distances and centroid size could be affected by substructure in the data (e.g., health, metabolism, or ancestry), all of which remain unknown in this study. Even if the factors affecting sample substructure were known, the lack of correlation for the entire sample would likely persist given the great dispersion of data across the full range of centroid sizes. Tracking individual growth longitudinally and averaging the change in module distances might eliminate or minimize some of these effects. However, such data are

not yet available, and so the patterns that this dissertation establishes refine current models of ontogeny (see discussion about future directions at the end of this chapter).

The Frontonasal Module

The frontonasal module maintains its relative distance from the overall centroid for the face throughout ontogeny in both females and males (Figure 5.1). However, among the Procrustes analysis and EDMA results, and as shown in Figure 5.6, the overall shape of this craniofacial unit does change throughout ontogeny, namely at the onset of the acceleration of growth during puberty. Most of these changes occur near to the frontonasal suture, with increases in the width and anterior projection of the nasal bones relative to the base of the frontal bone. Simultaneously, the nasal aperture unexpectedly shortens superoinferiorly, and the base of the nasal bones appears to shorten. This is contrary to overall patterns of craniofacial growth established in Chapter 3, where nasal lengthening has been documented to be the general trend throughout primary growth, though it is also possible that continued inferior growth of the nasal bones is outpacing the inferior displacement of the nasal aperture floor. The general pattern of increases in interlandmark distances (Table 5.13), though, does not suggest that this growth is a product of anterior displacement of the nasal bones. The net effect of these patterns of growth, then, is to change the overall shape of the nose inferiorly and, around the nasal bones, anteriorly and laterally.

The Left and Right Maxillary Modules

Like the frontonasal module, the left and right maxillary modules maintain a proportional distance from the overall centroid throughout ontogeny for both males and females (Figures 5.2

and 5.3). However, according to the Procrustes and EDMA results, shape changes in these modules are only statistically significant in females (Tables 5.11 and 5.12). These shape changes occur between 10-13 year olds and 14-17 year olds, indicating that the left and right maxillary modules change shape at or during the onset of puberty. As stated in Chapter 2, the zygomatic and maxillary bones experience rapid growth during postnatal ontogeny due to their interaction with the eye orbits, nasal region, and alveolar bone. Much of the shape change in the left and right maxillary modules is attributable to increases in interlandmark distances. Both the left and right maxillary modules show an increase in the lateral projection of the maxillary bones. This increase is consistent with the anterior displacement of the maxillae pushing the zygomatic bones in a posterior direction. As the zygomatic bones get displaced posteriorly, an increase in their vertical dimensions is expected, seen here as an increase in the landmarks defining the zygotemporale suture. Overall, the left and right maxillary modules are following the patterns of growth discussed in Chapter 2. Surprisingly, there is no increase in the interlandmark distance that defines the zygomaxillary suture. The ratio for the linear distance of the two landmarks defining this suture (zygomaxilare to zygoorbitale) are very close to 1.0 for both males and females, indicating little change between the two age groups being compared (10-13 year olds compared to 14-17 year olds). Increases in the size of the nasal region and eye orbits directly influence the growth taking place at the zygomaxillary suture. It is possible, though, that growth at this suture is minimal when compared to the zygotemporal suture, making it undetectable.

The Sphenoid Module

According to the results of the proportionality tests, the sphenoid module also maintains a proportional distance from the overall centroid throughout ontogeny (Figure 5.4). This result was unexpected since the sphenoid is continuously influenced throughout postnatal ontogeny by

many other growing parts of the skull (e.g., brain growth, orbital, nasal, oral, and pharyngeal growth). Even though it maintains proportional growth, according to the Procrustes and EDMA results, it experiences significant shape change later in ontogeny (i.e., when compared between 10-13 year olds and 14-17 year olds) (Tables 5.12 and 5.17). Overall, shape change of the sphenoid can be described as a lengthening in the anterior-posterior direction (Figure 5.9). An increase in the interlandmark distance between sella and sphenoethmoidal is likely an effect of bone resorption of the hypophyseal fossa, pulling sella in a posterior direction away from sphenoethmoidal. The dorsum of sella also increases in distance from sphenoethmoidal, consistent with the upward and backward movement of the sella turcica noted in Chapter 2. The sella turcica is reported to cease growth around seven years of age (Acheson and Archer 1959; Chilton et al. 1983; Latham 1972; Scheuer and Black 2000; Underwood et al. 1976). Contrary to this reported pattern, the height of the sella turcica increases during late ontogeny. This is potentially a by-product of the previously noted anterior-posterior increases in length of the sphenoid. This finding may also differ from the findings in the literature due to differences in analytical methods. As stated in Chapter 2, much of the previous research on the sphenoid bone used lateral radiographs (Bulygina et al. 2006; Ursi et al. 1992), limiting the ability for any type of three-dimensional analyses that would potentially detect minor directional changes taking place throughout ontogeny.

The Ethmoid Module

Unlike the other four modules, the ethmoid does not maintain a proportional distance from the overall centroid throughout ontogeny. While females show a significant shift in the ethmoid, the males show a trend of this pattern (significance at alpha 0.05 was lost after correcting for multiple comparisons). According to the scatterplots in Chapter 5 (Figure 5.5),

both males and females portray a negative slope in the ethmoid's module centroid distance from the overall centroid. This indicates that as age increases (as represented by an increase in centroid size) the size-scaled centroid distances decrease. As briefly stated in Chapter 5, a decrease in the distance measure means that the ethmoid module centroid is moving closer to the overall centroid throughout ontogeny, which translates into an anterior and inferior displacement of the whole ethmoid with age. This is likely an effect of the ethmoid slowing in growth throughout ontogeny (as indicated by the EDMA results) or a by-product of the frontonasal module pulling the ethmoid closer to the overall centroid. Perhaps this is due to the ethmoid's extended ossification period, as compared to the other four modules, throughout postnatal ontogeny (see Chapter 2). It is noteworthy that this shift in the location of the ethmoid occurs while the anteroposterior length of the cribriform plate increases before the onset of puberty. The shape changes in the ethmoid are discussed in more detail below.

Proportional Growth Results in Light of Craniofacial Development

As discussed in Chapter 2, each of the modules used in this study are independently derived. Thus, it is possible that some of the patterns revealed in the results are due to patterns of development that occur in the fetal period and/or in the early childhood growth stage. Developmentally, the frontonasal and left & right maxillary modules maintain a constant interaction throughout prenatal life. As stated in Chapter 2, the frontonasal module grows inferiorly while the maxillary modules grow medially around the sides of the face toward the midline. These three modules experience articulations and fusions with one another throughout prenatal life, which could potentially explain the similarity in their results. The sphenoid and ethmoid modules are in constant contact with each other and the other three facial modules; however, they are more likely influenced by their prenatal interactions with the basicranium and

developing meninges, brain, and eyes. Yet, even though they both undergo similar developmental interactions, they do not show similar patterns of proportional growth. This may be due to the variation in their ossification patterns. The sphenoid and ethmoid are especially notable given their extended ossification times. For instance, the sphenoid bone has six ossification centers that begin ossifying around nine weeks of gestation, with the last ossification center arising during the fifth fetal month and fusion completing around puberty. In contrast, the ethmoid has three ossification centers that are weakly ossified at birth, with its last fusion occurring as late as twenty to thirty years of age (see Chapter 2). The ethmoid's extended ossification into postnatal life may be contributing to its non-proportional growth, versus the prenatal ossification seen in the other four modules. In addition, the ethmoid plays a significant role in the prenatal development and postnatal growth of the nasal cavity and eye orbits. As discussed in Chapter 2, these two areas are highly variable among humans and throughout postnatal growth (variation in the orbital region is obvious in this sample based upon the EDMA results for the frontonasal module, discussed below). Unlike the frontonasal module's involvement in the nasal aperture opening, the ethmoid is more involved in the superior and internal nasal region. The nasal cavity increases its variance among human populations throughout growth (Noback et al. 2011), presumably due to interactions with multiple factors arising from interactions with other bones, soft tissues, and environmental factors. It remains surprising that, while the ethmoid responds to these factors, it is clear that the sphenoid does not in the same manner though it is more like the ethmoid than any of the other modules.

Synthesis of Results for the Five Developmental Modules

In light of the two hypothetical models concerning the origins of adult variation in postnatal ontogeny, this research provides support for the hypothesis that craniofacial variation is

set early in ontogeny and further accentuated throughout postnatal growth through parallel ontogenetic trajectories. Though this research does not directly evaluate these two models, it does provide evidence that modules of the face (with the exception of the ethmoid module), as defined by size-scaled centroids, maintain an equal (proportional) distance from the overall centroid throughout ontogeny. As stated in Chapter 4, it is possible that the differences between age groups are likely being driven by the disproportionate representation within the age groups. It is also important to remember that a limitation of this study is that individuals are not associated with ancestral information. Therefore, if the sample groups in this study are significantly skewed toward one particular population group, then potential differences in ontogenetic trajectories would not be detected. However, as discussed above, based upon the low r^2 values for each of the scatterplots shown in Chapter 5, this is an unlikely scenario for the current sample under study. Furthermore, as discussed in Chapter 3, while evidence supports population-based differences in craniofacial shape, patterns of modularity and integration (reflected in the analysis of proportionality) in the cranium should be similar for all humans.

It is important to note that the results of the proportionality tests are not entirely compatible with either model of postnatal growth. The results discussed above could also be interpreted as support for the non-proportionality model as well. Evidently, the ethmoid module does not portray proportional growth throughout ontogeny. Also, while the other four modules do not show statistically significant differences in the size-scaled centroid distances among age groups (indicating proportionality), the Procrustes and EDMA results reveal that each of them experience significant shape change during late ontogeny. It is possible that non-proportionality with significant shape change could be a result of the scale of the analysis. As discussed in Chapter 3, previous studies have only analyzed ontogenetic shape change by calculating

landmark distances from the overall centroid or through an analysis of scaled interlandmark distances. These studies, then, have evaluated global patterns of facial shape change. This produces results that resemble shape change throughout ontogeny; however, landmarks *within* modules may be remaining proportional throughout growth, shifting the entire module and creating morphological change. In other words, previous studies of global shape change may have potentially masked the shifts in the individual modules with significant changes in individual landmarks. Thus, the current models may have amplified the differences across ontogeny. Because the results can be interpreted as support for both models of proportionality, perhaps a better model would be one that 'hybridizes' the existing models. The hybridized model, then, would allow for some parts of the face to undergo proportional growth and others to experience significant shifts throughout ontogeny, with all modules universally undergoing shape changes.

A very significant, yet subtle, pattern emerges when examining the scatterplots of the five modules under study. With the non-significant exception of a slight difference in the slopes of the left maxillary module, males and females are showing the same patterns of proportional growth. The left and right maxillary modules are, in fact, the only modules to show a slight increase in the size-scaled module centroid distance throughout ontogeny. In other words, as age increases, the left and right maxillary modules move further away from the overall centroid while the centroids of the other three modules move closer to the overall centroid. This is likely occurring due to the growth processes that take place in the maxillary region. As discussed in Chapter 2, the infraorbital zygomaxillary suture shifts laterally throughout primary growth due to growth of the zygomatic and maxillary bones. An increase in the width of the face, at the maxillary regions, also occurs due to growth at the lateral borders of the eye orbits and at the

midpalatal suture. Therefore, an increase in the width of the face (as reflected in an increased size-scaled distance measure for the left and right maxillary modules) could be pulling the other three modules closer to the overall centroid (as reflected in a decrease in the size-scaled distance measures). As the overall centroid position and size was calculated from all 38 landmarks, and *not* the five module centroids, this is not likely a spurious result occurring from the calculation (where positive change in some module distances would necessitate negative change in other module distances).

Synthesis of Hypothesis Two Results

Hypothesis 2: Males and females have different developmental trajectories for the five modules under study.

Most researchers agree that adult sexual dimorphism in the face is the result of differential growth patterns between males and females (Bulygina et al. 2006; Ewing and Harris 2000; Ursi et al. 1992; Vioarsdottir 1999). However, it is still unclear in what ways postnatal growth contributes to establishing sexual differences or which regions of the face experience the most change during the two periods of accelerated growth (especially puberty). The results of this study support the hypothesis that differential growth patterns between males and females exist after the age of seven, and perhaps before that age. Surprisingly, the difference appears to be that females exhibit significant shape changes within the modules under study, while males do not. It is likely that the males do experience similar patterns of shape change as the females throughout ontogeny (based upon the confidence intervals), but not different enough among age groups to produce significant results. More importantly, the results of this research offer new

information for our understanding of postnatal growth by revealing how particular regions of the craniofacial complex change throughout ontogeny. In this section, the results for hypothesis two are discussed in detail individually for males and females. This is followed by a discussion of some potential explanations for the sexual differences in patterns of growth.

Female Patterns of Growth

The multivariate analysis of variance (MANOVA) and Euclidean distance matrix analysis (EDMA) results are very similar, except that the MANOVA indicated no significant difference between age groups for the sphenoid module while the EDMA results reveal a significant difference for this module during late ontogeny. This difference in results is likely due to the types of data being analyzed (principal components for the MANOVA versus Euclidean distances of individual landmarks for EDMA). Since the EDMA results reveal which age groups differ, they are discussed in further detail.

As revealed in the EDMA results, all developmental modules under study, with the exception of the ethmoid module, experience a significant amount of shape change later rather than earlier in ontogeny (i.e., after 13 years of age), but *only among females.* As discussed in Chapter 5 and noted above, the linear distances *collectively* produce an overall shape difference, but not *individually*. Even though no significant confidence intervals were found, the shape of each module can be described according to increases or decreases in the linear distances for each of the landmark pairs defining each module. This reveals which areas of the modules are experiencing the most change throughout ontogeny. Many of these shape changes were mentioned in the previous section and will only be mentioned here in reference to the specific interlandmark distances that contributed to shape changes.

The frontonasal module experiences an increase in the nasal bridge region and a decrease in the nasal aperture region (see Figure5.6 in Chapter 5). For instance, the distance between left and right nasale superius slightly increases as well as the distance between left and right nasomaxillary suture pinch and nasion. A decrease in nasal aperture height (as measured from rhinion to nasospinale) is also seen throughout late postnatal ontogeny. Thus, most of the changes occurring late in ontogeny in the frontonasal module are taking place in the nasal region and not in the premaxilla or the frontal processes of the maxillae.

The confidence intervals of the left and right maxillary modules include interlandmark distances that reveal the medial to lateral and inferior to superior length of the zygomatic bone. Overall, the shape change in the left and right maxillary module consists of increases in the length and height of the zygomatic bone during late ontogeny (from 10-17 years of age). For instance, the interlandmark distance between zygomaxilare and zygotemporale superior increases, widening the midface. An increase in the distance between zygotemporale superior and inferior for both the left and right sides contributes to the superioinferior height increase discussed in Chapter 2.

Most of the interlandmark distances defining the sphenoid show an increase during the later age comparison (Table 5.17; Figure 5.9). Thus, the sphenoid module experiences a lengthening in the anterior-posterior direction throughout late postnatal ontogeny. The sella turcica also increases in its depth, evidenced by the increase in the interlandmark distance between dorsum of sella and sella and between sella and superior sella. Both of these increases occur during the later age comparison (10-13 year olds versus 14-17 year olds). As mentioned in Chapter 2, the anterior-posterior lengthening of the sphenoid contributes to the overall anteroposterior lengthening of the face that occurs throughout ontogeny.

The ethmoid module was the only module to portray shape differences for the early postnatal age comparison (7-9 year olds compared to 10-13 year olds). A lengthening in the anterior-posterior direction of the ethmoid, measured as the linear distance between neck of crista galli and ethmoidale, occurred during the early ontogenetic age comparison. According to the current literature, the cribriform plate ceases growth around two to three years of age (Enlow 1968; Enlow and Bang 1965; Scheuer and Black 2000). Therefore, this increase in length between neck of crista galli and ethmoidale is likely due to movement of the neck of crista galli landmark and not the ethmoidale landmark. An increase in length also occurred in the distances between left and right medioorbitale and ethmoidale. Since it is expected that ethmoidale will not change position due to cessation of growth for the cribriform plate around two to three years of age, left and right medioorbitale are likely driving the increase in distance. This is potentially an effect of the widening of the frontonasal region near the nasal bridge, as previously discussed. Nevertheless, all of these increases in length are consistent with what is currently known about the movement of the ethmoid throughout postnatal ontogeny, that it experiences a downward and forward drift due to displacement (Enlow 1968; Enlow and Bang 1965).

The fact that the ethmoid module is the only one to display significant shape changes during early ontogeny reveals that it may not play a significant role, at least after the age of nine, in establishing adult craniofacial variation. It is the only module that shows no significant shape change after nine years of age, indicating that any growth that occurs after this period is internally proportional (though it does shift as a whole unit relative to the other modules). However, significant shape change is detected in early ontogeny (versus late ontogeny as shown in the other modules) since it continues to ossify after birth (unlike the ossification patterns of the other four modules under investigation). The sphenoeithmoidal synchondrosis, captured by

sphenoethmoidal (landmark 32), fuses around 6-7 years of age. Even though this is a landmark that is part of the sphenoid module, early fusion of this area is consistent with the absence of shape change seen in the ethmoid bone for the current sample under study. More research is needed to investigate the influence of the ethmoid bone on craniofacial growth throughout postnatal ontogeny. This is discussed in further detail in a later section of this chapter.

Male Patterns of Growth

As stated above, unlike females, males did not show any significant shape differences of the five modules under study for the later age comparison (10-13 year olds compared to 14-17 year olds). Potential reasons for this are discussed in the next section. In fact, the only significant male shape difference was found in the ethmoid module for the early age comparison (7-9 year olds versus 10-13 year olds). Even though significance at alpha 0.05 was lost after correcting for multiple comparisons, males display a trend of change across age groups for the ethmoid module. Based upon the results of the confidence interval testing, the same linear distances increased with age as seen in the females. This indicates that males and females experience similar growth patterns for this module, but not for the other four modules under investigation.

Explanations for Sexual Differences

The results of this study support the current hypothesis that adult sexual dimorphism is the result of differential growth patterns between males and females. According to this research, males and females portray different ontogenetic growth trajectories for four of the five modules under investigation (the frontonasal, left and right maxillary, and sphenoid modules). While all modules increase in size with age, it is apparent that males must establish definitive shape for

each module under examination prior to either of the increased growth periods under examination in this study.

When analyzing shape changes in different regions of the face, females show the greatest amount of shape change at or around the time of adolescence. This is evident from the absence of significant shape change for four modules in the first age comparison (7-9 year olds compared to 10-13 years olds). Males, on the other hand, show no significant shape changes for four of the five modules regardless of which ages are being compared. This pattern of results could be due to males experiencing rate or time hypermorphosis (German and Stewart 2001; Ravosa 1991; Shea 1986; Shea 1988).

Rate hypermorphosis occurs when one sex develops at a faster rate than the other sex, but both sexes attain maturity at the same chronological age (Figure 6.1). Time hypermorphosis, in comparison, occurs when both sexes develop at the same rate, but one has a longer developmental period. Multiple studies on primates have shown that these processes are present in establishing sexual dimorphism, from overall human size (German and Stewart 2001) to cranial traits in macaques, spider monkeys, capuchins, and squirrel monkeys (Corner and Richtsmeier 1992). These and other studies have established that both kinds of hypermorphosis occur across primate taxa.

Humans may experience both forms of hypermorphosis; females and males have different periods of growth (see Figure 3.1), as well as different rates. The males in the current sample could potentially be growing at a faster rate than females (i.e., developing dimorphic traits at an earlier age). Since the youngest age group under study is seven years, it is possible that the males have already experienced the majority of shape changes early in ontogeny.

Because the data do not include this younger group, such shape changes are undetectable in this sample.

Another possibility is that the males in this sample experienced time hypermorphosis (Figure 6.1). This means that males experience shape changes at a slower rate than females (i.e., shape changes are spread out over a longer duration during ontogeny). A slow rate of shape change, then, would not be statistically detectable. Females, on the other hand, may have experienced shape changes for a short duration of time, making them detectable when statistically compared among modules. The latter scenario is supported by this study, as shape change was only detected in females late in ontogeny. Without younger individuals, however, the possibility remains that males exhibit sexually dimorphic shape change earlier in primary growth.

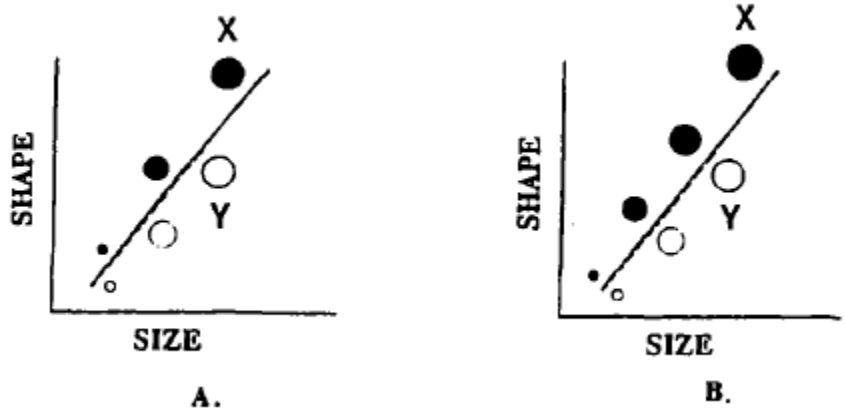

Figure 6.1. Rate (A) and time (B) hypermorphosis.
Differences in patterns of ontogeny for males and females could be explained by (A) males (X) growing at a faster rate than females (Y), referred to as rate hypermorphosis or (B) males growing for a longer duration of time, referred to as time hypermorphosis (adapted from Ravosa 1991).

As noted above, the only similarity in shape change observed between males and females occurs in the ethmoid during the first growth rate increase (between ages 7 and 9). In this study, the ethmoid is defined by four landmarks: neck of crista galli, left and right medio-orbitale, and ethmoidale (Phulari 2013; see also Chapters 2 and 4). When one considers the location of these four landmarks (i.e., two of the four landmarks are located in the orbital region), the differences in shape that occur early in ontogeny could potentially be explained as a by-product of significant changes taking place in the nasal and orbital regions from seven to nine years of age. For instance, research has shown that the medial walls of the orbits experience two major growth spurts, one during the first year of life and the second between six and eight years of age (Dixon et al. 1997). This typically occurs in an anterior direction, which matches the displacement observed in both left and right medioorbitale. The ethmoid's involvement in the nasal region could also be a driving force for the shape changes seen early in ontogeny (as discussed in Chapter 2). Perhaps one of the most noteworthy findings in this research is that unlike the other four modules under study, the ethmoid is the only one that does not differ in its growth trajectory between the sexes. This could potentially mean that after the age of nine, males and females do not portray sexual dimorphism of the ethmoid bone. There is currently no research available that investigates sexual dimorphism of the adult ethmoid bone.

Limitations and Future Directions of this Research

Potential Limitations

It is important to note some of the limitations in this study that could potentially be contributing to the observed differences and similarities between male and female ontogenetic trajectories of the five modules under study. Clearly, without elaboration and as noted above,

restricting the sample to be between ages seven and seventeen may not allow us to document sexually dimorphic growth earlier in primary growth. Also, the sample used in this study is skewed toward the median ages (9-15 years) and could be limiting the analysis. Expanding the sample to include younger individuals would address this.

As mentioned in Chapter 4, no information on ancestry was associated with the individuals in this study. Previous studies, as reviewed in Chapter 3, have established distinction in the growth trajectories of different human populations. Therefore, it is possible that a combination of groups with distinct but non-parallel growth trajectories could be contributing to the lack of statistically significant results for many of the dimensions observed; that is, undetected sample substructure could be adding variance to this study that obscures patterns. A study that could re-evaluate the current research hypotheses using a sample of known ancestry would be able to determine if the patterns revealed in this research are confounded by unexamined ancestral differences.

As stated in Chapters 4 and 5, the ethmoid module was comprised of the fewest number of landmarks. Also, according to the mean standard deviations, four landmarks used in this study showed a low precision rate (i.e., a value of 0.5 mm or greater). It is important to note that two of these four landmarks are located on the ethmoid. The fewer landmarks and increased error variance in precision rate could potentially be contributing to the significant results found for the ethmoid module. However, this is likely not the case since other landmarks are also contributing to the shape differences seen in the ethmoid, as revealed in the EDMA results (see Tables 5.18 and 5.19). Furthermore, unless this is systematic (i.e., the landmark placement error increases with age or is sex-specific), the effect should be minimal.

Perhaps the most important limitation of this study is the choice of landmarks. The results of this study are inherently contingent upon the number and types of landmarks that were chosen to analyze the two hypotheses. As discussed in the geometric morphometric literature (Bookstein 1991; O'Higgins 2000; Zelditch et al. 2004), landmark choice plays a significant role in any study that evaluates differences in shape. There is a chance that if some landmarks were taken out of the study and/or if other landmarks were added into the study, the results would be affected. As discussed in Chapter 2, the landmarks used in this study were chosen for particular reasons as each of them illuminates various growth processes and interactions between modules. All landmarks used in this study, therefore, are considered to be biologically meaningful and ontogenetically important. Nevertheless, it is important to keep in mind that since a particular number of landmarks and various types of landmarks define each module under study; the results of this research are inherently contingent upon landmark choice.

Future Directions

This dissertation is a first attempt to investigate the postnatal ontogenetic changes and interactions of developmental modules of the craniofacial complex. The results of this dissertation reveal that more research is needed to provide a complete synopsis of how postnatal ontogenetic growth processes contribute to ultimate adult morphologies. As with most research, obtaining a larger sample size would be the first step in improving this study. Of course, a larger sample size of known age, sex, and ancestry that encompassed a wider range of ages (e.g., birth to 18 years of age) would be the best type of data to utilize for the hypotheses being tested in this research. As discussed in Chapter 5, there are potential limitations in any study utilizing cross-sectional data. The most thorough analysis of postnatal growth would result from a longitudinal study. Also, as briefly discussed in the beginning of this chapter, using individual's biological

ages in this research may be masking the proportionality results. A future study, using tooth eruption to estimate the skeletal age of the individuals, is needed to determine if the growth trajectories of the individuals would change, potentially altering the results of this study. This would be especially useful for biological anthropologists who are often only able assess skeletal age. Additionally, the results of this research have revealed a number of questions pertaining to the ethmoid bone. A more extensive investigation of this bone and its potential role in the establishment of adult facial morphology is needed. The current research defined the ethmoid module using four three-dimensional landmarks; however, future research should include more landmarks to provide the most complete picture of the shape changes that take place in the ethmoid bone throughout postnatal growth.

Conclusions

In sum, this research provides an initial investigation into the postnatal changes that take place in the mid-face of human juveniles (ages 7-17) through an assessment of five developmental modules of the splanchnocranium. Three research questions were posed in the introductory chapter. The conclusions drawn from this research are therefore best summarized through a response to these three questions which includes implications that result from this study:

1) Are proportions among the facial modules set early in ontogeny?

With the exception of the ethmoid module, proportions among the facial modules under study are set earlier than age seven, and are further elaborated throughout postnatal growth. While most previous studies have utilized principal components to evaluate postnatal

ontogenies (Vioarsdottir and Cobb 2004; Vioarsdottir et al. 2002), this study took a different approach and assessed proportionality among modules of the face. If the results of this study hold true for other samples of larger size and of known sex, age, and ancestry, then this has an effect on how biological anthropologists describe patterns of growth in human juveniles, and the origins of sexual dimorphism. This, in turn, has implications from forensic applications to evolutionary models. From an evolutionary perspective, proportional growth among modules of the face implies that epigenetic or environmental factors occurring during postnatal growth after age six do not play a significant role in producing adult craniofacial variation, or affect the growth of all of the modules equally. A more interesting finding in response to this research question is that the ethmoid module does not portray proportionality throughout ontogeny. While the ethmoid bone is not often utilized in studies of ontogeny, due to the nature of the sample being utilized (i.e., archaeological or cadaveric samples), the results of this research warrants the need for more ontogenetic studies to use data obtained from clinical samples and to include more of the cranium than just surface facial landmarks when examining ontogenetic patterns.

2) Which modules of the splanchnocranium experience the most change during postnatal growth and development?

The results of this research reveal that the answer to this question depends on the sex under study (males or females). For females, at some point during postnatal ontogeny, all five modules experience significant shape change. The frontonasal, left and right maxillary, and sphenoid modules all experience significant shape changes late in ontogeny (after 13 years of age), while the ethmoid experiences change earlier in ontogeny (between 7-9 years of age). For males, only the ethmoid module experiences significant change during postnatal growth after age

six, but this change only occurs during the first accelerated growth period (between 7-9 years of age).

These results have many implications. First, they indicate that all regions of the face play a significant role in establishing adult craniofacial variation, especially dimorphic variation. Secondly, these results imply that at least for females, changes in independent regions of the face contribute to overall craniofacial variation. Lastly, these results echo the implications of the first research question. That is, the ethmoid should be included as part of the craniofacial complex in all studies of postnatal growth, as it plays a significant role in establishing variation early in ontogeny.

3) How do males and females differ in the developmental trajectories of the five independent craniofacial modules under study?

Males and females differ in the developmental trajectories of four of the five craniofacial modules under study. These four modules include the frontonasal, left and right maxillary, and the sphenoid modules. The ethmoid module portrayed the same growth trajectory for males and females. These results provide supporting evidence for the current hypothesis that adult facial dimorphism is established through differential growth trajectories between males and females, perhaps as a result of rate hypermorphosis. Within the field of anthropology, this implies that males and females should be studied separately, especially in research utilizing juveniles. These findings also reveal that the ethmoid may not be a useful indicator of sex after the age of nine; however, as argued above, this is a hypothesis that needs further investigation.

REFERENCES CITED

Acheson R, and Archer M. 1959. Radiological studies of the growth of the pituitary fossa in man. Journal of Anatomy 93:52-67.

Ackerman R, and Krovitz GE. 2002. Common patterns of facial ontogeny in the hominid lineage. Anatomical Record 269:142-147.

Ackermann R. 2005. Genetic integration of the hominoid face. Journal of Human Evolution 48:175-197.

Ackermann R, and Cheverud JM. 2004. Detecting genetic drift versus selection in human evolution. Proceedings of the National Academy of Sciences 101:17946-17951.

Ackermann R, and Krovitz GE. 2002. Common patterns of facial ontogeny in the Hominid lineage. The Anatomical Record 269:142-147.

Aldridge K, Boyadjiev S, Capone G, DeLeon V, and Richtsmeier J. 2005. Precision and error of three-dimensional phenotypic measures acquired from photogrammetric images. American Journal of Medical Genetics 15(138A(3)):247-253.

Bastir M, and Rosas A. 2004. Facial heights: Evolutionary relevance of postnatal ontogeny for facial orientation and skull morphology in humans and chimpanzees. Journal of Human Evolution 47:359-381.

Bastir M, and Rosas A. 2005. Hierarchical nature of morphological integration and modularity in the human posterior face. American Journal of Physical Anthropology 128:26-34.

Bastir M, Rosas A, and O'Higgins P. 2006. Craniofacial levels and morphological maturation of the human skull. Journal of Anatomy 209(5):637-654.

Björk A. 1966. Sutural growth of the upper face studies by the implant method. Acta Odontologica Scandinavica 24:109-129.

Björk A, and Skieller V. 1976. Postnatal growth and development of the maxillary complex. In: Jr JM, editor. Factors affecting the growth of the midface. Monograph No6, Craniofacial Growth Series, Center for Human Growth and Development. Ann Arbor, University of Michigan.

Boas F. 1912. Changes in bodily form of descendants of immigrants. New York: Columbia University Press.

Bogin B. 1999. Patterns of human growth. Cabridge: Cambridge University Press.

Bogin B. 2003. The human pattern of growth and development in paleontological perspective. In: Thompson J, Krovitz G, and Nelson A, editors. Patterns of growth and development in the Genus Homo. Cambridge: Cambridge University Press. p 15-44.

Bolker J. 2000. Modularity in development and why it matters to evo-devo. American Zoology 40(5):770-776.

Bookstein FL, editor. 1991. Morphometric tools for landmark data: geometry and biology: Cambridge University Press, Cambridge (UK), New York.

Bookstein FL, Gunz P, Mitteroecker P, Prossinger H, Schaefer K, and Seidler H. 2003. Cranial integration in Homo: singular warps analysis of the midsagittal plane in ontogeny and evolution. Journal of Human Evolution 44:167-187.

Buck T, and Vidarsdottir U. 2004. A proposed method for the identification of race in sub-adult skeletons: a geometric morphometric analysis of mandibular morphology. Journal of Forensic Sciences 49(6):1-6.

Bulygina E, Mitteroecker P, and Aiello L. 2006. Ontogeny of facial dimorphism and patterns of individual development within one human population. American Journal of Physical Anthropology 131:432-443.

Buschang R, Baume R, and Nass G. 1983. A craniofacial growth maturity gradient for males and females between 4 and 16 years of age. American Journal of Physical Anthropology 61:373-381.

Cameron N. 2002. Human growth and development. California: Academic Press.

Cattell R. 1966. The scree test for the number of factors. Multivariate Behavioral Research 1:629-637.

Chapman R. 1990. Conventional Procrustes approaches. In: Rohlf F, and Bookstein F, editors. Proceedings of the Michigan morphometrics workshop (Special publication No 2). Ann Arbor: Univerisity of Michigan Museum of Zoology. p 251-267.

Cheverud J. 1982. Phenotypic, genetic, and environmental integration in the cranium. Evolution 36:449-516.

Cheverud J. 1988. A comparison of genetic and phenotypic correlations. Evolution 42:958-968.

Cheverud J. 1995. Morphological integration in the saddle-back tamarin (Saguinus fuscicollis) cranium. American Naturalist 145:63-89.

Cheverud J. 1996. Developmental integration and the evolution of pleiotropy. American Zoologist 36:44-50.

Chilton L, Dorst J, and Garn S. 1983. The volume of the sella turcica in children: new standards. American Journal of Roentgenology 140:797-801.

Cobb S. 2001. Form variation in the postnatal facial skeleton of the African apes: University College London.

Cobb S, and O'Higgins P. 2004. Hominins do not share a common postnatal facial ontogenetic shape trajectory. Journal of Experimental Biology 302b:302-321.

Collard M, and O'Higgins P. 2001. Ontogeny and homoplasy in the papionin monkey face. Evolution and Development 3:322-331.

Corner B, and Richtsmeier J. 1992. Cranial growth in the squirrel monkey (Saimiri sciureus): a quantitative analysis using three dimensional coordinate data. American Journal of Physical Anthropology 87(1):67-81.

Cortella S, Shofer F, and Ghafari J. 1997. Transverse development of the jaw: norms for the posteroanterior cephalometric analysis. American Journal of Orthodontics and Dentofacial Orthopedics 112:519-522.

Cramon-Taubadel NV, Frazier B, and Lahr M. 2007. The problem of assessing landmark error in geometric morphometrics: theory, methods, and modifications. American Journal of Physical Anthropology 134:24-35.

Dixon A, Hoyte D, and Ronning O. 1997. Fundamentals of craniofacial growth. Boca Raton, Florida: CRC Press.

Edwards C, Marshall S, Qian F, Southard K, Franciscus R, and Southard T. 2007. Longitudinal study of facial skeletal growth completion in 3 dimensions. American Journal of Orthodontics and Dentofacial Orthopedics 132(6):762-768.

Enlow D. 1968. The Human Face: An account of the postnatal growth and development of the craniofacial skeleton. Row H, editor. New York.

Enlow D. 1990. Facial growth. Philadelphia: W B Saunders Co. 572 p.

Enlow D, and Bang S. 1965. Growth and remodeling of the human maxilla. American Journal of Orthodontics 51:446-464.

Enlow D, and Hans M. 1996. Essential of facial growth. Philadelphia: W.B. Saunders.

Enlow D, and Hunter W. 1966. A differential analysis of sutural and remodeling growth in the human face. American Journal of Orthodontics 52:823-830.

Ewing S, and Harris E. 2000. Craniofacial growth of Dutch-Americans: a longitudinal craniometric study. Journal of Dental Research 79:1468.

Field A. 2013. Discovering statistics using IBM SPSS Statistics. Los Angeles: Sage Publications Ltd.

Garvin H, and Ruff C. 2012. Sexual dimorphism in skeletal browridge and chin morphologies determined using a new quantitative method. American Journal of Physical Anthropology 147(4):661-670.

Gazi-Coklica V, Muretic Z, Brcic R, Kern J, and Milicic A. 1997. Craniofacial parameters during growth from the deciduous to permanent dentition-a longitudinal study. European Journal of Orthodontics 19:681-689.

German R, and Stewart S. 2001. Sexual dimorphism and ontogeny in primates. In: Minugh Purvis N, and McNamara K, editors. Human evolution through developmental change. Baltimore: John Hopkins University Press. p 207-222.

Gilbert S. 2006. Developmental biology. Associates S, editor. Sunderland, MA.

Gkantidis N, and Halazonetis D. 2011. Morphological integration between the cranial base and the face in children and adults. Journal of Anatomy 218:426-438.

Goodall C. 1991. Procrustes methods in the statistical analysis of shape. Journal of the Royal Statistical Society Series B 53:285-339.

Hallgrimsson B, Dorval C, Zelditch M, and German R. 2004. Craniofacial variability and morphological integration in mice susceptible to cleft lip and palate. Journal of Anatomy 205:501-517.

Harris E, Hicks J, and Barcroft B. 2001. Tissue contributions to sex and race: differences in tooth crown size of deciduous molars. American Journal of Physical Anthropology 115:223 237.

Hennessy RJ, and Stringer CB. 2002. Geometric morphometric study of the regional variation of modern craniofacial form. American Journal of Physical Anthropology 117:37-48.

Howells W. 1973. Cranial variation in man. A Study by multivariate analysis of patterns of differences among recent human populations. Papers of the Peabody Museum of Archaeology and Ethnology. Cambridge, Mass:Peabody Museum.

Hubbe M, Hanihara T, and Harvati K. 2009. Climate signatures in the morphological differentiation of worldwide modern human populations. The Anatomical Record 292(11):1720-1733.

Jungers W, Falsetti A, and Wall C. 1995. Shape, relative size, and size adjustments in morphometrics. Yearbook of Physical Anthropology 38:137-161.

Kimmerle E, Rosas A, and Slice D. 2008. Sexual dimorphism in America: Geometric morphometric analysis of the craniofacial region. Journal of Forensic Sciences 53(1):54 57.

Klingenberg C. 2008. Morphological integration and developmental modularity. Annual Review of Ecology, Evolution and Systematics 39:115-132.

Klingenberg C, Barluenga M, and Meyer A. 2002. Shape analysis of symmetric structures: quantifying variation among individuals and asymmetry. Evolution 56:1909-1920.

Klingenberg C, and McIntyre G. 1998. Geometric morphometrics of developmental instability: analyzing patterns of fluctuating asymmetry with Procrustes methods. Evolution 52:1363-1375.

Klingenberg CP. 2011. MorphoJ: an integrated software package for geometric morphometrics. Molecular Ecology Resources 11:353-357.

Korkmaz S, and Goksuluk D. 2014. MVN: Multivariate Normality Tests. R package version 3.5.

Krieg W. 1987. Early facial growth alterations. Angle Orthodontist 57:50-62.

Krovitz G. 2000. Three-dimensional comparisons of craniofacial morphology and growth patterns in Neandertals and modern humans: John Hopkins University.

Lande R. 1979. Quantitative genetic analysis of multivariate evolution, applied to brain:body size allometry. Evolution 33(1):402-416.

Lang J. 1989. Clinical anatomy of the nose, nasal cavity and paranasal sinuses. New York: Thieme.

Latham R. 1972. The sella point and postnatal growth of the human cranial base. American Journal of Orthodontics 61:156-162.

Lele S. 1993. Euclidean distance matrix analysis (EDMA): estimation of mean form and mean form difference. Mathematical Geology 25:573-602.

Lele S, and III TC. 1996. A new test for shape differences when variance-covariance matrices are unequal. Journal of Human Evolution 31:193-212.

Lele S, and Richtsmeier J. 1991. Euclidean distance matrix analysis: a coordinate-free approach for comparing biological shapes using landmark data. American Journal of Physical Anthropology 86(3):415-427.

Lele S, and Richtsmeier J. 1995. Euclidean distance matrix analysis: confidence intervals for form and growth comparison. American Journal of Physical Anthropology 98(1):73-86.

Lele S, and Richtsmeier J. 2000. An invariant approach to the statistical analysis of shapes. London: Chapman & Hall/CRC Press.

Leon MS, and Zollikofer CP. 2001. Neanderthal cranial ontogeny and its implications for late hominid diversity. Nature 412:534-538.

Lieberman D, Carlo J, Leon MPd, and Zollikofer C. 2007. A geometric morphometric analysis of heterochrony in the cranium of chimpanzees and bonobos. Journal of Human Evolution 52:647-662.

Lieberman D, Krovitz G, Yates F, Devlin M, and Claire MS. 2004. Effects of food processing on masticatory strain and craniofacial growth in a retrognathic face. Journal of Human Evolution 46:655-677.

Lieberman D, Pearson O, and Mowbray K. 2000. Basicranial influence on overall cranial shape. Journal of Human Evolution 38:291-315.

Lieberman D. 2011. The evolution of the human head. Cambridge, MA: The Belknap Press of Harvard University Press.

Lieberman D, McBratney BM, and Krovitz G. 2002. The evolution and development of cranial form in Homo sapiens. Proceedings of the National Academy of Sciences 99:1134-1139.

Little BB, Buschang PH, Reyes MEP, Tan SK, and Malina RM. 2006. Craniofacial dimensions in children in rural Oaxaca, Southern Mexico: secular change, 1968-2000. American Journal of Physical Anthropology 131:127-136.

Maddux S. 2011. A quantitative assessment of infraorbital morphology in Homo: testing for character independence and evolutionary significance in the human midface. University of Iowa.

Marroig G, and Cheverud J. 2001. A comparison of phenotypic variation and covariation patterns and the role of phylogeny, ecology and ontogeny during cranial evolution of New World monkeys. Evolution 55:576-600.

Martin R. 1956. Lehrbuch der anthropologie. Revised 3rd Edition, Volume 3, edited by Karl S Saller. Gustav Fischer Verlag: Stuttgart.

Martin R, Willner L, and Dettling A. 1994. The evolution of sexual dimorphism in primates. In: Short R, and Balaban E, editors. The differences between the sexes. Cambridge: Cambridge University Press. p 159-200.

Martinez-Abadia N, Esparza M, Sjovold T, Gonzalez-Jose R, Santos M, and Hernandez M. 2009. Heritability of human cranial dimensions: comparing the evolvability of different cranial regions. Journal of Anatomy 214:19-35.

May R, and Sheffer D. 1999. Growth changes in measurements of upper facial positioning. American Journal of Physical Anthropology 108(3):269-280.

McCarthy R. 2004. Constraints on primate craniofacial growth and architecture [Dissertation]. New Brunswick: The George Washington University.

McCarthy R, and Lieberman D. 2001. The posterior maxillary (PM) plane and anterior cranial architecture in primates. Anatomical Record 264:247-260.

Mitteroecker P, and Bookstein F. 2007. The conceptual and statistical relationship between modularity and morphological integration. Systematic Biology 56:818-836.

Mitteroecker P, and Bookstein F. 2008. The evolutionary role of modularity and integration in the hominoid cranium. Evolution 62(4):943-958.

Mitteroecker P, Gunz P, Bernhard M, Schaefer K, and Bookstein FL. 2004. Comparison of cranial ontogenetic trajectories among great apes and humans. Journal of Human Evolution 46:679-697.

Molleson T, and Cox. 1993. The Spitalfields Project. Volume 2-The Anthropology-The Middling Sort, Research Report 86. London: Council for British Archaeology.

Mooney M, and Siegel M. 2002. Understanding craniofacial anomalies: The etiopathogenesis of craniosynotoses in facial clefting. New York: Wiley-Liss, Inc.

Moss M. 1968. The primacy of functional matrices in orofacial growth. Dental Practitioner 19:63-73.

Moss M, and Bromberg B. 1968. The passive role of nasal septal cartilage in mid-facial growth. Plastic and Reconstructive Surgery 41:536-542.

Moss M, and Salentijn L. 1969. The primary role of functional matrices in facial growth. American Journal of Orthodontics 55:566-577.

Moss M. 1997. The functional matrix hypothesis revisited. 1. The role of mechanotransduction. American Journal of Orthodontics and Dentofacial Orthopedics 112:8-11.

Moss M, and Young RW. 1960. A functional approach to craniology. American Journal of Physical Anthropology 18:281-292.

Noback ML, Harvati K, and Spoor F. 2011. Climate-related variation of the human nasal cavity. American Journal of Physical Anthropology 145(4):599-614.

O'Higgins P. 2000. The study of morphological variation in the hominid fossil record: biology, landmarks and geometry. Journal of Anatomy 197:103-120.

O'Higgins P, and Collard M. 2002. Sexual dimorphism and facial growth in Papionin monkeys. Journal of Zoology 257:255-272.

O'Higgins P, and Dryden I. 1993. Sexual dimorphism in hominoids: further studies of craniofacial shape differences in Pan, Gorilla and Pongo. Journal of Human Evolution 24:183-205.

O'Higgins P, and Vioarsdottir U. 1999. New approaches to the quantitative analysis of craniofacial growth and variation. In: Hoppa R, and FitzGerald C, editors. Human Growth in the Past: studies from bones and teeth. Cambridge: Cambridge University Press. p 128-160.

Olson E, and Miller R. 1958. Morphological integration. Chicago: University of Chicago Press.

Pearson O, and Lieberman D. 2004. The aging of Wolff's "law": ontogeny and responses to mechanical loading in cortical bone. American Journal of Physical Anthropology 39:63 99.

Phulari B. 2013. An atlas on cephalometric landmarks: Jaypee Brothers, Medical Publishers.

Pinhasi R, Eshed V, and Shaw P. 2008. Evolutionary changes in the masticatory complex following the transition to farming in the Southern Levant. American Journal of Physical Anthropology 135:136-148.

Plavcan J, Schaik v, Schaik Cv, and Kappeler P. 1995. Competition, coalitions and canine size in primates. Journal of Human Evolution 28:245-276.

Plavcan JM, and Cope DA. 2001. Metric variation and species recognition in the fossil record. Evolutionary Anthropology 10(6):204-222.

Polly PD. 2012. Euclidean distance matrix analysis. Department of Geological Sciences, Indiana University.

Raff R. 1996. The shape of life: genes, development and the evolution of animal form. Press UoC, editor. Chicago.

Ranly D. 1988. A synopsis of craniofacial growth. Lange AA, editor. Norwalk.

Ravosa M. 1991. The ontogeny of cranial sexual dimorphism in two old world monkeys: Macaca fascicularis (Cercopithecinae) and Nasalis larvatus (Colobinae). International Journal of Primatology 12(4):403-426.

Ravosa M, and Shea B. 1994. Pattern in craniofacial biology: evidence from the Old World monkeys (Cercopithecidae). International Journal of Primatology 15:801-822.

Relethford JH. 1994. Craniometric variation among modern human populations. American Journal of Physical Anthropology 95:53-62.

Relethford JH. 1998. Genetics of modern human origins and diversity. Annual Review of Anthropology 27:1-23.

Relethford JH. 2004. Global patterns of isolation by distance based on genetic and morphological data. Human Biology 76(4):499-513.

Richtsmeier J, Cheverud J, Danahey S, Corner B, and Lele S. 1993. Sexual dimorphism of ontogeny in the crab eating macaque (Macaca fasciularis) Journal of Human Evolution 25:130.

Richtsmeier J, Cheverud J, and Lele S. 1992. Advances in anthropological morphometrics. Annual Review of Anthropology 21:231-253.

Richtsmeier J, DeLeon V, and Lele S. 2002. The promise of geometric morphometrics. Yearbook of Physical Anthropology 45:63-91.

Richtsmeier J, III TC, Valeri C, Krovitz G, and Lele S. 1998. Pre-operative morphology and development in sagittal synostosis. Journal of Craniofacial Genetic and Developmental Biology 18(2):64-78.

Richtsmeier J, and Lele S. 1993. A coordinate-free approach to the analysis of growth patterns: models and theoretical considerations. Biological Reviews 68(3):381-411.

Richtsmeier J, Paik C, Elfert P, III TC, and Dahlman H. 1995. Precision, repeatability and validation of the localization of cranial landmarks using computed tomography scans. Cleft Palate-Craniofacial Journal 32(3):217-227.

Rohlf F. 2000. Statistical power comparisons among alternative morphometric methods. American Journal of Physical Anthropology 111:463-478.

Rohlf F, and Slice D. 1990. Extensions of the Procrustes method for the optimal superimposition of landmarks. Systematic Zoology 39:40-59.

Rohlf F, and Marcus L. 1993. A revolution in morphometrics. TREE 8:129-132.

Rolian C. 2014. Genes, development and evolvability in primate evolution. Evolutionary Anthropology 23(3):93-104.

Rosas A, and Bastir M. 2002. Thin-plate spline analysis of allometry and sexual dimorphism in the human craniofacial complex. American Journal of Physical Anthropology 117(3):236-245.

Roseman C, and Weaver T. 2007. Molecules versus morphology? Not for the human cranium. BioEssays 29(12):1185-1188.

Roseman C, Weaver T, and Stringer C. 2011. Do modern humans and Neandertals have different patterns of cranial integration? Journal of Human Evolution 60:684-693.

Roseman C. 2004. Detecting interregionally diversifying natural selection on moden human cranial form using matched molecular and morphometric data. Proceedings of the National Academy of Sciences 101:12824-12829.

Royston J. 1983. Some techniques for assessing multivariate normality based on the Shaprio Wilk W. Applied Statistics 32(2):121-133.

Royston J. 1995. Remark as r94: a remark on algorithm AS 181: The W test for normality.

Applied Statistics 44(4):547-551.

Sardi M, Novellino P, and Pucciarelli H. 2006. Craniofacial morphology in the Argentine Center-West: consequences of the transition to food production. American Journal of Physical Anthropology 130:333-343.

Sardi M, and Ramirez RF. 2012. Different cranial ontogeny in Europeans and Southern Africans. PLoS ONE 7(4).

Sardi M, and Rozzi F. 2005. A cross-sectional study of human craniofacial growth. Annals of Human Biology 32:390-396.

Scheuer J, and Black S, editors. 2000. Developmental juvenile osteology. London.

Schlosser G, and Wagner G. 2004. Modularity in development and evolution. UC Press, editor. Chicago.

Schoenwolf G, Bleyl S, Brauer P, Francis-West P, and Larsen W. 2015. Development of the pharyngeal apparatus and face. Larsen's human embryology. 5th ed. Philadelphia: Elsevier/Churchill Livingstone.

Shea B. 1986. Ontogenetic approaches to sexual dimorphism in anthropoids. In: Evolution H, editor. 1: 97-110.

Shea B. 1988. Heterochrony in primates. In: McKinney M, editor. Heterochrony in evolution. New York: Plenum Press. p 175-205.

Sherwood RJ, Duren DL, Demerath EW, Czerwinski SA, Siervogel RM, and Towne B. 2008. Quantitative genetics of modern human cranial varaition. Journal of Human Evolution 54:909-914.

Sholts S, Walker P, Kuzminsky S, Miller K, and Warmlander S. 2011. Identification of group affinity from cross-sectional contours of the human midfacial skeleton using digital morphometrics and 3D laser scanning technology. Journal of Forensic Sciences

56(2):334-338.

Sparks CS, and Jantz RL. 2002. A reassessment of human cranial plasticity: Boas revisited. Proceedings of the National Academy of Sciences 99:14636-14639.

Sperber G, Guttmann G, and Sperber S. 2001. Craniofacial development. Canada: PMPH-USA.

Strauss A, and Hubbe M. 2010. Craniometric similarities within and between human populations in comparison with neutral genetic data. Human Biology 82(3):315-330.

Trevor. 1950. Osteometry. In *Chamber's Encyclopedia,* vol. I, pp. 458-462. London: George Newnes.

Underwood L, Radcliffe W, and Guinto F. 1976. New standards for the assessment of the sella turcica in children. Radiology 119:651-654.

Ursi W, Trotman C, McNamara J, and Behrents R. 1992. Sexual dimorphism in normal craniofacial growth. The Angle Orthodontist 63(1):47-56.

Vioarsdottir U. 2003. MorFIDS: morphometric forensic identification of sub-adults. American Journal of Physical Anthropology Suppl 36:202.

Vioarsdottir U. 1999. Changes in the facial skeleton during growth: a comparative morphemetric study of modern humans and Neanderthals. University of London (United Kingdom).429.

Vioarsdottir U, and Cobb S. 2004. Inter- and intra-specific variation in the ontogeny of the hominoid facial skeleton: testing assumptions of ontogenetic variability. Annals of Anatomy 186:423-428.

Vioarsdottir U, O'Higgins P, and Stringer C. 2002. A geometric morphometric study of regional differences in the ontogeny of the modern human facial skeleton. Journal of Anatomy 201:211-229.

Wagner G. 1996. Homogenous, natural kinds and the evolution of modularity. American Zoology 36:307-325.

Waitzman A, Posnick J, Armstorng D, and Pron G. 1992. Craniofacial skeletal measurements based on computed tomography: Part II. Normal values and growth trends. The Cleft Palate-Craniofacial Journal 29:118-128.

Weaver TD, Roseman CC, and Stringer CB. 2007. Were neandertal and modern human cranial differences produced by natural selection or genetic drift? Journal of Human Evolution 53:135-145.

Webster M, and Sheets H. 2010. A practical introduction to landmark-based geometric morphometrics. In: Alroy J, and Hunt G, editors. Quantitative methods in paleobiology, pp. 163-188, Paleontological Society Short Course, October 30th, 2010: The Paleontological Society.

Weinberg S, Andreasen N, and Nopoulos P. 2009. Three-dimensional morphometric analysis of brain shape in nonsyndromic orofacial clefting. Journal of Anatomy 214(6):926-936.

Weinberg S, Putz D, Mooney M, and Siegal M. 2002. Nonmetric population variation in perinatal human skulls. American Journal of Physical Anthropology Suppl 34:162.

Weston E, Friday A, and Lio P. 2007. Biometric evidence that sexual selection has shaped the Hominin face. Plos ONE 2(8):e710.

Wood C, and Lynch J. 1996. Sexual dimorphism in the craniofacial skeleton of modern humans. In: Marcus L, editor. Advances in morphometrics. New York: Plenum Press. p 407-414.

Zelditch M, Swiderski D, Sheets H, and Fink W. 2004. Geometric morphometrics of biologists: a primer. San Diego: Elsevier Academic Press

APPENDICES

APPENDIX A: Internal review board proposal.

FORM A

Certification for Exemption from IRB Review for Research Involving Human Subjects

---

A. PRINCIPAL INVESTIGATOR(s) and/or CO-PI(s):

Principal Investigator:
Amber D. Wheat
Graduate Student, Anthropology
University of Tennessee, Knoxville

Faculty Advisor:
Dr. Benjamin M. Auerbach
Assistant Professor, Anthropology
University of Tennessee, Knoxville

Co-PI:
Dr. David Hatcher, D.D.S.
Diagnostic Digital Imaging Center
Sacramento, California

B. DEPARTMENT:
Department of Anthropology, College of Arts & Sciences

C. COMPLETE MAILING ADDRESS AND PHONE NUMBER OF PI(s) and CO-PI(s):
Department of Anthropology
University of Tennessee, Knoxville
250 South Stadium Hall
Knoxville, TN 37996
Tel: 865-974-4408

Diagnostic Digital Imaging Center
99 Scripps Drive #101
Sacramento, CA 95824
Tel: 916-646-3740

D. TITLE OF PROJECT:
Investigating Postnatal Ontogeny in the Craniofacial Complex of Human Juveniles

E. EXTERNAL FUNDING AGENCY AND ID NUMBER:
N/A

F. GRANT SUBMISSION DEADLINE:
N/A

G. STARTING DATE:
December 1, 2013

H. ESTIMATED COMPLETION DATE:
May 1, 2015

I. RESEARCH PROJECT

1. Objective(s) of Project:

The purpose of this IRB review proposal is to obtain approval for research based upon the analysis of de-identified CT scans detailed in the sections to follow. After obtaining IRB approval from the University of Tennessee, the co-PI, Dr. David Hatcher, will allow me to obtain CT scans from the Digital Imaging Center located in Sacremento, California.

Introduction

This project explores the correspondence of skeletal traits of the face throughout primary growth among human juveniles. I will utilize anonymous (i.e., de-identified) DICOM images of juveniles (under the age of 18) to assess the correlation and covariation of the mid-face throughout growth and development. The PI will use these data for the purpose of her dissertation research, which also will be published in a scholarly journal.

Research Objective

Studies of craniofacial variation in humans are a central focus for multiple subdisciplines within biological anthropology. Researchers have analyzed the developmental processes contributing to craniofacial variation from genetic, evolutionary, biomechanical, and forensic perspectives. These studies have long established that craniofacial morphology varies among adults in covariance with geography (Relethford 1994; Relethford 2004; Roseman 2004), as well as between the sexes (Kimmerle et al. 2008; Rosas and Bastir 2002). This variation is the product of functional and structural interactions that occur during ontogeny, overlying genetically controlled growth processes(Enlow and Hans 1996). While this research has helped to unravel the many factors that play a role in producing craniofacial variation, little research exists on how postnatal development contributes to this variation.

This dissertation will document the developmental changes that take place throughout ontogeny in the mid-face of human juveniles to gain a better understanding of how developmental variance and covariance of the facial skeleton establish adult human craniofacial variation. Previous studies, as reviewed below, have established the processes & patterns of development, the covariance of morphological traits of the facial skeleton, and hypotheses of how these relate to adult craniofacial form and variation. Yet, these studies have not clearly established the relationship of ontogenetic developmental variation of the splachnocranium—namely variance in the postnatal facial skeleton—with ultimate adult morphologies.

The main goal of this research is to investigate and describe the developmental changes that take place throughout ontogeny in the mid-face of human juveniles. As previously stated, many studies have documented patterns of ontogeny in non-human primates, hominids, and humans to evaluate how postnatal ontogeny contributes to observed adult craniofacial variation. However, these studies have opposing ideas about how postnatal ontogeny contributes to establishing adult craniofacial variation. This dissertation will use a model-bound approach in an attempt to illuminate the exact role that postnatal ontogeny plays in producing craniofacial variation. Longitudinal data would offer the most precise assessment of postnatal ontogeny, however, if the sample size is large enough, cross-sectional data can provide, with some margin of error, a picture of the average overall postnatal ontogenetic trajectory. To this end, this project will use more than 300 CT scans of juvenile heads (6 months-18 years) to examine the anatomical changes that take place during ontogeny to produce craniofacial variation.

Using a model-bound approach, this research will assess the developmental trajectories of five developmentally independent regions of the face. These include the left and right maxillary processes, the frontonasal process, the ethmoid, and the sphenoid. Here, a model of proportionality among these five regions is proposed to test the hypothesis that proportions of the face are set at birth. By using a model of proportionality, I can address the two opposing hypotheses related to the influence of postnatal ontogeny. If my results fit the model, this indicates support for the hypothesis that facial proportions are set prenatally and are further elaborated throughout postnatal life through parallel developmental processes. This means that each developmental region of the face maintains an independent variance throughout postnatal ontogeny. If my results do not fit the model, this indicates that developmental processes occurring during postnatal ontogeny play a role in producing adult craniofacial variation.

2. Subjects:

To construct our sample, more than 300 de-identified head CT facial scans that are associated with demographic information (age and sex) will be used. These scans come from the Diagnostic Digital Imaging Center located in Sacramento, California. These scans are HIPPA-compliant. All scans will be anonymized by the PI and saved to a CD-R/CD-RW and used for further analyses (see Methods and Procedures section). Therefore, the sample for this research will be constructed from pre-existing data without collecting identifiers. To qualify for selection to be used in the study, the individuals must be under the age of eighteen, portray no facial anomalies, and be associated with demographic information (age and sex).

3. Methods or Procedures:

For this study, three-dimensional surface reconstructions will be produced from the CT images. To investigate ontogenetic trajectories of mid-face morphology, the sample will be divided into different age groups and separated according to sex. Specific anthropometric

landmarks that define mid-face shape will be placed on the three-dimensional images using morphometric software such as Stratovan Checkpoint and/or Amira. These landmarks will be used to define linear distances as well as mid-face contour. To test the model of proportionality, multivariate analysis will be used.

Specific Risks and Protection Measures
The participants of this study do not fall within any known vulnerable population category and will not suffer any physical harm as a result of this study. Since data are being collected from pre-existing scans without collecting identifiers, all subjects will remain anonymous.
Benefits
Participants will receive no direct benefits from this study. Once data are obtained and analyzed, the results of this study will be published through a peer-reviewed journal.

4. **CATEGORY(s) FOR EXEMPT RESEARCH PER 45 CFR 46**:
Category 4: "Research involving the collection or study of existing data, documents, records, pathological specimens or diagnostic specimens, if these sources are publicly available or if the information is recorded by the investigator in such a manner that subjects cannot be identified, directly or through identifiers linked to the subjects."

J. CERTIFICATION: The research described herein is in compliance with 45 CFR 46.101(b) and presents subjects with no more than minimal risk as defined by applicable regulations.

Principal Investigator: Amber D. Wheat (Name) _____ (Signature) 2.18.14 (Date)

Student Advisor: BENJAMIN M. AUERBACH (Name) _____ (Signature) 2/25/2014 (Date)

Department Review Committee Chair: Michael H. Logan (Name) _____ (Signature) 2/18/2014 (Date)

APPROVED:
Department Head: ANDREW KRAMER (Name) _____ (Signature) 3/4/2012 (Date)

COPY OF THIS COMPLETED FORM MUST BE SENT TO COMPLIANCE OFFICE IMMEDIATELY UPON COMPLETION.

Rev. 01/2005

ddi
imaging·center

February 23, 2014

To Whom It May Concern,

I am granting Amber Wheat permission to use de-identified head Cone Beam CT scans from the Diagnostic Digital Imaging Center in California. These studies have already been obtained for clinical purposes and no prospective scans will be obtained for the purpose of research. These scans are HIPPA-compliant. The CBCT scans of juveniles (0-18 years of age) will be anonymized and used by Amber Wheat for her dissertation research.

Sincerely,

David C. Hatcher, D.D.S., M.Sc., M.R.C.D. (c)
Oral & Maxillofacial Radiologist

99 Scripps Drive, Suite 101, Sacramento, California 95825
Telephone (916) 646-3740 Facsimile (916) 646-3742 http://www.ddicentral.com

APPENDIX B: Mean interlandmark distances for 7-9 year old females.

Frontonasal Module															
	NAS	LDAC	RDAC	LNSU	RNSU	LSPI	RSPI	LNIN	RNIN	RHI	LALA	RALA	NSP	SSP	PRO
NAS	0.00														
LDAC	13.23	0.00													
RDAC	13.64	18.43	0.00												
LNSU	6.63	7.03	15.87	0.00											
RNSU	6.92	15.67	7.13	10.78	0.00										
LSPI	8.51	8.20	14.89	4.94	10.75	0.00									
RSPI	8.48	14.68	8.40	10.53	5.01	8.18	0.00								
LNIN	18.88	16.29	21.89	16.03	19.73	11.47	15.26	0.00							
RNIN	19.60	22.47	16.59	20.24	16.71	15.90	12.14	12.17	0.00						
RHI	19.35	21.87	21.86	19.28	19.46	14.88	14.89	8.94	9.27	0.00					
LALA	36.76	29.77	35.46	32.84	36.13	28.67	31.56	19.13	24.66	23.64	0.00				
RALA	36.86	35.77	29.47	36.19	32.87	31.65	28.78	25.05	18.62	23.77	21.22	0.00			
NSP	44.85	41.43	41.15	42.78	42.82	38.02	38.06	27.86	27.31	27.99	15.53	15.64	0.00		
SSP	48.02	44.02	43.68	45.77	45.76	41.07	41.09	31.17	30.56	31.76	17.18	17.12	4.29	0.00	
PRO	60.69	56.66	56.27	58.46	58.44	53.77	53.76	43.54	42.86	43.71	28.43	28.28	16.15	13.01	0.00

Left Maxillary Module						
	LZYM	LZYO	LCHI	LCHS	LZTI	LZTS
LZYM	0.00					
LZYO	28.40	0.00				
LCHI	5.26	25.56	0.00			
LCHS	21.28	11.35	20.22	0.00		
LZTI	27.89	47.71	32.04	38.98	0.00	
LZTS	24.13	38.79	28.03	29.38	11.73	0.00

Right Maxillary Module						
	RZYM	RZYO	RCHI	RCHS	RZTI	RZTS
RZYM	0					
RZYO	28.92	0				
RCHI	5.554	26	0			
RCHS	21.4	11.5	20.3	0		
RZTI	28.13	48.6	32.6	39.8	0	
RZTS	24.11	39.7	28.4	30.2	11.6	0

Sphenoid Module							
	DOS	SEL	LCLI	RCLI	SPE	SPH	SSE
DOS	0.00						
SEL	4.32	0.00					
LCLI	15.32	13.39	0.00				
RCLI	15.86	13.74	24.20	0.00			
SPE	34.70	30.45	28.70	28.93	0.00		
SPH	10.13	6.06	12.27	12.45	25.01	0.00	
SSE	3.51	5.37	14.81	15.29	34.71	9.78	0.00

Ethmoid Module				
	NCRG	LMO	RMO	ETH
NCRG	0.00			
LMO	12.81	0.00		
RMO	12.97	16.86	0.00	
ETH	14.65	24.97	25.01	0.00

APPENDIX C: Mean interlandmark distances for 10-13 year old females.

Frontonasal Module															
	NAS	LDAC	RDAC	LNSU	RNSU	LSPI	RSPI	LNIN	RNIN	RHI	LALA	RALA	NSP	SSP	PRO
NAS	0.00														
LDAC	13.56	0.00													
RDAC	14.10	18.47	0.00												
LNSU	7.38	6.53	16.20	0.00											
RNSU	7.54	15.90	6.96	11.47	0.00										
LSPI	9.48	8.41	15.13	5.70	11.41	0.00									
RSPI	9.22	14.97	8.58	11.21	5.49	8.45	0.00								
LNIN	19.37	16.92	22.34	16.42	20.22	11.22	15.36	0.00							
RNIN	19.76	22.94	17.14	20.61	16.86	15.64	11.89	12.27	0.00						
RHI	21.34	24.33	24.13	21.67	21.67	16.78	16.81	10.45	9.91	0.00					
LALA	39.70	32.53	37.76	35.35	38.70	30.64	33.77	21.68	27.11	26.41	0.00				
RALA	39.70	38.26	31.96	38.74	35.28	33.54	30.90	27.13	21.40	26.18	22.03	0.00			
NSP	48.47	44.95	44.42	46.17	46.13	40.75	40.99	30.96	30.65	30.66	16.70	16.65	0.00		
SSP	51.35	47.17	46.58	48.78	48.71	43.45	43.69	33.99	33.70	34.34	17.87	17.73	4.50	0.00	
PRO	65.97	61.86	61.24	63.48	63.41	58.14	58.36	48.24	47.89	47.83	30.99	30.82	17.64	15.03	0.00

Left Maxillary Module						
	LZYM	LZYO	LCHI	LCHS	LZTI	LZTS
LZYM	0.00					
LZYO	29.60	0.00				
LCHI	5.01	27.34	0.00			
LCHS	21.79	12.36	21.27	0.00		
LZTI	29.67	49.97	33.75	40.25	0.00	
LZTS	26.17	41.19	30.13	30.83	11.85	0.00

Right Maxillary Module						
	RZYM	RZYO	RCHI	RCHS	RZTI	RZTS
RZYM	0.00					
RZYO	30.17	0.00				
RCHI	5.37	27.75	0.00			
RCHS	22.10	12.57	21.44	0.00		
RZTI	29.32	50.43	33.69	40.72	0.00	
RZTS	25.93	41.65	30.18	31.29	11.99	0.00

Sphenoid Module							
	DOS	SEL	LCLI	RCLI	SPE	SPH	SSE
DOS	0.00						
SEL	4.70	0.00					
LCLI	15.37	13.47	0.00				
RCLI	15.57	13.49	24.47	0.00			
SPE	35.46	30.84	29.70	29.83	0.00		
SPH	10.37	6.02	12.39	12.72	25.51	0.00	
SSE	3.72	5.57	14.68	14.98	35.03	9.71	0.00

Ethmoid Module				
	NCRG	LMO	RMO	ETH
NCRG	0.00			
LMO	13.25	0.00		
RMO	13.63	16.95	0.00	
ETH	16.82	27.27	27.54	0.00

APPENDIX D: Mean interlandmark distances for 14-17 year old females.

Frontonasal Module															
	NAS	LDAC	RDAC	LNSU	RNSU	LSPI	RSPI	LNIN	RNIN	RHI	LALA	RALA	NSP	SSP	PRO
NAS	0.00														
LDAC	15.18	0.00													
RDAC	16.06	18.59	0.00												
LNSU	9.30	7.32	15.80	0.00											
RNSU	9.96	16.16	7.21	11.56	0.00										
LSPI	11.96	9.50	15.32	6.30	11.34	0.00									
RSPI	12.15	15.75	9.70	12.31	6.82	9.37	0.00								
LNIN	22.97	19.39	23.75	18.47	21.47	12.79	17.04	0.00							
RNIN	23.33	24.75	18.83	21.94	18.37	16.50	14.15	12.66	0.00						
RHI	24.70	26.03	25.46	23.12	22.87	17.66	18.36	10.19	10.29	0.00					
LALA	43.02	34.76	39.42	37.14	39.82	31.81	35.23	21.85	27.77	26.33	0.00				
RALA	42.87	40.71	33.89	40.51	36.85	34.79	33.01	27.79	22.37	26.79	22.95	0.00			
NSP	50.40	46.68	45.61	47.15	46.89	41.27	42.16	30.43	30.66	30.12	16.84	16.75	0.00		
SSP	53.54	48.93	47.89	49.96	49.62	44.17	44.69	33.65	33.91	34.00	18.06	17.94	5.04	0.00	
PRO	68.90	64.66	63.46	65.57	65.17	59.74	60.41	48.67	48.82	48.18	31.78	31.36	18.82	16.42	0.00

Left Maxillary Module						
	LZYM	LZYO	LCHI	LCHS	LZTI	LZTS
LZYM	0.00					
LZYO	31.51	0.00				
LCHI	7.17	29.17	0.00			
LCHS	23.05	12.81	22.50	0.00		
LZTI	32.26	51.03	34.25	41.32	0.00	
LZTS	30.15	44.76	33.10	34.37	14.09	0.00

Right Maxillary Module						
	RZYM	RZYO	RCHI	RCHS	RZTI	RZTS
RZYM	0.00					
RZYO	30.72	0.00				
RCHI	5.51	27.80	0.00			
RCHS	22.75	14.87	22.69	0.00		
RZTI	30.37	51.22	34.96	40.42	0.00	
RZTS	29.26	43.79	33.30	32.88	14.67	0.00

Sphenoid Module							
	DOS	SEL	LCLI	RCLI	SPE	SPH	SSE
DOS	0.00						
SEL	5.32	0.00					
LCLI	15.47	13.22	0.00				
RCLI	16.13	14.08	24.83	0.00			
SPE	36.58	31.44	30.33	30.76	0.00		
SPH	11.64	7.09	12.78	13.08	25.82	0.00	
SSE	4.56	6.80	15.33	15.77	36.04	10.59	0.00

Ethmoid Module				
	NCRG	LMO	RMO	ETH
NCRG	0.00			
LMO	13.33	0.00		
RMO	14.35	17.44	0.00	
ETH	17.27	27.50	27.23	0.00

Appendix E: Mean interlandark distances for 7-9 year old males.

Frontonasal Module															
	NAS	LDAC	RDAC	LNSU	RNSU	LSPI	RSPI	LNIN	RNIN	RHI	LALA	RALA	NSP	SSP	PRO
NAS	0														
LDAC	14	0													
RDAC	13.9	19.3	0												
LNSU	6.65	7.66	16.02	0											
RNSU	6.49	16.1	7.764	10.3	0										
LSPI	8.29	8.77	14.77	4.75	10.08	0									
RSPI	8.12	15.2	8.616	10.2	4.638	7.75	0								
LNIN	20.3	17.3	22.74	17.3	20.74	13	16.5	0							
RNIN	20.5	23.6	17.14	21.1	17.51	16.7	13.3	12.6	0						
RHI	20.6	23	22.5	20.4	20.34	16.1	16	9.34	8.93	0					
LALA	38.5	31.4	36.68	34.6	37.53	30.6	33.3	19.2	25.2	23.8	0				
RALA	38.4	37.5	30.63	37.6	34.38	33.2	30.6	25.4	19.1	23.8	21.5	0			
NSP	46.8	43.4	42.72	44.7	44.63	40.2	40.2	28.4	28.3	28.4	15.7	16.1	0		
SSP	50.6	46.6	45.81	48.3	48.17	43.8	43.8	32.2	32.1	32.7	17.8	18.1	4.64	0	
PRO	62.5	58.5	57.69	60.3	60.13	55.8	55.8	44	43.7	44.1	28.6	28.5	15.9	12.3	0

Left Maxillary Module						
	LZYM	LZYO	LCHI	LCHS	LZTI	LZTS
LZYM	0.00					
LZYO	30.75	0.00				
LCHI	5.56	27.45	0.00			
LCHS	22.09	13.20	20.65	0.00		
LZTI	28.96	50.61	33.68	40.44	0.00	
LZTS	25.41	41.95	29.75	31.08	11.69	0.00

Right Maxillary Module						
	RZYM	RZYO	RCHI	RCHS	RZTI	RZTS
RZYM	0.00					
RZYO	30.41	0.00				
RCHI	5.71	26.99	0.00			
RCHS	21.99	12.74	20.37	0.00		
RZTI	29.52	50.90	34.45	41.01	0.00	
RZTS	25.66	41.77	30.13	31.27	12.09	0.00

Sphenoid Module							
	DOS	SEL	LCLI	RCLI	SPE	SPH	SSE
DOS	0.00						
SEL	4.49	0.00					
LCLI	16.07	13.96	0.00				
RCLI	16.22	13.98	24.86	0.00			
SPE	35.47	31.02	29.17	29.55	0.00		
SPH	10.45	6.12	12.59	12.80	25.48	0.00	
SSE	3.86	5.64	15.54	15.65	35.45	10.11	0.00

Ethmoid Module				
	NCRG	LMO	RMO	ETH
NCRG	0.00			
LMO	13.81	0.00		
RMO	13.93	17.31	0.00	
ETH	12.87	24.65	24.74	0.00

APPENDIX F: Mean interlandmark distances for 10-13 year old males.

Frontonasal Module															
	NAS	LDAC	RDAC	LNSU	RNSU	LSPI	RSPI	LNIN	RNIN	RHI	LALA	RALA	NSP	SSP	PRO
NAS	0.00														
LDAC	14.17	0.00													
RDAC	15.06	19.36	0.00												
LNSU	7.45	7.19	17.09	0.00											
RNSU	7.70	16.69	7.88	11.82	0.00										
LSPI	9.29	8.56	15.59	5.32	11.38	0.00									
RSPI	9.17	15.34	8.89	11.21	5.19	8.48	0.00								
LNIN	20.37	17.73	23.35	17.30	21.18	12.53	16.41	0.00							
RNIN	20.87	23.92	17.76	21.59	17.74	16.77	13.16	12.73	0.00						
RHI	21.73	24.59	24.54	21.79	21.87	17.23	17.32	10.11	10.21	0.00					
LALA	40.70	33.21	38.42	36.32	39.72	31.89	34.86	21.74	27.26	26.59	0.00				
RALA	40.88	39.29	32.53	39.91	36.42	34.89	32.22	27.56	21.45	26.65	22.23	0.00			
NSP	49.66	45.86	45.15	47.28	47.28	42.21	42.38	31.22	30.85	31.21	16.84	16.80	0.00		
SSP	52.79	48.32	47.54	50.17	50.16	45.15	45.33	34.50	34.13	35.08	18.21	18.18	4.58	0.00	
PRO	66.85	62.43	61.63	64.31	64.29	59.28	59.44	48.20	47.79	48.12	30.80	30.65	17.40	14.47	0.00

Left Maxillary Module						
	LZYM	LZYO	LCHI	LCHS	LZTI	LZTS
LZYM	0.00					
LZYO	30.93	0.00				
LCHI	5.60	28.20	0.00			
LCHS	22.62	12.87	21.79	0.00		
LZTI	30.47	51.67	35.04	41.73	0.00	
LZTS	27.01	42.70	31.38	32.09	12.30	0.00

Right Maxillary Module						
	RZYM	RZYO	RCHI	RCHS	RZTI	RZTS
RZYM	0.00					
RZYO	31.17	0.00				
RCHI	5.58	28.39	0.00			
RCHS	22.72	13.06	21.78	0.00		
RZTI	30.44	52.12	35.03	42.08	0.00	
RZTS	27.24	43.48	31.64	32.78	12.13	0.00

Sphenoid Module							
	DOS	SEL	LCLI	RCLI	SPE	SPH	SSE
DOS	0.00						
SEL	4.81	0.00					
LCLI	15.93	13.87	0.00				
RCLI	16.17	13.91	25.03	0.00			
SPE	36.03	31.28	29.64	30.14	0.00		
SPH	10.54	5.99	12.73	12.93	25.84	0.00	
SSE	3.78	6.01	15.43	15.75	36.00	10.37	0.00

Ethmoid Module				
	NCRG	LMO	RMO	ETH
NCRG	0.00			
LMO	13.76	0.00		
RMO	14.21	17.97	0.00	
ETH	16.84	27.76	28.18	0.00

APPENDIX G: Mean interlandmark distances for 14-17 year old males.

Frontonasal Module															
	NAS	LDAC	RDAC	LNSU	RNSU	LSPI	RSPI	LNIN	RNIN	RHI	LALA	RALA	NSP	SSP	PRO
NAS	0.00														
LDAC	15.17	0.00													
RDAC	16.24	20.39	0.00												
LNSU	8.31	7.32	18.29	0.00											
RNSU	8.42	17.65	8.38	12.85	0.00										
LSPI	9.93	9.25	16.84	5.65	12.30	0.00									
RSPI	9.68	16.35	9.83	12.09	5.58	9.14	0.00								
LNIN	20.61	18.94	24.84	17.70	21.93	12.71	16.87	0.00							
RNIN	20.88	24.97	18.96	22.08	17.99	16.99	13.12	12.92	0.00						
RHI	22.47	26.64	26.81	23.18	23.27	18.45	18.48	10.82	10.80	0.00					
LALA	42.71	34.97	40.59	37.92	41.75	33.35	36.61	23.99	29.52	29.36	0.00				
RALA	42.71	41.09	34.18	41.64	37.99	36.39	33.58	29.50	23.69	29.23	23.26	0.00			
NSP	51.99	48.31	47.74	49.50	49.61	44.16	44.39	33.44	33.31	33.76	17.85	17.85	0.00		
SSP	55.16	50.72	50.04	52.37	52.46	47.12	47.34	36.87	36.71	37.81	19.04	18.99	4.80	0.00	
PRO	70.86	66.50	65.78	68.17	68.24	62.91	63.11	52.13	51.93	52.26	33.19	33.05	19.04	16.14	0.00

Left Maxillary Module						
	LZYM	LZYO	LCHI	LCHS	LZTI	LZTS
LZYM	0.00					
LZYO	33.04	0.00				
LCHI	5.67	30.20	0.00			
LCHS	23.73	13.91	22.78	0.00		
LZTI	31.67	54.16	36.22	43.13	0.00	
LZTS	28.52	44.59	32.77	32.91	13.30	0.00

Right Maxillary Module						
	RZYM	RZYO	RCHI	RCHS	RZTI	RZTS
RZYM	0.00					
RZYO	32.94	0.00				
RCHI	5.58	30.29	0.00			
RCHS	23.74	13.94	22.92	0.00		
RZTI	32.16	54.43	36.57	43.45	0.00	
RZTS	28.76	44.62	32.91	33.00	13.52	0.00

Sphenoid Module							
	DOS	SEL	LCLI	RCLI	SPE	SPH	SSE
DOS	0.00						
SEL	5.09	0.00					
LCLI	16.15	14.08	0.00				
RCLI	16.84	14.47	25.65	0.00			
SPE	38.25	33.22	31.75	31.87	0.00		
SPH	11.11	6.39	12.93	13.44	27.61	0.00	
SSE	4.17	6.35	15.51	16.24	37.96	10.54	0.00

Ethmoid Module				
	NCRG	LMO	RMO	ETH
NCRG	0.00			
LMO	14.14	0.00		
RMO	14.46	18.78	0.00	
ETH	17.14	28.42	28.79	0.00

APPENDIX H: Principal components and corresponding eigenvalues for each module for females.

Table A.1. Principal components for the frontonasal module

Landmark	Principal Components							
(x,y,z coordinate)	PC1	PC2	PC3	PC4	PC5	PC6	PC7	PC8
NASx	0.150	0.152	-0.152	0.092	0.061	-0.169	0.071	-0.112
NASy	0.005	-0.023	0.006	-0.001	-0.002	-0.036	-0.045	-0.023
NASz	0.069	-0.077	-0.016	-0.124	-0.165	0.150	0.070	-0.105
LDACx	0.110	-0.021	-0.136	-0.024	-0.102	0.094	-0.026	0.025
LDACy	0.003	0.160	0.065	0.104	0.232	0.105	-0.042	-0.043
LDACz	0.033	0.066	0.061	-0.218	0.067	0.100	-0.039	-0.005
RDACx	0.082	-0.012	-0.074	-0.033	-0.016	-0.014	-0.051	-0.049
RDACy	-0.002	-0.143	-0.103	-0.089	-0.246	-0.155	-0.063	0.084
RDACz	0.020	0.122	0.009	-0.177	0.043	0.176	-0.075	0.150
LNSUx	0.130	-0.128	-0.071	0.041	-0.006	-0.032	0.006	0.005
LNSUy	0.017	0.296	-0.077	0.135	0.101	-0.121	-0.111	-0.020
LNSUz	0.057	0.184	-0.111	-0.110	-0.113	-0.016	-0.010	-0.086
RNSUx	0.112	-0.135	-0.064	0.067	-0.019	-0.037	-0.009	-0.016
RNXUy	-0.019	-0.296	0.057	-0.165	-0.175	0.073	0.020	0.054
RNSUz	0.059	0.196	-0.084	-0.091	-0.073	-0.019	0.002	-0.058
LSPIx	0.100	-0.244	-0.080	-0.007	-0.033	0.019	0.100	0.049
LSPIy	0.021	0.244	0.013	0.056	0.085	-0.041	-0.028	0.071
LSPIz	0.082	-0.018	-0.068	0.057	-0.035	0.007	0.034	-0.003
RSPIx	0.092	-0.244	-0.037	-0.005	-0.026	0.041	0.049	0.093
RSPIy	-0.023	-0.254	-0.007	-0.046	-0.166	0.038	-0.009	-0.022
RSPIz	0.074	-0.024	-0.105	0.036	0.010	0.023	0.034	-0.052
LNINx	-0.590	0.122	-0.157	0.033	-0.188	-0.035	-0.545	0.164
LNINy	0.162	0.117	0.157	0.089	0.201	0.033	0.175	0.145
LNINz	-0.154	-0.076	-0.037	0.415	-0.093	-0.215	0.120	0.504
RNINx	-0.606	0.044	-0.010	-0.027	0.156	0.204	0.507	-0.261
RNINy	-0.154	-0.071	-0.098	-0.114	-0.113	0.130	0.067	-0.223
RNINz	-0.137	-0.071	0.036	0.352	0.086	-0.042	0.294	0.164
RHIx	-0.112	-0.022	0.665	-0.367	0.098	-0.357	0.014	0.107
RHIy	-0.006	0.001	-0.046	0.023	0.029	0.044	-0.045	0.014
RHIz	0.010	-0.396	0.300	0.245	0.049	0.000	-0.211	-0.186
LALAx	0.119	0.184	0.205	0.093	-0.135	0.408	-0.130	0.116
LALAy	-0.011	-0.010	0.105	0.071	0.199	0.034	-0.064	0.086
LALAz	-0.030	0.010	-0.027	-0.094	0.174	-0.202	-0.174	-0.104
RALAx	0.126	0.166	0.238	0.089	-0.085	0.364	-0.072	0.144
RALAy	0.012	0.004	-0.102	-0.028	-0.214	-0.061	0.070	-0.062
RALAz	-0.033	-0.041	-0.029	-0.104	0.150	-0.224	-0.157	-0.115
NSPx	0.105	0.153	0.076	0.168	-0.154	-0.290	0.054	-0.276
NSPy	0.003	-0.022	-0.007	-0.024	0.078	-0.015	0.038	-0.031
NSPz	-0.027	-0.137	-0.021	0.088	0.214	0.284	-0.145	-0.135

Table A.1 (cont.). Principal components for the frontonasal module

Landmark (x,y,z coordinate)	Principal Components							
	PC1	**PC2**	**PC3**	**PC4**	**PC5**	**PC6**	**PC7**	**PC8**
SSPx	0.110	0.106	-0.033	0.168	-0.068	-0.176	0.042	-0.246
SSPy	0.000	-0.004	0.006	0.002	0.021	-0.015	0.039	-0.021
SSPz	-0.038	0.066	0.101	0.026	-0.022	0.034	-0.045	-0.232
PROx	0.072	-0.121	-0.369	-0.288	0.517	-0.019	-0.012	0.257
PROy	-0.009	0.000	0.031	-0.014	-0.029	-0.014	-0.002	-0.010
PROz	0.016	0.196	-0.010	-0.301	-0.293	-0.056	0.301	0.263

Table A.2. Eigenvalues and percent sample variance for principal components one through eight for the frontonasal module

Principal Components	Eigenvalues	Total Variance (%)
1	0.00	39.24
2	0.00	10.96
3	0.00	7.08
4	0.00	6.62
5	0.00	5.25
6	0.00	3.46
7	0.00	3.18
8	0.00	2.93
Total		78.75

Table A.3. Principal components for the left maxillary module

Landmarks	Principal Component					
(x,y,z coordinate)	PC1	PC2	PC3	PC4	PC5	PC6
LZYMx	0.510	0.565	-0.012	-0.124	0.307	0.245
LZYMy	0.004	0.090	-0.324	-0.353	0.140	-0.348
LZYMz	0.024	0.100	0.058	0.071	0.264	-0.480
LZYOx	-0.479	0.232	0.308	0.181	-0.010	-0.165
LZYOy	0.297	-0.048	0.189	0.230	0.040	-0.010
LZYOz	-0.227	0.267	0.040	-0.035	-0.174	0.230
LCHIx	0.316	-0.199	0.028	-0.067	-0.683	-0.255
LCHIy	-0.119	-0.130	-0.296	-0.443	-0.040	0.199
LCHIz	0.004	-0.215	0.045	-0.054	-0.112	0.412
LCHSx	0.180	-0.510	0.008	0.193	0.290	0.188
LCHSy	0.098	0.210	0.287	0.052	-0.250	0.092
LCHSz	0.173	-0.191	-0.094	0.015	0.063	-0.308
LZTIx	-0.295	-0.127	0.285	-0.512	0.084	-0.009
LZTIy	-0.165	-0.224	0.188	0.195	0.297	0.127
LZTIz	-0.028	0.101	-0.222	0.084	-0.129	0.253
LZTSx	-0.232	0.039	-0.617	0.330	0.012	-0.004
LZTSy	-0.114	0.102	-0.044	0.318	-0.187	-0.060
LZTSz	0.054	-0.064	0.173	-0.081	0.088	-0.108

Table A.4. Eigenvalues and percent sample variance for principal components one through six for the left maxillary module

Principal Components	Eigenvalues	Total Variance (%)
1	0.00	28.69
2	0.00	20.16
3	0.00	15.4
4	0.00	12.78
5	0.00	5.78
6	0.00	4.26
Total		87.08

Table A.5. Principal components for the right maxillary module

Landmarks (x,y,z coordinate)	Principal Component				
	PC1	PC2	PC3	PC4	PC5
RZYMx	0.163	0.694	-0.211	0.305	0.153
RZYMy	0.045	-0.102	-0.409	0.345	0.109
RZYMz	-0.097	-0.024	-0.048	-0.044	-0.190
RZYOx	0.536	-0.099	0.352	-0.135	0.140
RZYOy	-0.163	0.268	0.175	-0.099	0.196
RZYOz	-0.265	0.033	-0.014	0.105	0.389
RCHIx	-0.388	0.089	0.025	0.005	-0.513
RCHIy	-0.008	-0.334	-0.257	0.312	-0.192
RCHIz	0.150	0.074	-0.066	-0.031	-0.010
RCHSx	-0.562	-0.121	0.072	-0.209	0.182
RCHSy	0.037	0.289	0.230	-0.049	-0.351
RCHSz	0.185	-0.053	0.052	-0.072	-0.305
RZTIx	0.097	-0.345	0.297	0.425	-0.093
RZTIy	-0.035	-0.164	0.281	-0.117	0.297
RZTIz	-0.022	-0.054	0.188	0.241	0.210
RZTSx	0.155	-0.217	-0.534	-0.391	0.132
RZTSy	0.124	0.044	-0.020	-0.391	-0.059
RZTSz	0.049	0.023	-0.112	-0.199	-0.093

Table A.6. Eigenvalues and percent sample variance for principal components one through five for the right maxillary module

Principal Components	Eigenvalues	Total Variance (%)
1	0.00	28.40
2	0.00	20.39
3	0.00	14.69
4	0.00	10.93
5	0.00	6.445
Total		80.86

Table A.7. Principal components for the sphenoid module

Landmarks (x,y,z coordinate)	Principal Component				
	PC1	PC2	PC3	PC4	PC5
DOSx	-0.206	-0.141	-0.293	-0.215	-0.080
DOSy	0.063	0.268	-0.209	0.237	-0.070
DOSz	0.015	-0.010	0.010	-0.022	0.101
SELx	-0.082	-0.162	-0.126	0.109	-0.048
SELy	0.125	0.192	-0.236	0.236	0.126
SELz	0.009	-0.023	-0.015	-0.050	0.154
LCLIx	0.418	0.237	0.272	-0.278	0.178
LCLIy	-0.043	-0.426	0.290	-0.164	-0.157
LCLIz	-0.376	0.319	0.353	0.210	-0.068
RCLIx	0.406	0.283	0.210	-0.172	-0.211
RCLIy	-0.033	-0.421	0.277	-0.183	-0.102
RCLIz	0.334	-0.261	-0.368	-0.076	-0.093
SPEx	-0.497	0.106	0.166	-0.062	0.075
SPEy	-0.079	0.160	-0.188	0.029	-0.166
SPEz	0.012	0.017	-0.025	0.022	-0.121
SPHx	0.154	-0.239	0.138	0.709	-0.242
SPHy	0.085	-0.047	0.170	0.121	0.699
SPHz	-0.006	-0.034	0.044	-0.041	0.014
SSEx	-0.193	-0.085	-0.367	-0.092	0.328
SSEy	-0.119	0.274	-0.105	-0.275	-0.331
SSEz	0.011	-0.008	0.001	-0.043	0.014

Table A.8. Eigenvalues and percent sample variance for principal components one through five for the sphenoid module

Principal Components	Eigenvalues	Total Variance (%)
1	0.00	32.84
2	0.00	24.72
3	0.00	13.07
4	0.00	6.21
5	0.00	5.02
Total		81.86

Table A.9. Principal components for the ethmoid module

Landmarks (x,y,z coordinate)	Principal Component			
	PC1	PC2	PC3	PC4
NCRGx	-0.695	0.495	0.085	0.014
NCRGy	-0.067	-0.234	0.821	0.063
NCRGz	0.004	-0.018	0.009	0.219
LMOx	0.107	-0.321	-0.093	0.591
LMOy	0.066	0.044	-0.265	0.016
LMOz	-0.344	-0.466	-0.190	-0.276
RMOx	0.088	-0.331	0.005	-0.592
RMOy	0.063	0.043	-0.256	-0.056
RMOz	0.336	0.468	0.214	-0.259
ETHx	0.500	0.157	0.003	-0.013
ETHy	-0.062	0.147	-0.300	-0.024
ETHz	0.003	0.017	-0.034	0.316

Table A.10. Eigenvalues and percent sample variance for principal components one through four for the ethmoid module

Principal Components	Eigenvalues	Total Variance (%)
1	0.01	40.49
2	0.01	32.84
3	0.00	20.73
4	0.00	3.88
Total		97.94

APPENDIX I: Principal components and corresponding eigenvalues for each module for males.

Table A.11. Principal components for the frontonasal module

Landmark	Principal Components				
(x,y,z coordinate)	PC1	PC2	PC3	PC4	PC5
NASx	0.118	0.035	-0.179	-0.017	0.058
NASy	0.004	-0.014	-0.007	-0.002	-0.022
NASz	0.078	-0.286	0.160	-0.064	-0.030
LDACx	0.103	-0.139	-0.091	0.056	0.155
LDACy	0.008	0.240	-0.017	0.101	-0.083
LDACz	0.076	0.119	0.120	-0.240	-0.176
RDACx	0.087	-0.150	-0.053	0.035	0.069
RDACy	0.003	-0.227	0.021	-0.126	0.043
RDACz	0.057	0.161	0.118	-0.188	-0.126
LNSUx	0.125	-0.122	-0.031	-0.023	-0.031
LNSUy	-0.013	0.324	-0.202	-0.057	0.069
LNSUz	0.052	0.009	-0.083	-0.180	0.064
RNSUx	0.117	-0.087	-0.035	0.020	-0.046
RNXUy	0.009	-0.315	0.238	0.053	-0.062
RNSUz	0.022	-0.002	-0.124	-0.154	0.074
LSPIx	0.112	-0.152	-0.002	0.087	-0.069
LSPIy	-0.009	0.258	-0.148	0.014	0.057
LSPIz	0.045	-0.016	-0.068	-0.003	0.065
RSPIx	0.103	-0.154	0.012	0.083	-0.065
RSPIy	0.009	-0.256	0.154	-0.020	-0.095
RSPIz	0.034	-0.053	-0.086	-0.096	0.067
LNINx	-0.611	-0.029	-0.089	-0.102	-0.207
LNINy	0.147	0.203	-0.122	0.092	0.091
LNINz	-0.156	0.021	-0.205	0.301	0.195
RNINx	-0.605	0.013	0.088	-0.121	0.154
RNINy	-0.145	-0.186	0.098	-0.051	-0.023
RNINz	-0.182	-0.051	-0.121	0.329	0.310
RHIx	-0.017	0.397	0.460	0.197	-0.368
RHIy	-0.007	-0.024	-0.027	0.009	0.020
RHIz	0.066	-0.014	0.225	0.382	-0.011
LALAx	0.108	0.161	0.157	-0.252	0.281
LALAy	-0.010	0.072	-0.074	0.052	-0.039
LALAz	-0.058	0.040	-0.049	0.130	-0.194
RALAx	0.099	0.155	0.130	-0.241	0.319
RALAy	0.003	-0.086	0.059	-0.047	0.012
RALAz	-0.021	0.028	-0.095	0.136	-0.236
NSPx	0.087	0.085	0.116	0.204	0.136
NSPy	-0.008	-0.010	-0.037	-0.017	0.014

Table A.11 (cont.). Principal components for the frontonasal module

Landmark (x,y,z coordinate)	Principal Components				
	PC1	PC2	PC3	PC4	PC5
NSPz	-0.011	-0.019	-0.006	0.062	-0.054
SSPx	0.058	0.027	0.023	0.192	0.060
SSPy	0.004	-0.004	0.005	-0.006	0.019
SSPz	-0.008	0.054	0.122	-0.110	0.107
PROx	0.115	-0.041	-0.508	-0.118	-0.445
PROy	0.003	0.026	0.062	0.004	-0.001
PROz	0.005	0.007	0.092	-0.306	-0.055

Table A.12. Eigenvalues and percent sample variance for principal components one through five for the frontonasal module

Principal Components	Eigenvalues	Total Variance (%)
1	0.00	32.7
2	0.00	11.88
3	0.00	8.14
4	0.00	6.864
5	0.00	5.155
Total		64.74

Table A.13. Principal components for the left maxillary module

Landmarks (x,y,z coordinates)	Principal Components					
	PC1	PC2	PC3	PC4	PC5	PC6
LZYMx	0.338	0.365	-0.058	-0.473	-0.418	-0.303
LZYMy	-0.088	-0.398	-0.165	-0.370	0.025	0.195
LZYMz	-0.052	0.062	0.044	-0.106	-0.173	0.013
LZYOx	-0.483	0.354	0.161	0.123	-0.104	0.266
LZYOy	0.318	0.195	0.158	0.115	-0.101	0.038
LZYOz	-0.242	0.217	-0.097	-0.158	0.356	-0.176
LCHIx	0.350	-0.165	-0.106	-0.141	0.410	0.448
LCHIy	-0.173	-0.372	-0.068	-0.160	-0.146	-0.414
LCHIz	0.066	-0.098	0.122	0.175	-0.007	-0.003
LCHSx	0.335	-0.213	0.179	0.435	0.167	-0.362
LCHSy	0.096	0.300	0.004	-0.142	0.193	0.255
LCHSz	0.192	-0.201	0.009	0.106	-0.301	0.268
LZTIx	-0.325	-0.237	0.486	-0.211	0.157	-0.105
LZTIy	-0.116	0.015	0.188	0.325	-0.300	0.162
LZTIz	0.015	0.077	-0.282	0.028	0.179	-0.165
LZTSx	-0.214	-0.104	-0.662	0.268	-0.212	0.056
LZTSy	-0.037	0.260	-0.116	0.231	0.329	-0.236
LZTSz	0.021	-0.055	0.203	-0.044	-0.054	0.063

Table A.14. Eigenvalues and percent sample variance for principal components one through six for the left maxillary module

Principal Components	Eigenvalues	Total Variance (%)
1	0.00	31.23
2	0.00	20.27
3	0.00	13.77
4	0.00	11.54
5	0.00	6.11
6	0.00	4.61
Total		87.53

Table A.15. Principal components for the right maxillary module

Landmarks (x,y,z coordinate)	Principal Component				
	PC1	PC2	PC3	PC4	PC5
RZYMx	-0.528	-0.372	-0.439	0.031	-0.327
RZYMy	0.064	-0.117	-0.063	0.021	-0.076
RZYMz	-0.138	-0.164	0.474	-0.185	-0.004
RZYOx	0.391	-0.483	0.096	-0.045	0.062
RZYOy	0.117	-0.260	0.139	0.016	0.119
RZYOz	0.293	0.080	-0.014	0.141	0.126
RCHIx	-0.233	0.274	-0.056	-0.026	0.699
RCHIy	-0.019	0.149	0.009	-0.111	-0.090
RCHIz	-0.237	-0.274	0.203	-0.148	0.070
RCHSx	-0.192	0.446	0.434	-0.254	-0.352
RCHSy	-0.090	0.217	-0.156	0.049	0.057
RCHSz	0.195	0.194	-0.121	0.167	-0.402
RZTIx	0.448	0.053	-0.205	-0.439	0.004
RZTIy	-0.100	-0.019	0.165	0.196	0.089
RZTIz	-0.160	-0.047	-0.161	0.100	0.193
RZTSx	0.114	0.083	0.169	0.732	-0.087
RZTSy	0.028	0.029	-0.094	-0.171	-0.098
RZTSz	0.047	0.211	-0.381	-0.075	0.016

Table A.16. Eigenvalues and percent sample variance for principal components one through six for the right maxillary module

Principal Components	Eigenvalues	Total Variance (%)
1	0.00	28.72
2	0.00	18.19
3	0.00	14.53
4	0.00	11.30
5	0.00	6.59
Total		79.33

Table A.17. Principal components for the sphenoid module

Landmarks (x,y,z coordinate)	Principal Component				
	PC1	PC2	PC3	PC4	PC5
DOSx	0.092	0.206	-0.341	-0.144	0.009
DOSy	0.006	-0.243	-0.191	0.090	0.054
DOSz	0.035	0.049	0.017	0.011	0.023
SELx	-0.071	0.087	-0.237	-0.266	-0.145
SELy	-0.007	-0.219	-0.142	0.201	-0.128
SELz	0.022	0.034	0.001	0.030	0.013
LCLIx	-0.155	-0.270	0.386	0.160	0.168
LCLIy	-0.141	0.464	0.317	-0.007	0.102
LCLIz	0.433	-0.106	0.255	-0.134	-0.203
RCLIx	-0.158	-0.404	0.361	0.154	0.132
RCLIy	-0.118	0.464	0.312	0.000	0.126
RCLIz	-0.501	0.039	-0.302	0.152	0.071
SPEx	0.505	0.171	0.085	-0.025	-0.084
SPEy	0.105	-0.128	-0.208	-0.113	0.149
SPEz	0.009	-0.038	-0.003	-0.014	0.014
SPHx	-0.350	-0.012	0.002	-0.516	-0.141
SPHy	-0.069	-0.111	0.047	0.096	-0.759
SPHz	-0.009	-0.001	0.037	0.013	0.024
SSEx	0.137	0.221	-0.256	0.636	0.060
SSEy	0.224	-0.227	-0.135	-0.267	0.457
SSEz	0.011	0.023	-0.004	-0.057	0.058

Table A.18. Eigenvalues and percent sample variance for principal components one through five for the sphenoid module

Principal Components	Eigenvalues	Total Variance (%)
1	0.00	28.27
2	0.00	21.23
3	0.00	18.19
4	0.00	7.56
5	0.00	6.21
Total		81.45

Table A.19. Principal components for the ethmoid module

Landmarks (x,y,z coordinate)	Principal Component			
	PC1	PC2	PC3	PC4
NCRGx	0.736	0.443	0.006	0.036
NCRGy	0.155	-0.250	-0.801	0.081
NCRGz	0.032	-0.041	-0.090	-0.238
LMOx	-0.094	-0.320	0.005	-0.593
LMOy	-0.081	0.051	0.235	-0.059
LMOz	0.250	-0.477	0.284	0.279
RMOx	-0.152	-0.317	0.076	0.572
RMOy	-0.091	0.058	0.254	0.005
RMOz	-0.289	0.496	-0.199	0.274
ETHx	-0.490	0.194	-0.088	-0.015
ETHy	0.017	0.140	0.312	-0.027
ETHz	0.006	0.023	0.006	-0.314

Table A.20. Eigenvalues and percent sample variance for principal components one through four for the ethmoid module

Principal Components	Eigenvalues	Total Variance (%)
1	0.01	42.08
2	0.01	34.12
3	0.00	18.01
4	0.00	3.64
Total		97.85

APPENDIX J: Scree Plots

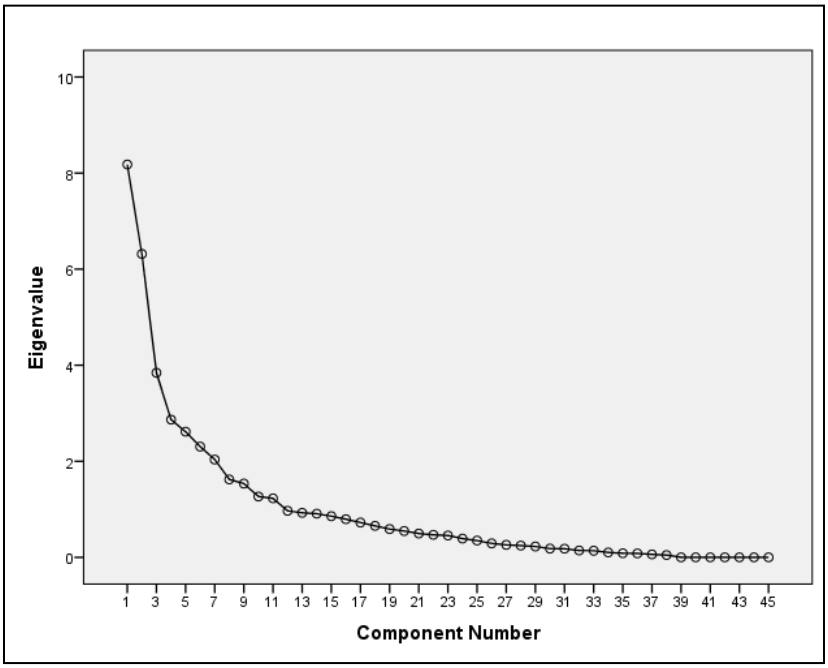

Figure A.1: Scree plot for the frontonasal module for females.

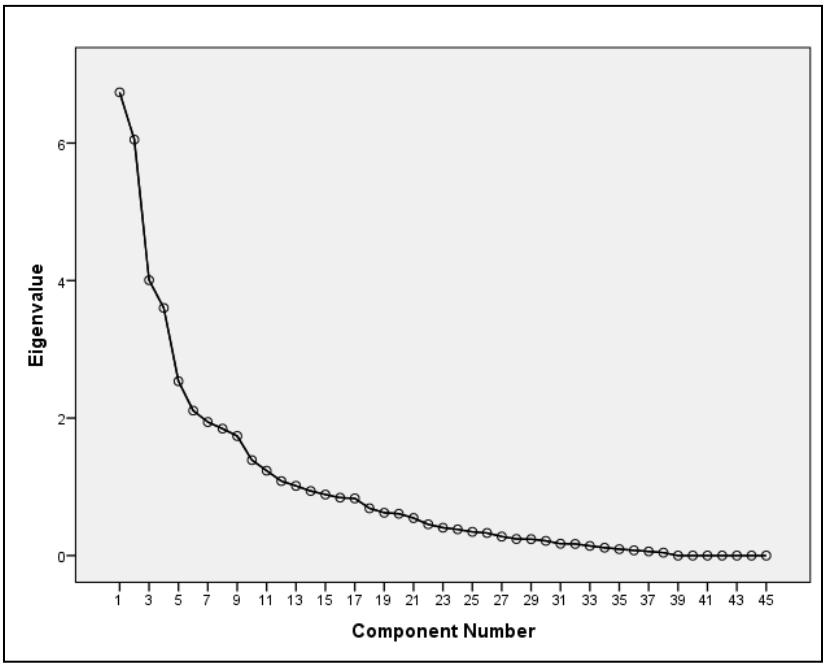

Figure A.2. Scree plot for the frontonasal module for males.

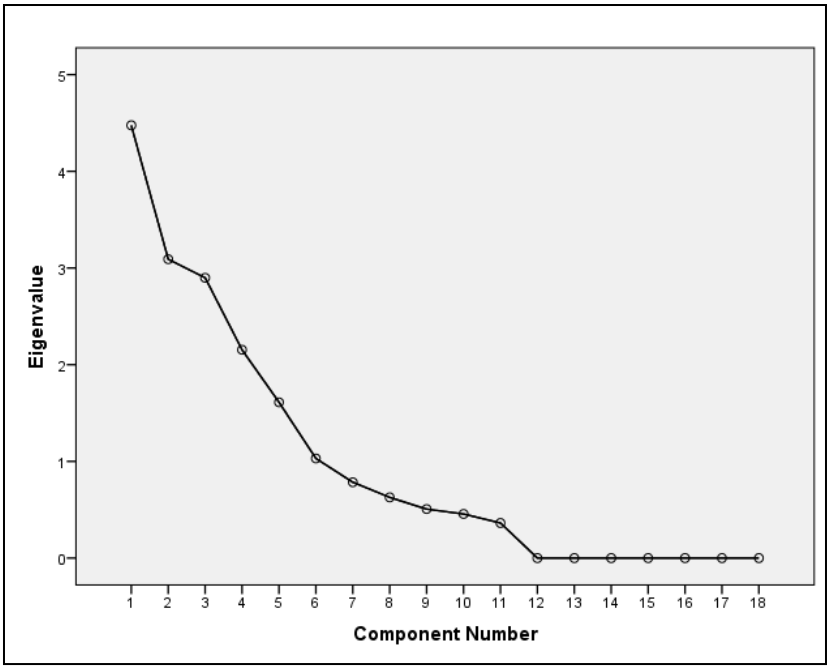

Figure A.3. Scree plot for the left maxillary module for females.

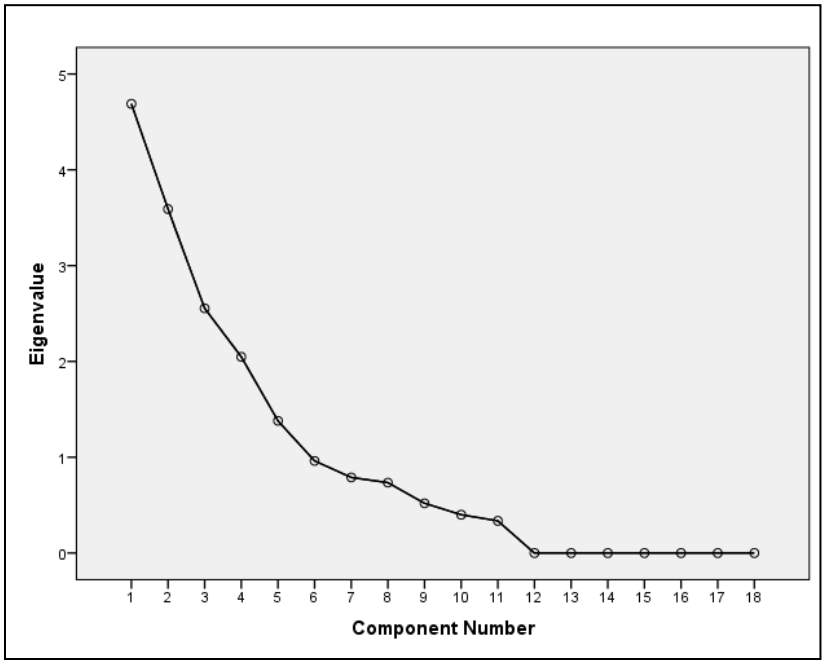

Figure A.4. Scree plot for the left maxillary module for males.

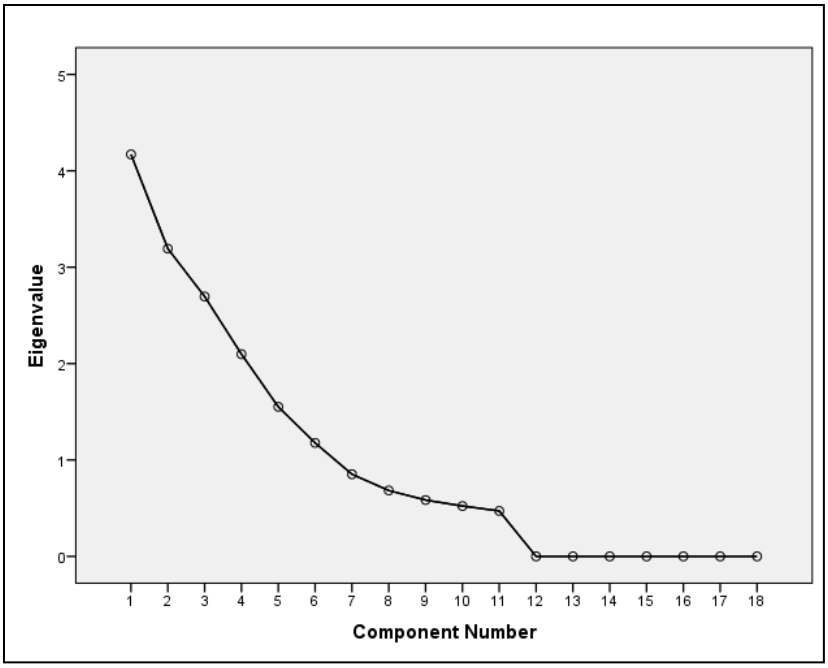

Figure A.5. Scree plot for the right maxillary module for females.

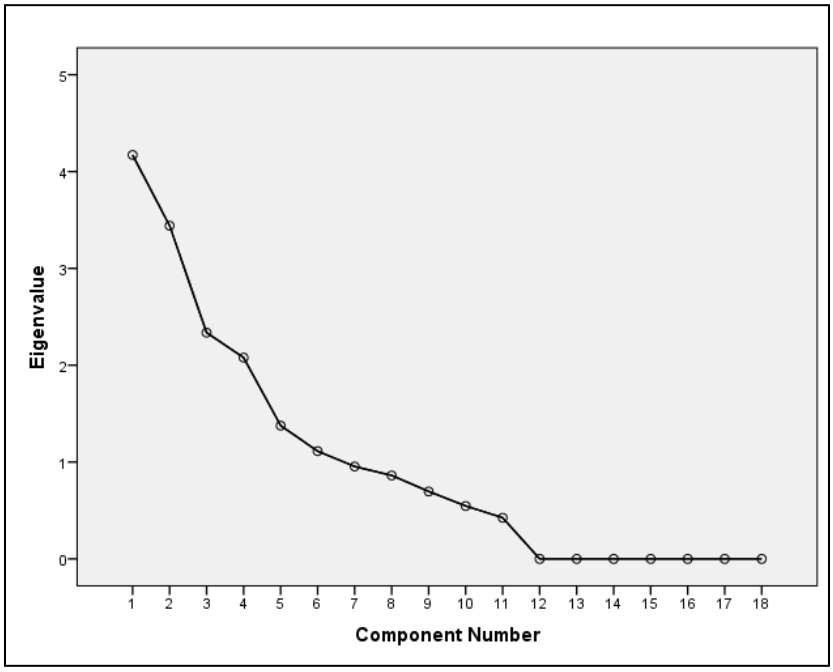

Figure A.6. Scree plot for the right maxillary module for males.

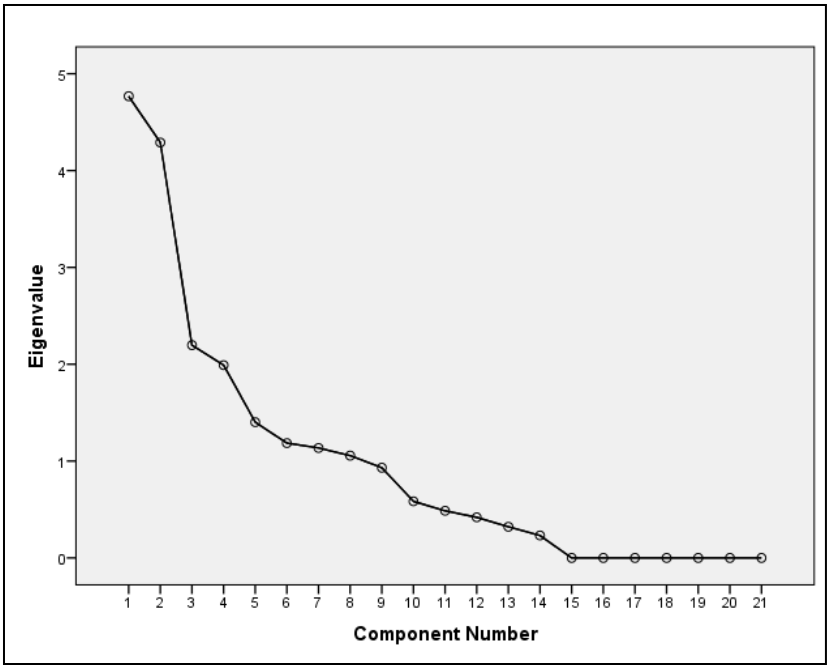

Figure A.7. Scree plot for the sphenoid module for females.

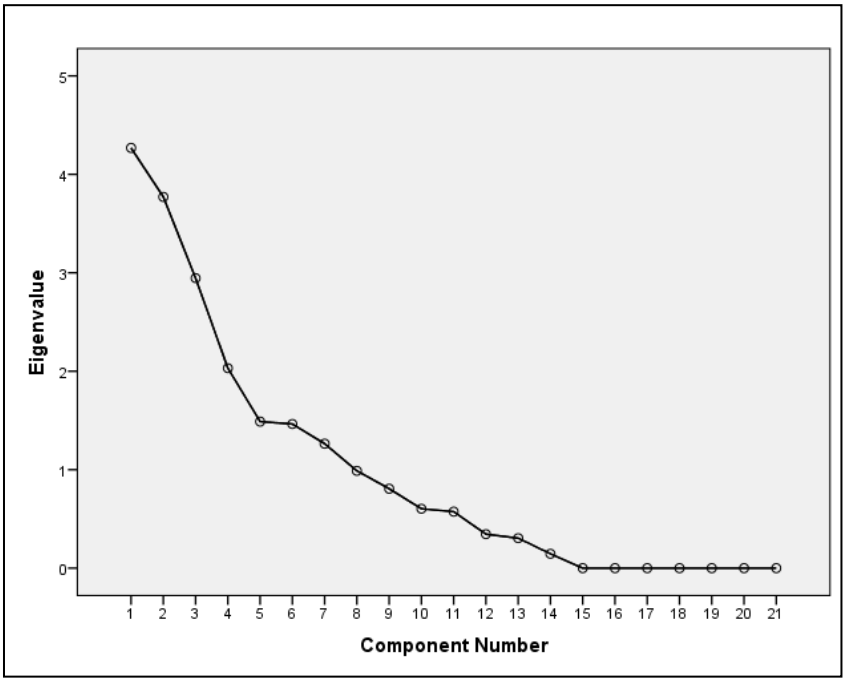

Figure A.8. Scree plot for the sphenoid module for males.

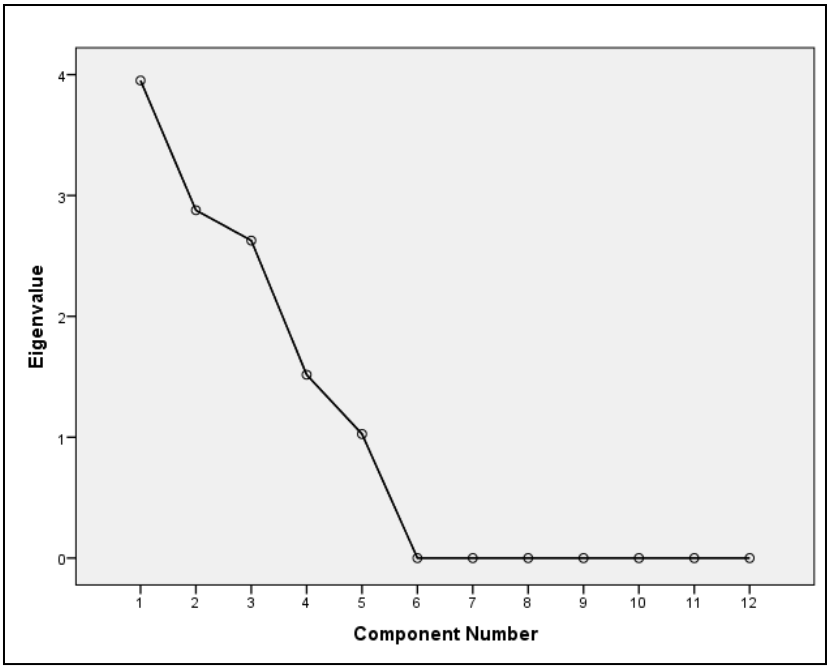

Figure A.9. Scree plot for the ethmoid module for females.

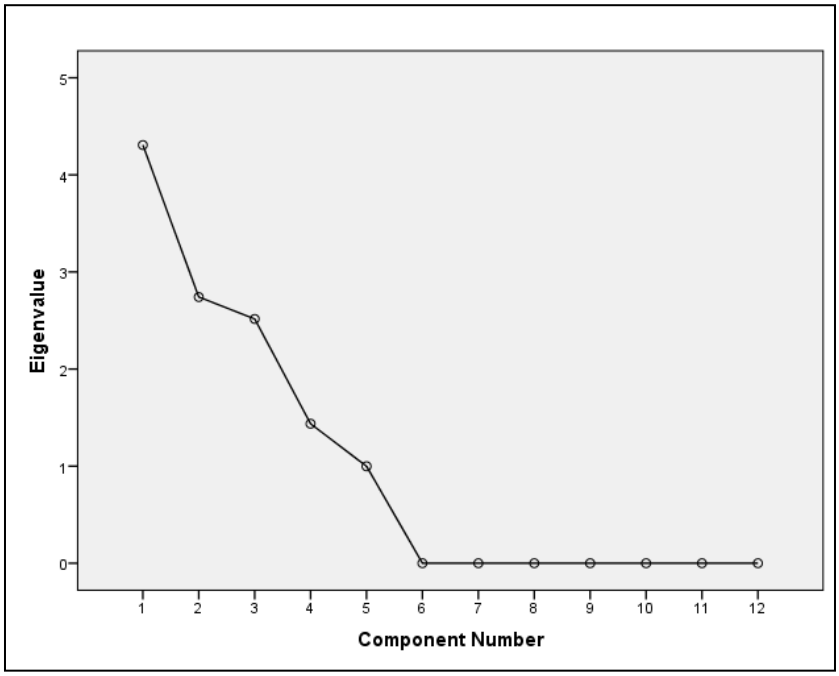

Figure A.10. Scree plot for the ethmoid module for males.

APPENDIX K: Plots of PC1 versus PC2 for each module for females.

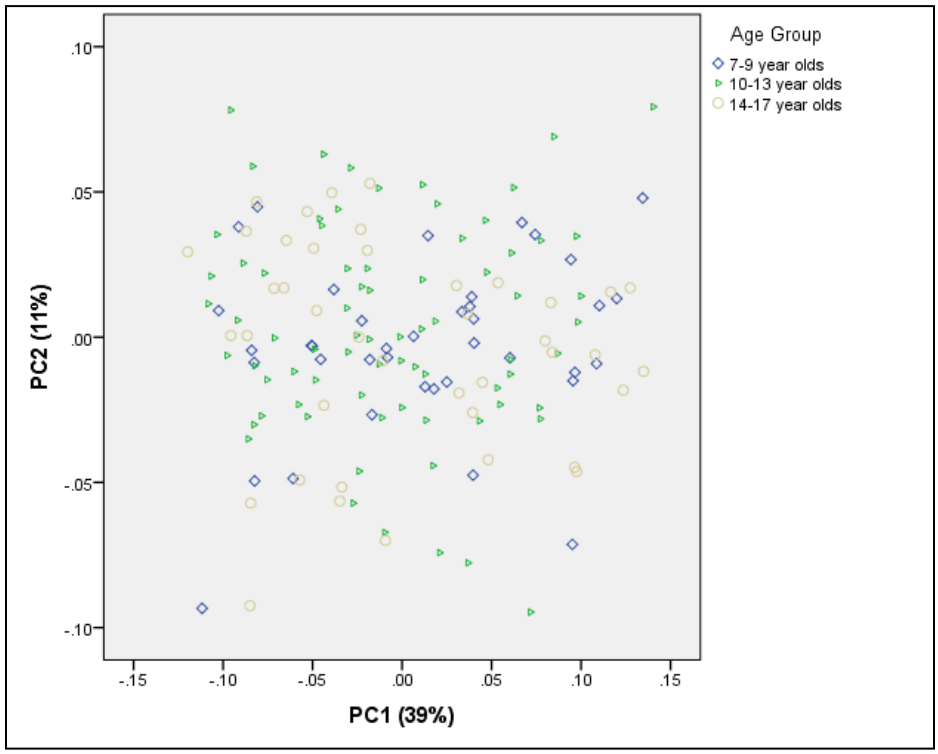

Figure A.11. PC1 versus PC2 for the frontonasal module for females.

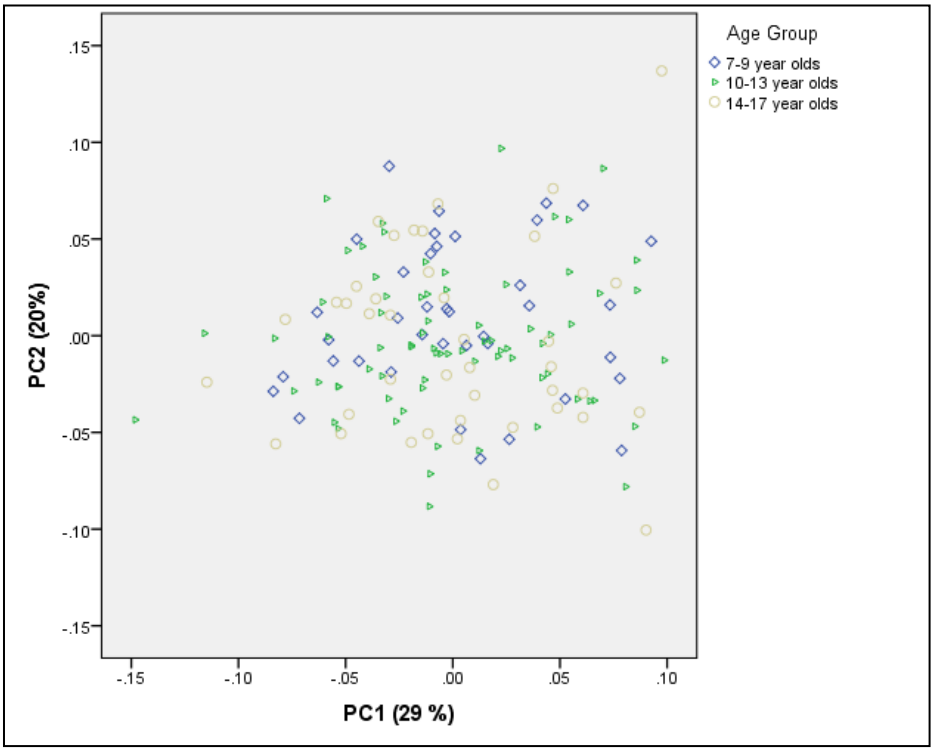

Figure A.12. PC1 versus PC2 for the left maxillary module for females.

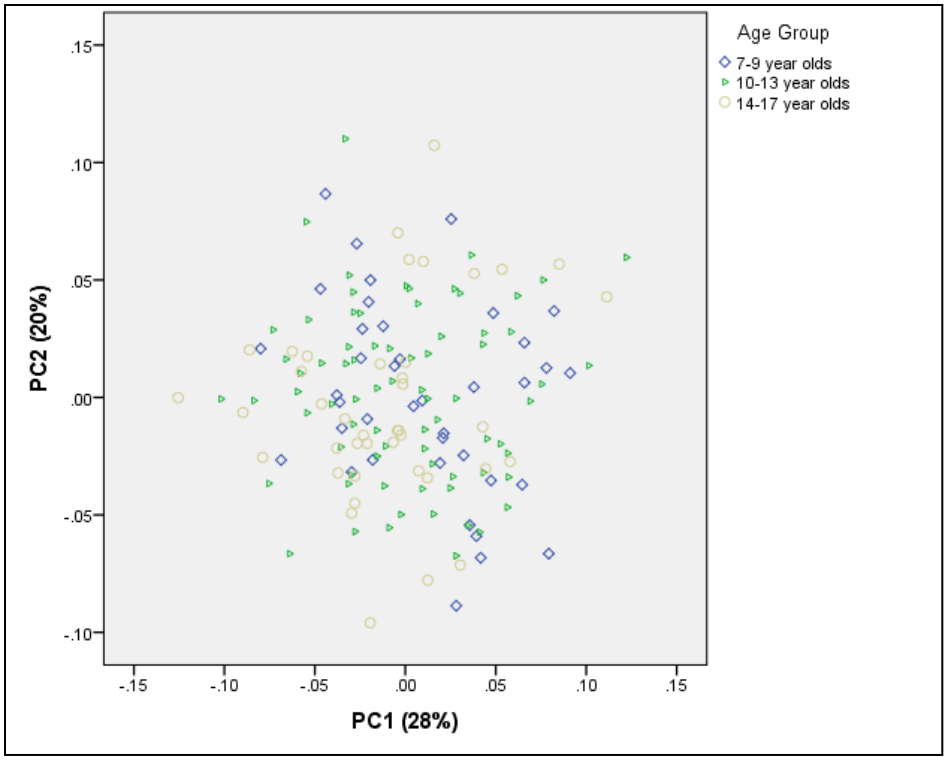

Figure A.13. PC1 versus PC2 for the right maxillary module for females.

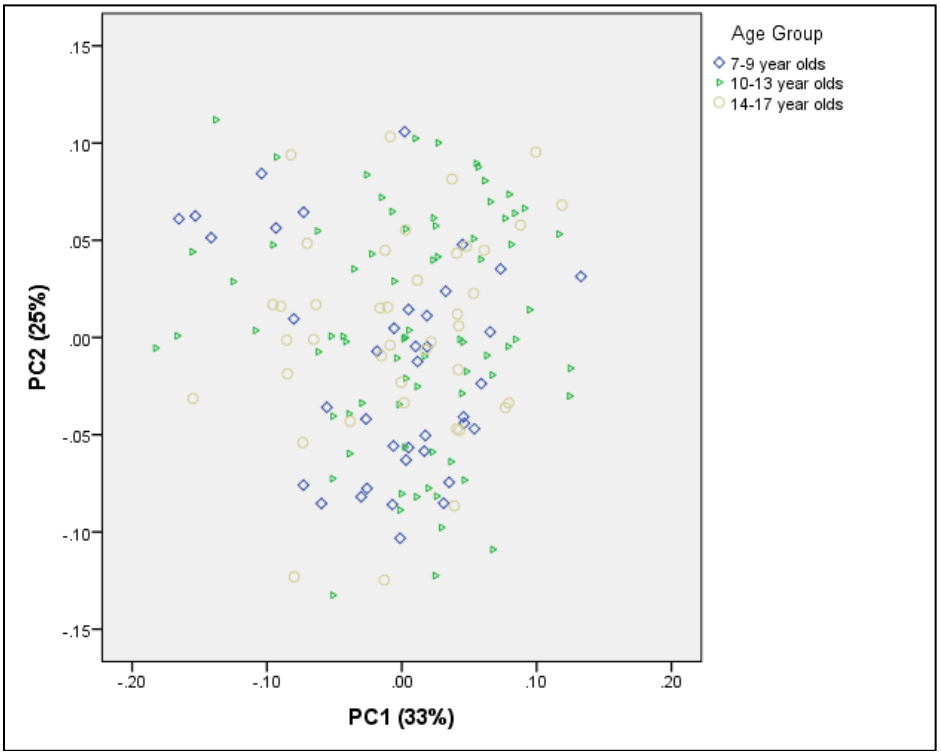

Figure A.14. PC1 versus PC2 for the sphenoid module for females.

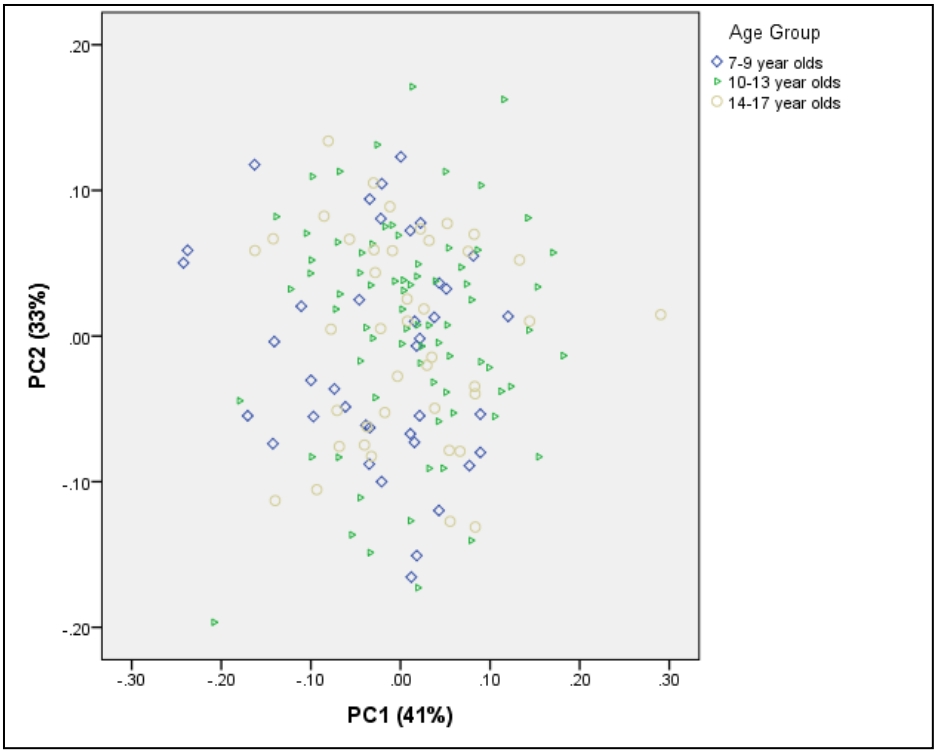

Figure A.15. PC1 versus PC2 for the ethmoid module for females.

APPENDIX L: Plots of PC1 versus PC2 for each module for males.

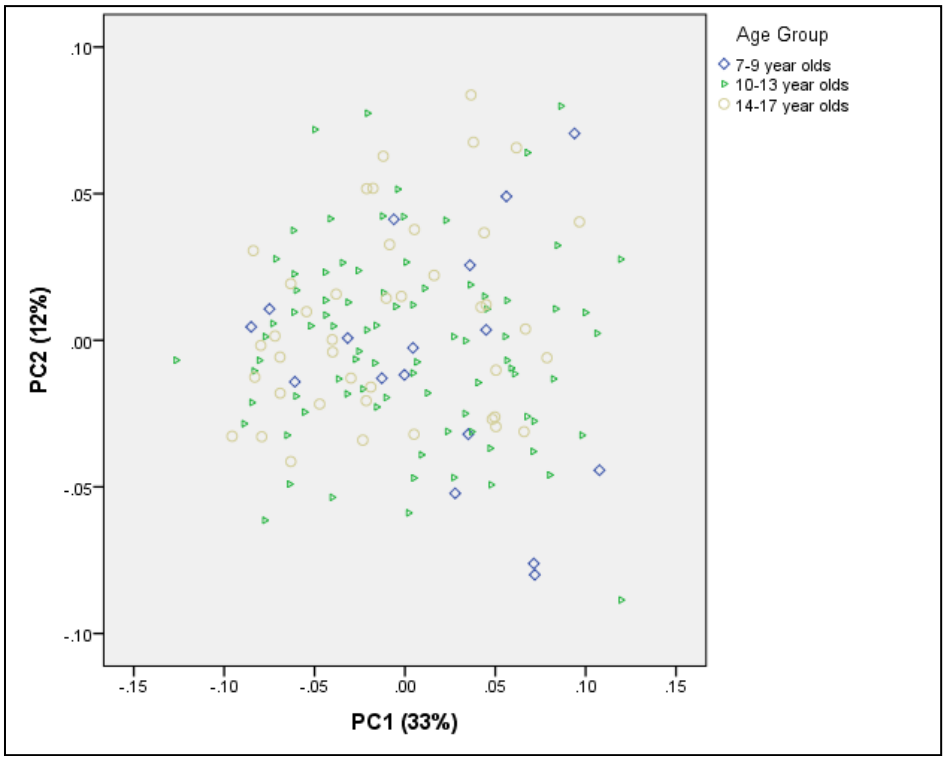

Figure A.16. PC1 versus PC2 for the frontonasal module for males.

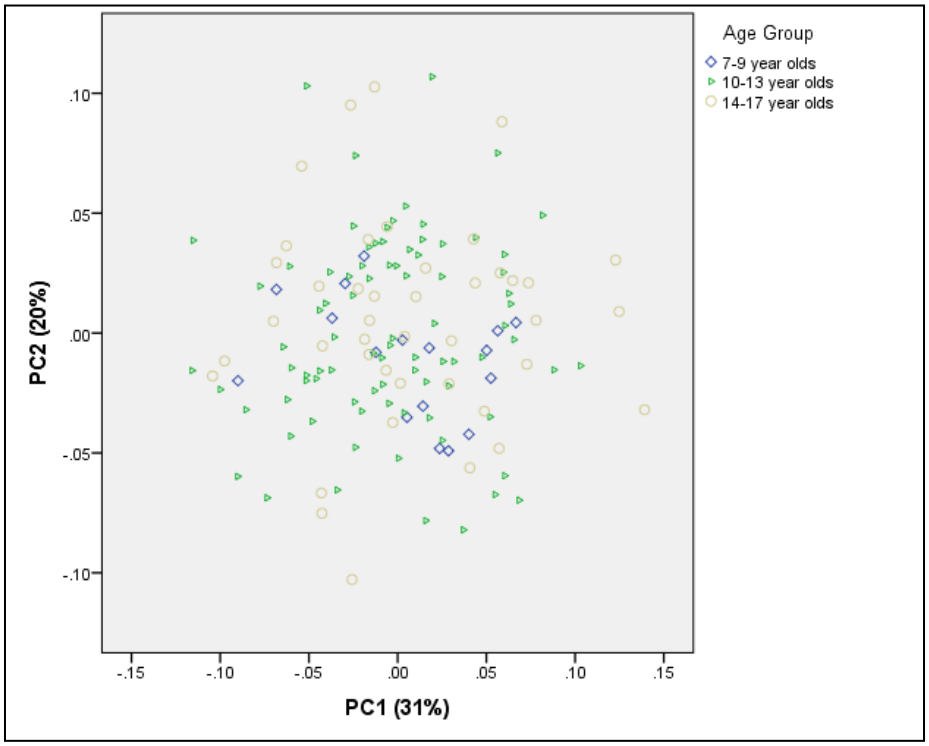

Figure A.17. PC1 versus PC2 for the left maxillary module for males.

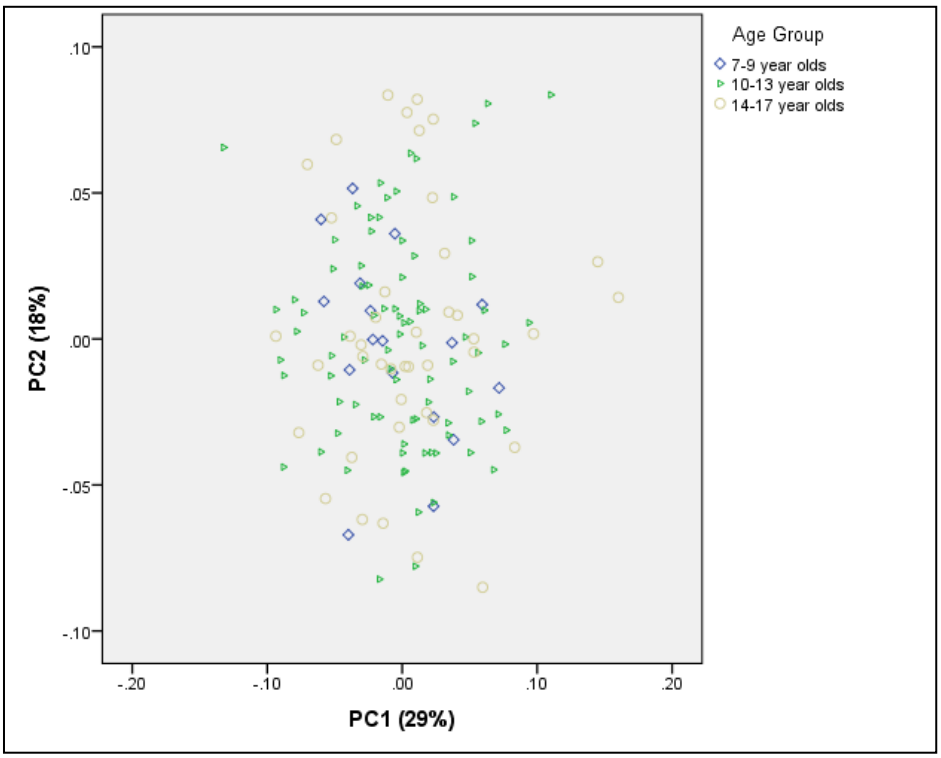

Figure A.18. PC1 versus PC2 for the right maxillary module for males.

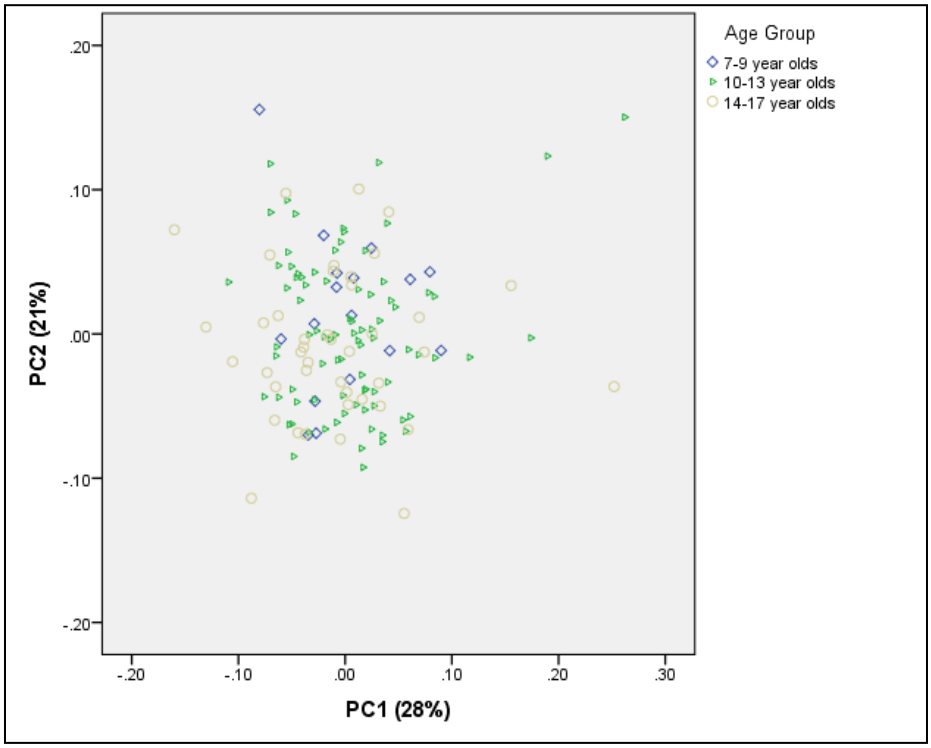

Figure A.19. PC1 versus PC2 for the sphenoid module for males.

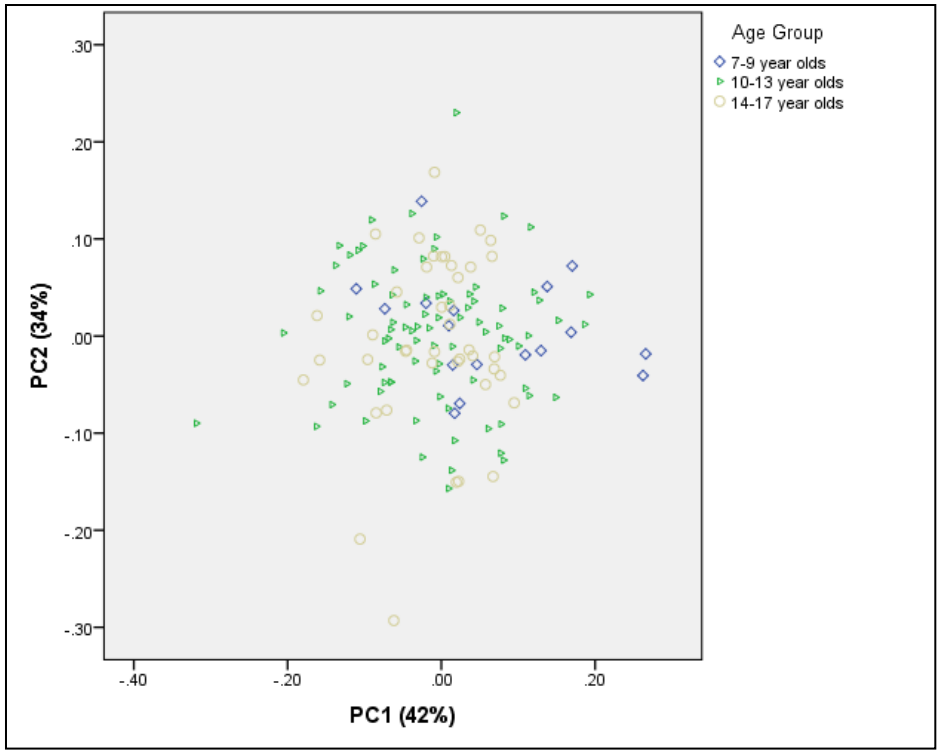

Figure A.20. PC1 versus PC2 for the ethmoid module for males.

VITA

Amber Wheat was born in Baton Rouge, Louisiana to parents Jimmy and Leslie Davis. She studied and completed her undergraduate education at Louisiana State University, graduating with a B.A. in Anthropology in 2007. She attended Texas State University-San Marcos to pursue her interests in biological anthropology, graduating with an M.A. degree in 2009. She continued her graduate education at the University of Tennessee, earning her Ph.D. in May 2015. During her tenure in graduate school, Amber was a Graduate Teaching Assistance for many classes including Human Origins, Human Osteology, Introduction to Cultural Anthropology, and Introductory Forensic Anthropology. She was also a Graduate Teaching Associate for Human Origins during her time at the University of Tennessee. Amber continues to pursue both teaching and research opportunities.